INFORMATION TO USERS

This manuscript has been reproduced from the microfilm master. UMI films the text directly from the original or copy submitted. Thus, some thesis and dissertation copies are in typewriter face, while others may be from any type of computer printer.

The quality of this reproduction is dependent upon the quality of the copy submitted. Broken or indistinct print, colored or poor quality illustrations and photographs, print bleedthrough, substandard margins, and improper alignment can adversely affect reproduction.

In the unlikely event that the author did not send UMI a complete manuscript and there are missing pages, these will be noted. Also, if unauthorized copyright material had to be removed, a note will indicate the deletion.

Oversize materials (e.g., maps, drawings, charts) are reproduced by sectioning the original, beginning at the upper left-hand corner and continuing from left to right in equal sections with small overlaps. Each original is also photographed in one exposure and is included in reduced form at the back of the book.

Photographs included in the original manuscript have been reproduced xerographically in this copy. Higher quality 6" x 9" black and white photographic prints are available for any photographs or illustrations appearing in this copy for an additional charge. Contact UMI directly to order.

UMI

A Bell & Howell Information Company
300 North Zeeb Road, Ann Arbor MI 48106-1346 USA
313/761-4700 800/521-0600

Downloaded from SHAREOK. Persistent Handle URL: https://hdl.handle.net/11244/5769

UNIVERSITY OF OKLAHOMA

GRADUATE COLLEGE

SURFACTANT-CYCLODEXTRIN BINDING, MIXED SURFACTANT MICELLES, AND NEW SURFACE TENSION METHODS

A Dissertation

SUBMITTED TO THE GRADUATE FACULTY

in partial fulfillment of the requirements for the degree of

Doctor of Philosophy

By

Andrew Randall Slagle
Norman, Oklahoma
1998

UMI Number: 9914422

UMI Microform 9914422
Copyright 1999, by UMI Company. All rights reserved.

This microform edition is protected against unauthorized copying under Title 17, United States Code.

UMI
300 North Zeeb Road
Ann Arbor, MI 48103

©Copyright by Andrew Randall Slagle 1998
All Rights Reserved

SURFACTANT-CYCLODEXTRIN BINDING, MIXED SURFACTANT MICELLES, AND NEW SURFACE TENSION METHODS

A dissertation APPROVED FOR THE

DEPARTMENT OF CHEMISTRY AND BIOCHEMISTRY

BY

Prof. Sherril D. Christian

Prof. Dick van der Helm

Prof. Richard W. Taylor

Prof. John F. Scamehorn

Prof. Brian P. Grady

Acknowledgments

Professor Christian has been a tremendously supportive advisor whose guidance and experience have made every aspect of this research possible. I will always be grateful for his patience and generosity. Every member of my research committee has been inspirational. Professors van der Helm, Taylor, Scamehorn and Grady have been examples of researchers with enthusiastic exuberance for science and engineering. They have all been mentors willing to make time for guidance, and I am very appreciative to each committee member.

All of my family has provided endless support in one way or another, whether they know it or not, and I am very grateful for their support and understanding. I am especially grateful to my wife, Afsaneh, for her patience while I have spent way too much time in pursuit of a degree.

The encouragement and friendship of Kurt Grafton, Paul Kerr, Jim Roach, Kevin Raymond and Kris Wise have helped me immensely. Besides occasionally discussing issues related to research, these guys could also be counted on to provide distractions in the way of Disc Golf or late night Poker games. I am also grateful for the friendships of Qi Qu, Carlos Rodriguez, Connie Dunaway, Katsuhiko Fujio and Dr. Ed Tucker. I am further indebted to Dr. Ed Tucker for being an endless supplier of equipment, tools, computers, and general laboratory expertise.

I am very grateful to Dr. Edwin Quiñones, Sanjay Wategaonkar and Tim Nelson for friendships made during my Masters studies at Kansas State University. These guys are good friends and were always available for research discussions.

Everyone that I worked with at Amoco made working there a pleasure. I am specially grateful for the invaluable friendships of Dan Phelps, Dan Crosby, Andy Weber, Bruce Barnes, Bob Stewart, and Dutch Frame who are among the best people I have ever had to opportunity to work with. Dutch has been a mentor since I first met him during my undergraduate studies at Southwestern Oklahoma State University and I will always be grateful for his steadfast encouragement and friendship.

Nonionic surfactants used for the mixed micelle studies were provided by Prof. Yoshihiro Saito from the Nihon University School of Pharmacy, Chiba, Japan. During Yoshi's sabbatical in our labs, we became very good friends and I greatly appreciate his support even after he returned to Japan.

Considerable financial, technical, and clerical support has been provided by the Department of Chemistry and Biochemistry. Glassblowing work by Jim Cornell and Ron Stermer, and the electronics and technical support of Alan Rees and John Black, have been invaluable. Of course, it would be impossible to accomplish anything without the departmental office staff and I am especially indebted to Karen Hinkle and Arlene Crawford.

Exceptional opportunity is provided to each student who works with Surfactant Associates and the Institute for Applied Surfactant Research. I am very thankful for the financial support of Surfactant Associates and the honor of being associated with both of these groups.

Table Of Contents

List Of Tables viii

List Of Figures x

Abstract xiii

Chapter

1. Using Surfactant Sensitive Electrodes to Measure the Binding of *n*-Alkylammonium Cations by Cyclodextrins

   Introduction 1

   Experimental 15

   Results and Discussion 20

   Conclusions 49

   References 51

2. Synergism in Nonionic/Cationic Mixed Micelle Systems

   Introduction 57

   Experimental 59

   Results and Discussion 64

   Conclusions 89

   References 91

   Appendix To Chapter 2 93

3. Inverted Vertical Pull Surface Tension Methods

Introduction 96

Experimental 107

Results and Discussion 123

Conclusions 126

References 130

Appendix To Chapter 3 132

List of Tables

Table		Page
1.1	Select physical properties of α-, β- and γ-cyclodextrin.	5
1.2	CMC Determination of CTAB	22
1.3	CMC Determination of MTAB	22
1.4	CMC Determination of DDTAB	22
1.5	Calibration data for CTAB, MTAB, DDTAB	31
1.6	Titration of DDTAB with α-CD	33
1.7	Titration of MTAB with α-CD	33
1.8	Titration of CTAB with α-CD	33
1.9	Titration of DTAB with β-CD	34
1.10	Titration of MTAB with β-CD	34
1.11	Titration of CTAB with β-CD	34
1.12	Titration of DDTAB with γ-CD	35
1.13	Titration of MTAB with γ-CD	35
1.14	Titration of CTAB with γ-CD	35
1.15	Stepwise equilibrium constants for inclusion complexes of DDTAB, MTAB, and CTAB with α-, β-, and γ-cyclodextrins	39
1.16	Results of SSE studies by Wyn-Jones	47
2.1	S.T. (Surface Tension, mN/m) data for BL7SY	69
2.2	S.T. (Surface Tension, mN/m) data for BD8SY	71
2.3	S.T. (Surface Tension, mN/m) data for BL8SY	73

2.4 S.T. (Surface Tension, mN/m) data for BM8SY 75

2.5 Critical micelle concentration data for BL7SY-CTAB Mixtures 81

2.6 Critical micelle concentration data for BD8SY-CTAB Mixtures 81

2.7 Critical micelle concentration data for BL8SY-CTAB Mixtures..... 81

2.8 Critical micelle concentration data for BM8SY-CTAB Mixtures..... 81

2.9 β parameters calculated based on the one parameter model..... 87

List of Figures

Figure		Page
1.1	Cyclodextrin structures demonstrating size and relative arrangement of hydroxyl groups	6
1.2	Illustration of an inclusion complex between a cyclodextrin and CTAB	9
1.3	K_{sp} dependent model of electrode operation	13
1.4	Adsorption dependent model of electrode operation.	14
1.5	Surfactant Sensitive Electrode (SSE) construction	15
1.6	Configuration of system used for electrode measurements	17
1.7	CMC determination of CTAB, MTAB, DDTAB in 0.010 M NaCl	23
1.8	Surfactant counterion activity relative to surfactant activity	24
1.9	Calibration curves used at the beginning of each binding measurement to determine free surfactant concentration	32
1.10	Millivolt response as a function of α-CD complexation	36
1.11	Millivolt response as a function of β-CD complexation	37
1.12	Millivolt response as a function of γ-CD complexation	38
1.13	Free cationic surfactant concentration as a function of α-CD complexation	41
1.14	Free cationic surfactant concentration as a function of β-CD complexation	42
1.15	Free cationic surfactant concentration as a function of γ-CD complexation	43
1.16	Simplified structures illustrating some possible binding configurations of surfactant:CD complexes	44

2.1 Structures of compounds used in mixed micelle studies. 63

2.2 Log(total surfactant concentration) vs. surface tension used to determine CMC for BL7SY/CPC mixtures 77

2.3 Log(total surfactant concentration) vs. surface tension used to determine CMC for BD8SY/CPC mixtures 78

2.4 Log(total surfactant concentration) vs. surface tension used to determine CMC for BL8SY/CPC mixtures 79

2.5 Log(total surfactant concentration) vs. surface tension used to determine CMC for BM8SY/CPC mixtures 80

2.6 Mole Fraction BL7SY vs. CMC with a line representing the fit of the one parameter model to determine Beta for BL7SY/CPC mixtures 82

2.7 Total Mole Fraction BL7SY vs. Mole fraction in the Micelle with a line representing the fit of the one parameter mode. 83

2.8 Mole Fraction BD8SY vs. CMC with a line representing the fit of the one parameter model to determine Beta for BD8SY/CPC mixtures 84

2.9 Mole Fraction BL8SY vs. CMC with a line representing the fit of the one parameter model to determine Beta for BL8SY/CPC mixtures 85

2.10 Mole Fraction BM8SY vs. CMC with a line representing the fit of the one parameter model to determine Beta for BM8SY/CPC mixtures 86

3.1 Illustrations of Wilhelmy Plate and du Noüy ring methods 99

3.2 The important parameters needed to calculate force for the rod pull method 100

3.3 Force curve for water (72.3 mN/m @ 23 °C) as a function of rod height above the free surface 105

3.4 Inverse Rod Pull (IRP) Tensiometer: Micrometer and liquid cell arrangement for vertical pull measurement 108

3.5 Directional Converted Rod Pull (DCIRP) Tensiometer 109

3.6 Depiction of rod pulling liquid surface 110

3.7 Surface tension dependence on the rod radius 113

3.8 Force vs. height curves for a series of CTAB solutions. Lines are calculated from theory (knowing the surface tension 115

3.9 CMC determination of CTAB 120

3.10 Comparison of present measurements with du Noüy ring measurements of Dharmawardana, et. al. (20) and Wilhelmy plate measurements of Aveyard, et. al. (19) 121

3.11 CMC Determination for SDS 122

Abstract

Cyclodextrins are macrocyclic compounds with the unusual and useful structural feature of having a shape like a cup open at both ends. The macrocyclic structure is made up of 6, 7 or 8 glucopyranose units for α, β, or γ-cyclodextrin, respectively. With a hydrophobic cavity, cyclodextrins are capable of forming *inclusion complexes* in which a nonpolar structural feature of a guest molecule is bound inside the cavity. Hydroxyl groups lining the structures openings help make cyclodextrins water soluble and can also affect their natural tendency for forming complexes. Nonpolar compounds or compounds with nonpolar branches, such as a hydrocarbon tail, have demonstrated a strong propensity to act as guests in cyclodextrin inclusion complexes. In the work presented here, the binding constants for cyclodextrin (CD) with a series of *n*-alkyl trimethylammonium bromide (TAB) cationic surfactants have been determined. The activity of the TAB compounds was measured in solution by using a surfactant sensitive electrode. The electrode response was used in a least-squares regression fit to model the equilibrium constants. Results show that the TAB surfactants, with carbon tail lengths of C12, C14, and C16, form complexes of varying strength and different stoichiometries with α, β, and γ-cyclodextrins. The ability to form complexes with TAB:CD ratios of 1:1, 1:2, and 2:1 are shown to depend on the relative length of the surfactants hydrocarbon tail and on the size of the cyclodextrins cavity.

Mixtures of surfactants are of great practical and theoretical interest. The natural tendency of surfactants to form aggregates (micelles) in solution can be substantially enhanced when present as mixtures compared to either of the pure surfactants. This enhancement is referred to as a synergistic effect. The synergistic lowering of the critical micelle concentration (CMC) of a series of binary cationic/nonionic mixed surfactant systems is the subject of the present work. Despite the importance of understanding mixed surfactant behavior, surprisingly little data has been published for cationic surfactants with the nonionic surfactants used here, probably because of the extremely high cost of monodisperse nonionic surfactants. The cationic surfactant used was cetylpyridinium chloride (CPC). The series of nonionic surfactants used were polyethylene oxides (PEO's) with 7 and 8 EO linkages, and hydrocarbon tails of C12, C14, and C16. The surface tensions of the pure surfactants and binary mixtures were measured and used to determine the critical micelle concentrations. The CMC values for the mixtures were used in a model for which a single parameter β, is a measure of the magnitude of the enhancement. Results show that the CMC lowering enhancement is stronger as the hydrocarbon tail of the PEO increases (coming closer to the C16 tail length of the CTAB) and that the enhancement increases as the number of ethylene oxide subunits decreases.

Conventional vertical pull surface tension techniques are typically conducted by contacting a probe, of well defined shape, with the surface of a solution to be tested, and slowly pulling the probe upward. The most common probes are the du Noüy ring and Wilhelmy plate, although for the present work a stainless steel rod with precisely known radius is used. The most common instruments use a microbalance or torsion wire mounted above the test system to measure the force acting on the probe. The first new surface tension method presented here measures the force by weighing the liquid sample, while a probe is allowed to contact the surface of the solution and then pulled slowly upward. A second method is presented in which the solution is not weighed, but the force measurements are still made from below rather than above the test system. One of the most important aspects in measuring the forces from below is that a top-loading analytical laboratory balance of 0.1 to 1 mg precision which is commonly available in most academic and research laboratories, can be used. Hence, the largest cost of the instrument is already covered and the measurements are extremely cost effective. Results indicate that another very important feature of these methods is that the probe can be held rigidly above the solution, instead of being swung freely from a balance above. This advantage is especially important when measurements are to be made on small samples where the probe may be in close proximity to the sample vessel wall. Although the methods can be used with traditional platinum rings or plates, it is demonstrated here that a stainless steel rod with precisely know radius provides excellent results.

Chapter 1

Using Surfactant Sensitive Electrodes to Measure the Binding of *n*-Alkylammonium Cations by Cyclodextrins

Introduction

The most widely used ion selective electrode (ISE) is the glass pH electrode. Early in the present century Cremer (1) and Haber (2-3) developed the prototype hydrogen electrodes. Use these electrodes has obviously flourished as evidenced by their widespread utilization since that time. Some success in developing electrodes selective for other ions was realized beginning in the 1930s but it was not until the early 1960s (4) that a wide range of ISEs began to be developed. The dramatic increase in development from the 1960s forward was mainly facilitated by the successful application of heterogeneous-membrane electrodes. The heterogeneous-membrane electrode used in the present studies, a surfactant sensitive electrode (SSE) was constructed of a polymer membrane with an aqueous filling solution containing the specific ion to be measured. The polymer membrane was impregnated with a "carrier complex" to facilitate charge transfer and ion exchange at the membrane surface.

Published studies show that tailoring the SSE to actually be selective for surfactants of the same charge and similar structure has been successful, although it is difficult to make an electrode respond reproducibly to different samples of the same mixture (5-9). For the present study, however, it was not the intent to detect a particular cationic surfactant in the presence of others, but to monitor the effect of varying concentrations of a single surfactant in solution. Therefore, the electrodes constructed here are designed to be sensitive to, but not necessarily selective for, cationic surfactants. Further, the experiments are designed to produce a calibration curve with each experimental measurement; therefore, difficulties with reproducible response between samples are avoided.

Surfactant sensitive electrodes have been used to study the molecular interactions for a variety of applications. Cationic surfactants have been investigated alone in aqueous solution to determine intrinsic surfactant solution characteristics such as aggregation and counterion binding (10-15), micellar exchange rates (16-17) and critical micelle concentrations (10,18-22). Wyn-Jones et. al., have also studied micellization in non-aqueous solutions using a SSE (23-24). Many of the same types of studies have been reported for anionic (25-47) and zwitterionic surfactants (48).

The earliest examples of SSEs were made using liquid-ion-exchanger membranes requiring a liquid organic phase to hold the ion-exchanger complex (14, 25-26, 33-36, 43). The electrode construction design used here was based mainly on work reported by Rippin and Laskowski (49), although very similar variations have been in much of the literature reviewed. The basic electrode design included a

polymeric (usually PVC) membrane with a plasticizer (dioctylpthalate in the present study). An active complex (a 1:1 precipitate of a cationic/anionic surfactant) impregnated the membrane and is believed to facilitate ion exchange providing the sensitivity, and selectivity, of the electrode. The main difference between this electrode design and the earlier liquid-ion-exchanger designs was that the active-complex is immobilized in the PVC. This PVC membrane design is also easier to maintain and there is no concern about a liquid organic membrane phase being solubilized by micelles in the test solution.

Since the electrodes described above can measure the surfactant monomer activity in solution, they have been used to investigate the binding and interactions of ionic surfactants with various other compounds and solids. Cationic and anionic surfactants have been studied in the presence of oppositely charged polyelectrolytes (50-60), DNA (61-62) and neutral, water soluble polymers (63-64). One paper was found that discussed the "binding" of cationic surfactants to nonionic (polyethyleneoxide) surfactant micelles (65) and one that discussed mixed micelles of ionic surfactants with *n*-alkyl alcohols (66). The limited number of publications regarding nonionic surfactants may be due to the interference of nonionic surfactants with the surfactant sensitive electrode. The adsorption of cationic surfactants to colloidal clay and coal fine particles has also been investigated (67-68). The results were contrasted to those obtained by more complicated techniques such as equilibrium dialysis, or other techniques of separating the surfactant-bound clay from the bulk solution for analysis.

Cyclodextrins are compounds capable of forming complexes with many different compounds. Among the important classes of compounds that form complexes with cyclodextrins are drugs, perfumes and surfactants. In the present work, the binding constants for cyclodextrins and a series of cationic surfactants were investigated using a surfactant sensitive electrode to measure the free surfactant activity in the presence of cyclodextrin(s) in aqueous solution.

Cyclodextrins (CDs) are natural, cyclic oligosaccharides of 6, 7 or 8 glucopyranose units called α, β or γ-cyclodextrin, respectively. They are produced by the enzymatic action of cyclodextrin glycosyltransferase (CGTase) on starches resulting in α-1,4 linkages to form a macrocyclic structure. Cyclodextrins were actually discovered at the end of the 19th century, but factors such as cost and problems of large scale production prevented extensive research until the 1970's. A vast amount of literature is available on the structures and chemistry of these three naturally occurring cyclodextrins and of the many derivatives thereof. Szejtli has written two books (69-70), and contributed to another (71) on the subject since 1982. Another book (72) has also been written by other authors. The structures, shape and dimensions of these CDs are shown in Figure 1.1 and some pertinent properties are listed in Table 1.1. The data in Table 1.1 are related not just to the relative size of each cyclodextrin but, more importantly, to the size of the cyclodextrin cavity.

	α-CD	β-CD	γ-CD
Molecular Weight (g mol^{-1})	973	1135	1297
Internal cavity diameter (Å)	5.2	6.6	8.4
CD height (Å)	7.9	7.9	7.9
Cavity volume ($Å^3$)	174	262	427
Water solubility (g/100mL @ 25°C)	14.2	1.85	23.2
Melting range (°C)	255-260	255-265	240-245
Water molecules in cavity	6	11	17

Table 1.1. Select physical properties of α-, β- and γ-cyclodextrin from Fromming and Szejtli (70).

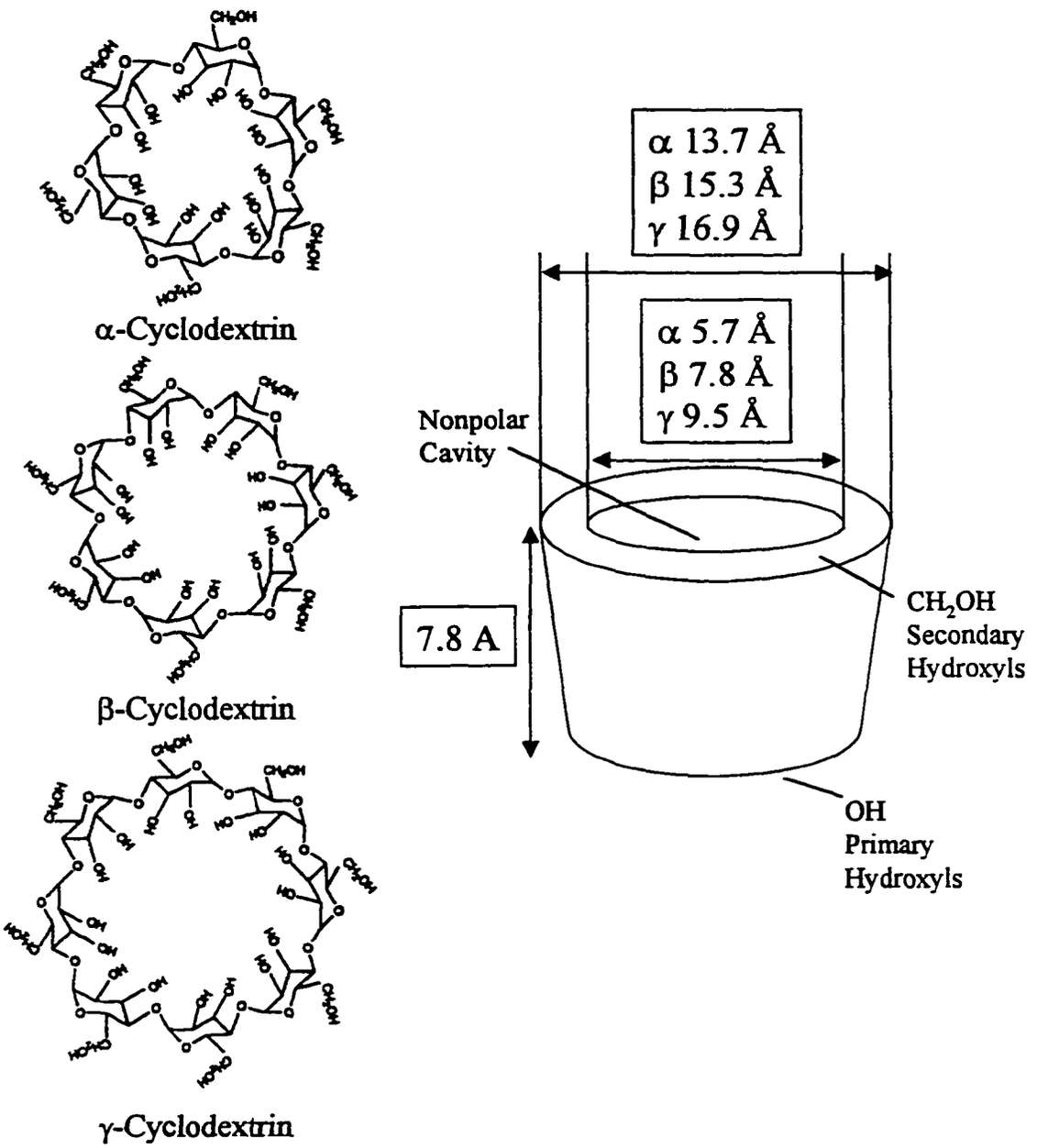

Figure 1-1. Cyclodextrin structures demonstrating size and relative arrangement of hydroxyl groups (70,73).

The cavity volume of each CD increases with the number of glucopyranose subunits. This size variation indicates that molecules of varying size might be able to fit into the cavity forming an *inclusion complex*. Besides the size of the cavity, other factors may also strongly influence the ability of CD to act as a "host" to a "guest" molecule. The hydroxyl groups of each glucopyranose monomer unit are directed similarly for all natural CDs. At the top (wider end) of the CD molecules are secondary hydroxyl groups, while at the bottom end there are primary hydroxyl groups. CD molecules are typically drawn as truncated cones, or toroids, and their structure is largely determined by the free rotation of the primary hydroxyl groups restricting the diameter of one end of the cavity. The interaction between hydroxyls, hydrogen bonds, may be responsible for the peculiar solubility drop of β-CD (69). Therefore, not only is the size of the cavity important in determining binding interactions, but the interaction of the polar regions of the guest molecule with the CD hydroxyl groups may be of importance.

The interior of cyclodextrin has been shown to behave as a nonpolar environment. Evidence is given by researchers comparing the spectral characteristics of 4-tert-butylphenol in an α-CD solution to the spectrum in the apolar solvent dioxane (74). In addition, the UV spectra of 1,4-dimethoxybenzene in 0.1 M aqueous α-CD was shown to be very close to the spectrum in cyclohexane (75). Fluorescence spectroscopy has also been used to conclude that the environment inside the CD cavity much more closely resembles a hydrophobic solvent than the aqueous medium in which CD is most often studied (73, 76-77). Sufficient evidence exists to conclude

that the nonpolar environment of the cyclodextrin cavity differs significantly from the polar environment of the aqueous solvent. The CD has a rigid structure so, when in aqueous solution, water molecules will enter the structure and be held until replaced by a more suitable, less polar or non-polar, guest molecule or molecules.

One of the most active areas of research involving cyclodextrin binding is the use of cyclodextrins in drug delivery by the pharmaceutical industry (70). The solubility of a drug in fats or in blood may be effectively altered by including it into a CD cavity. Other applications involve the use of CDs to prolong the slow release of perfume compounds for the cosmetic and toiletry industries, and as stabilizers for food flavors (69). Complexes with pesticides could allow the time-controlled release of active agents in agricultural applications (69, 72). Many other examples of industrial and chemical applications of cyclodextrin complexes can be found in references 69-72. Many forms of cyclodextrins are approved in many countries as consumables for food and pharmacy industries. Szejtli (70) predicts that one particular cyclodextrin derivative (hydroxypropyl-β–CD) will be produced for pharmaceutical applications on the scale of 100 ton/year by the year 2000. A World Wide Web search for cyclodextrin information returns literally hundreds of pages devoted to the various aspects of cyclodextrin investigation and application.

In the present work, the formation of cyclodextrin-cationic surfactant inclusion complexes is of interest. The non-polar tail of a surfactant molecule such as CTAB (cetyltrimethylammonium bromide) may permit it to bind within the nonpolar cavity of a cyclodextrin molecule as illustrated in Figure 1.2. The formation of a

stable complex implies an equilibrium between the bound and unbound species. The effectiveness of the CD at binding any compound is determined by the solubility of the compound in the matrix outside the CD cavity, the van der Waals forces within the cavity, and possible hydrogen bonding between the bound species and the cyclodextrin rim hydroxyl groups.

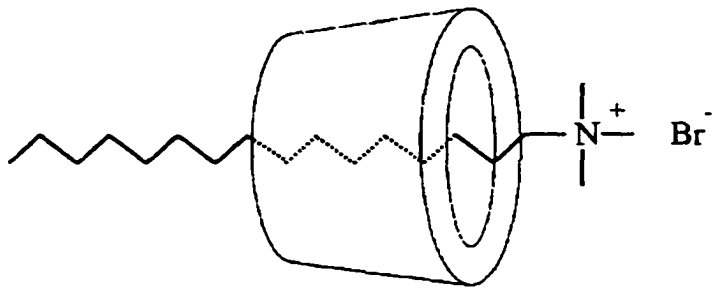

Figure 1.2. Illustration of an inclusion complex between a cyclodextrin and CTAB.

Given that the van der Waals (cross sectional) radius of the surfactant is such that it fits into the cavity of the CD, the polarity of the guest molecule will be an important factor determining the extent of complex formation for the linear *n*-alkyl cationic surfactants used in the present study. The cationic surfactants consist of a linear hydrophobic tail (C12, C14 and C16) and an ionic head group ($-N(CH_3)_3^+$). The non-polar tail is expected to be the most significant component in determining the binding strength of the surfactant with CD.

The stoichiometry of the linear *n*-alkyl surfactant complexes may be described as 1:1, 1:2 or 2:1 in S:CD, the ratio of surfactant to cyclodextrin in the complex (also see Figure 1.16 in the Results and Discussion section). The convention of indicating

cyclodextrin as CD and surfactant as S will be adopted for simplicity, particularly in describing the equilibrium model in the discussion section. The ability to form such surfactant-CD complexes is expected to depend on the length of the hydrocarbon tail, which should affect how well it fits into the CD cavity.

How the Surfactant Sensitive Electrode Works

The sensitivity of the surfactant electrode is thought to occur by either or both of two mechanisms. The membrane (described in detail in the experimental section of this chapter) was made sensitive by impregnating a flexible polyvinylchloride (PVC) substrate with an insoluble complex. This "active complex" consisted of the cationic surfactant of interest, with an anionic surfactant. The cationic surfactants being investigated were the linear *n*-alkyl derivatives (C12, C14 and C16) of trimethylammonium bromide. As a mater of convenience sodium dodecyl sulfate was used as the counterion for these studies. In the membrane the complex (shown here)

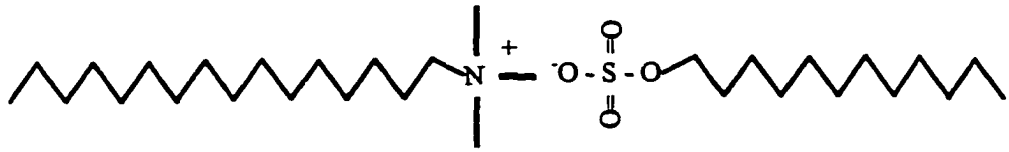

is of course held within the body of the membrane but, more importantly, it is also present at the surface.

The commonly accepted cause for a potential across the membrane boundary is attributed to the difference between two potentials, V_1 and V_2, at each of the liquid/PVC interfaces (4, 78-80). The potentials at each boundary are represented by

$$V_1 = j_1 + 2.303\frac{RT}{nF}\log\frac{a_1}{a_1'} \quad \text{and} \quad V_2 = j_2 + 2.303\frac{RT}{nF}\log\frac{a_2}{a_2'} \qquad \text{Equations 1.1}$$

where a_1 and a_2 are the activities of the surfactants in the solutions on either side of the membrane and a_1' and a_2' are the activities of the surfactant held at sites at the surface in the membrane. If the same number of sites is available for binding on both sides of the membrane then the constants j_1 and j_2 will be identical. Therefore, the boundary potential can be expressed as

$$E_b = V_1 - V_2 = 2.303\frac{RT}{nF}\log\frac{a_1}{a_2} \qquad \text{Equation 1.2}$$

Moreover, since the concentration on one side of the membrane, the filling solution, is constant this equation can be expressed as

$$E_b = I + 2.303\frac{RT}{nF}\log a_1 \qquad \text{Equation 1.3}$$

where I is simply a constant. For a system that satisfies "Nernstian" behavior a plot of measured potential vs. surfactant concentration should yield a slope of 59.1 millivolts per decade, assuming an activity coefficient of one.

Figure 1.3 illustrates how a mechanism of ion equilibration might occur with the complex at the surfaces of the membrane. Here, the charge on either surface would depend on the solubility product, K_{sp}, of the active complex. To allow this

mechanism to occur, the active complex is impregnated into the PVC membrane such that it is distributed homogeneously throughout the membrane. At the membrane surface, some of the active complex would be extending out of the PVC so part of the molecules are exposed to the solutions on both sides of the membrane, as illustrated in the Figure. On either side, an equilibrium will exist between one ion of the active complex, and the counter ion which would remain in the substrate. This equilibrium will be especially affected by the concentration of other molecules in the solutions that might be capable interacting similarly with the active complex. If there are no other ionic species similar to the added free cationic surfactant in solution, the charge at the surface should only be determined by the concentration of that surfactant.

Figure 1.4 illustrates a second possible mechanism of how a charge difference might occur even without active complex in the membrane. In the second mechanism, the charge difference across the membrane surface would be caused by the adsorption of the hydrocarbon tail of the surfactant. Since adsorption coverage should be proportional to solution concentration, the potential difference across the membrane would be a function of concentration on either side of the membrane. Although cursory experiments indicated that the membrane without active complex does respond to varying concentration of cationic surfactant, results were not reliably reproducible. For the intent of the present work, the electrode construction with the active complex was used exclusively.

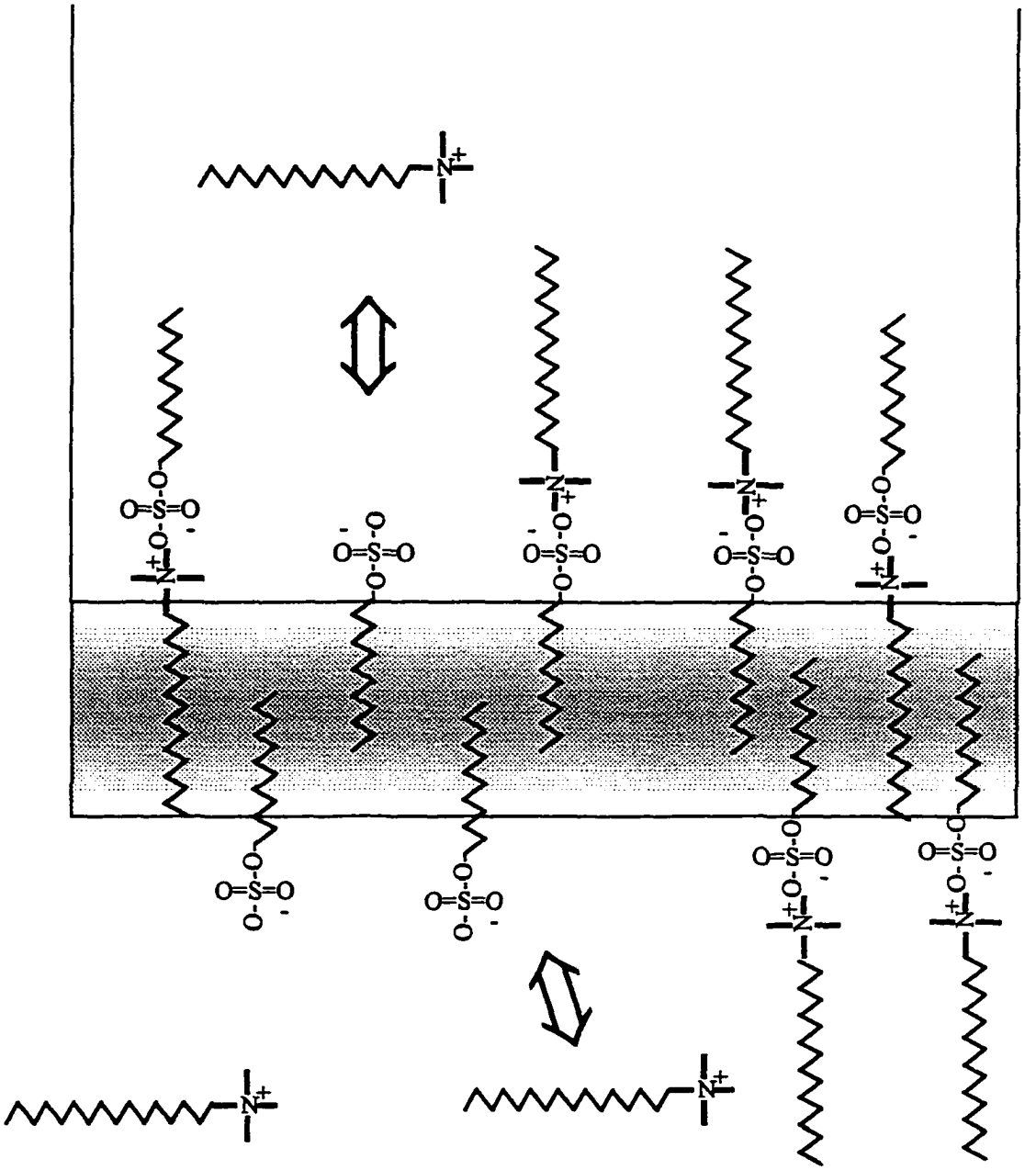

Figure 1.3. The K_{sp} dependent mechanism of electrode response.

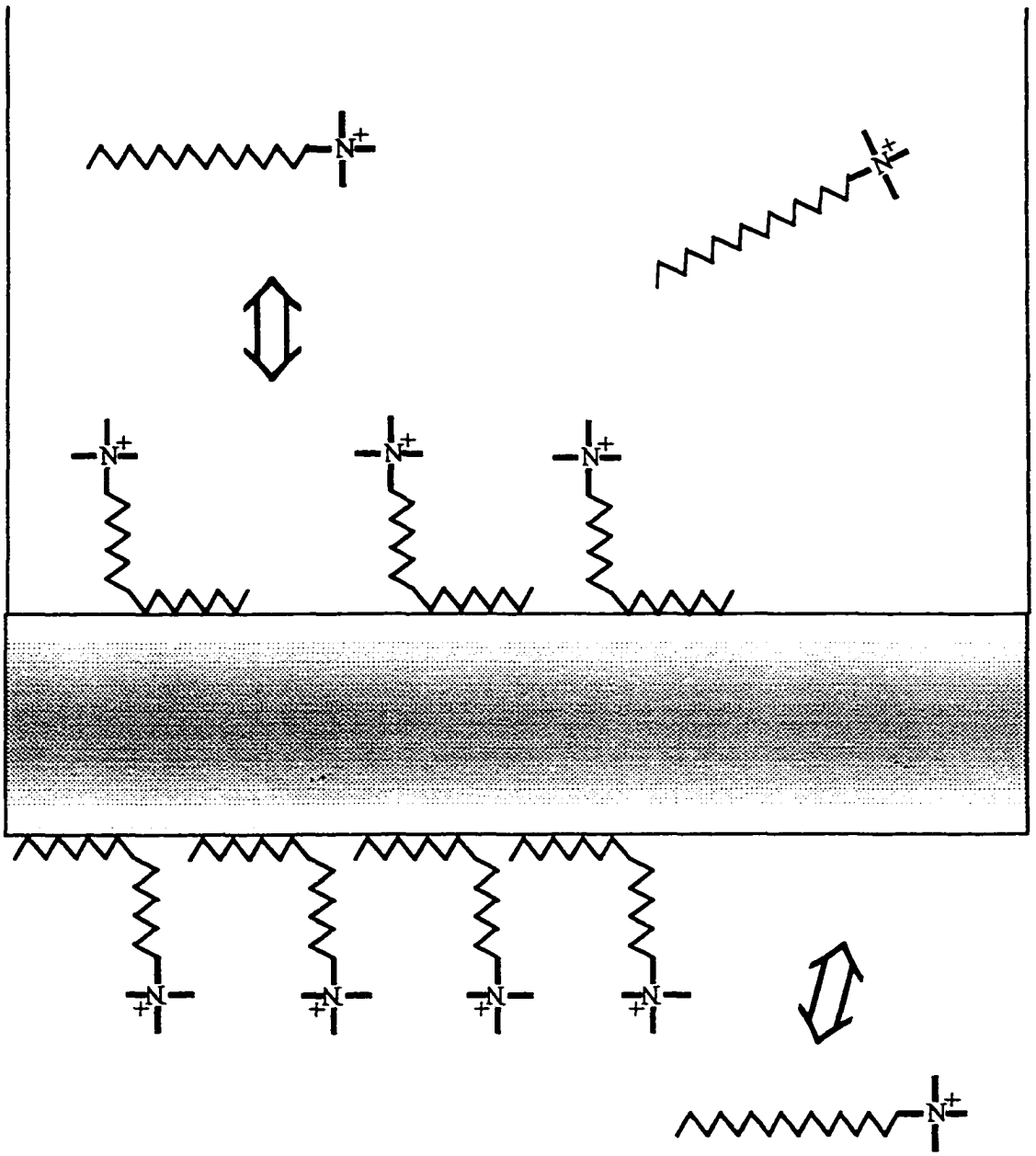

Figure 1.4. The adsorption dependent mechanism of electrode response.

Experimental

As Figure 1.5 illustrates, the surfactant sensitive electrode was made by attaching a polyvinylchloride (PVC) membrane to the end of a body of PVC pipe. Membranes were made by dissolving approximately 0.35 g PVC powder (Aldrich Cat# 34,675-6, High Molecular Weight), 0.80 g dioctylpthalate (Aldrich, 99%) and 0.01 g active complex in approximately 50 mL of tetrahydrofuran, (THF, Aldrich, HPLC Grade). This solution was poured into a 10 cm Petri dish and covered with filter paper to slow the evaporation of THF. The THF was allowed to evaporate overnight in the hood at room temperature (23.0 ± 0.5 °C). This method produced enough membrane material to assemble several electrodes.

To attach the membrane to the PVC pipe, the end of the pipe was dipped for approximately 5 seconds in a shallow volume (generally in a watch plate) of THF. The THF wetted pipe end was contacted firmly with the membrane material (still in the Petri dish) and allowed to stand upright overnight to allow the THF to evaporate. The membrane was trimmed with a razor blade around the edges of the pipe's end.

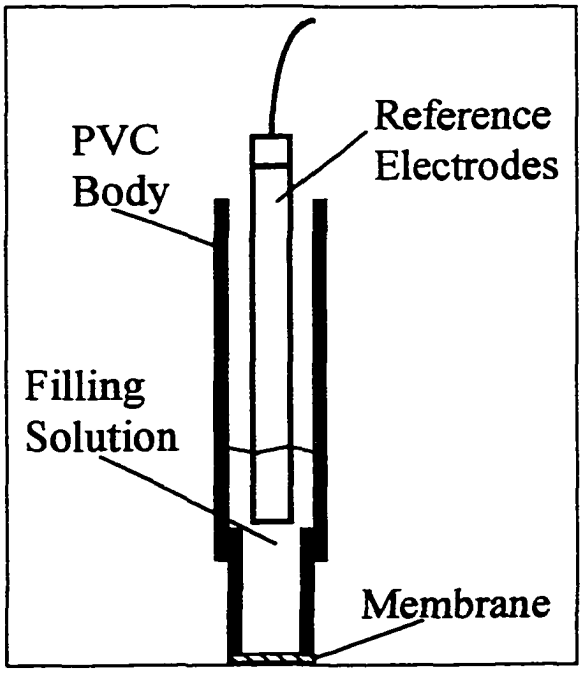

Figure 1.5. Surfactant Sensitive Electrode construction.

The body of the surfactant electrode was constructed using standard white PVC pipe from Ace Hardware. Initial construction was with 3/4 inch outer diameter pipe since the inner diameter (5/8 inch) accommodated the reference electrodes, required for potential measurement. However, it was found that the membrane was so elastic that when filling solution was added the membrane bulged excessively. By using 7/8 inch outer diameter pipe (5/8 inch inner diameter) as an extension of the 3/4 inch outer diameter pipe, (see Figure 1.5) the problem with the bulging membrane was reduced and the reference electrode could still be accommodated in the upper portion of the electrode body.

All voltage readings were made using a FLUKE 8050A Digital Multimeter. The reference electrodes were either $Ag^{+}/AgCl$ or Calomel (Hg^{2+}/Hg_2Cl_2). The general configuration illustrated in Figure 1.6 was always used with one of the matching reference electrodes immersed in a filling solution in the PVC electrode. A small Teflon stirrer bar was used and the test solution was continuously stirred.

The PVC electrode filling solution was 0.01 M NaCl (Mallinkrodt, 99.9%), and 0.1 mM cetyltrimethylammonium bromide (CTAB or hexadecyl-trimethylammonium bromide, Sigma, 99%), or the ionic surfactant to be determined. The other two surfactants used in this study were myristyltrimethylammonium bromide (MTAB or tetradecyltrimethylammonium bromide, Aldrich, 99%) and dodecyltrimethylammonium bromide (DDTAB, Aldrich 99%). The term trimethylammonium bromides or TABs may be used to refer to these compounds in general.

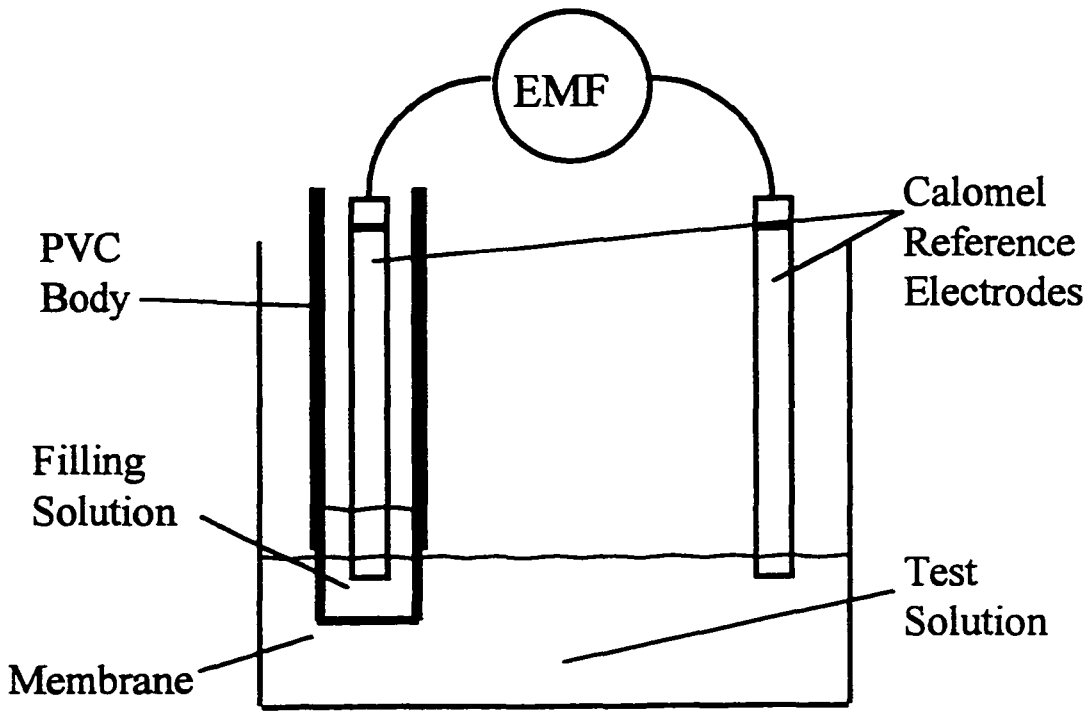

Figure 1.6. Configuration of system used for electrode measurements.

In all binding experiments, the test solution was maintained at 0.01 M NaCl concentration as the concentration of a TAB was gradually increased by adding a concentrated stock solution that was also 0.01 M in NaCl. To conduct a typical titration, two stock solutions were prepared. The first stock solution contained a fixed concentration of cationic surfactant about 10 to 20 times more concentrated than the CMC (e.g. 20 mM TAB). This solution was added serially to an initial volume of 0.01 M NaCl solution in the test beaker. After each serial aliquot, a voltage reading was taken. Aliquots were made over the linear part of the concentration/mV curve but the concentration was not allowed to exceed the CMC. The resulting data were used to determine a calibration curve that allowed calculation of surfactant monomer concentrations. Table 1.5 and Figure 1.9 are the calibration data for each CD-surfactant binding measurement.

A second stock solution, of ~10 mM cyclodextrin (and 0.01 M NaCl), was added serially after the last aliquot of surfactant had been added. A voltage reading was also made after each CD aliquot. Figures 1.10 – 1.12 show the shapes of the titration curves, as raw millivolt readings vs. concentration of surfactant. Figures 1.13 – 1.15 show the titration curves as free surfactant monomer, $[surfactant]_{free}$, vs the total cyclodextrin added, $[CD]_{total}$. The data for those plots are given in Tables 1.6 – 1.14. In those tables, the total surfactant concentration is decreasing slowly due to the dilution effect of adding the cyclodextrin solution. It was important to keep track of total concentrations since these values were required in fitting the data to the equilibrium model. The last column in each of the Tables (1.6 – 1.14) is the

concentration of free monomer determined using the millivolt readings in the previous column and the slope and intercept of the calibration curve (Table 1.5). The abbreviations CTAB, MTAB and DDTAB stand for cetyl-, myristyl- and dodecyl-trimethylammonium bromide or the C16, C14 and C12 *n*-alkyl analogs respectively.

Each titration required from 15 to 45 minutes to complete. A period of one minute was typically required for the mV reading to equilibrate between each aliquot. This equilibration time was sometimes longer (~3 minutes) at significantly lower surfactant concentration.

The SSE was also used to determine the critical micelle concentration for the three cationic surfactants. To demonstrate the usefulness of the electrode as a tool to measure CMCs, it was illustrative to conduct some measurements without added salt. Figure 1.7, a plot of millivolt vs. [TAB], is indicative of the type of data obtained as the surfactant concentration increased past the CMC with no added salt.

The lifetime of the SSEs was not determined during the course of these experiments. Over a period of approximately three months a single electrode was used for most of the measurements made for the work reported here and for other experiments. No wear was visibly detected on the electrode membrane. Indeed, the electrode membranes look as clear over a year later as they did when they were first cast. It was determined that it was *not* necessary to make a new electrode for each of the three surfactants studied. Instead, both sides of the electrode membrane were soaked in a concentrated surfactant solution (about 10 times the CMC, with 0.01 M NaCl) of a given surfactant, overnight, prior to being used. Both sides of the

electrode were rinsed with the appropriate filling solution, then allowed to stand in that solution for at least an hour before use. The model presented in the discussion section pertaining to how the electrode works provides the argument for using this technique.

Results and Discussion

Critical Micelle Concentration Determinations

The critical micelle concentration (CMC) for each cationic surfactant was determined with the SSE following the procedure described in the experimental section. For these CMC measurements, no sodium chloride was added to the solutions. Figure 1.7 and Tables 1.2-1.4 show typical data obtained for CMC titrations. The results for each surfactant were analyzed by plotting data as E (mV) vs log(surfactant concentration) on expanded scales (on individual graphs not shown here), drawing straight lines through the two linear portions of the graph, and marking the intersection of the lines as the CMC. Since the CMC values are determined graphically, the error limits are only estimated. Values for CTAB, MTAB, and DDTAB were determined to be 0.81 ± 0.02 mM, 3.6 ± 0.1 mM, and 14.5 ± 0.5 mM respectively. The agreement with literature values was very good. Mukerjee and Mysels (81) give 0.8 mM, 3.5 mM, and 14.0 mM for CTAB, MTAB, and DDTAB respectively as determined by surface tension measurements.

In each of the measurements (Figure 1.7), after the CMC is reached, the voltage value begins to decrease indicating a decrease in the surfactant monomer activity. This at first seems contrary to the concept that the monomer activity should remain constant once the CMC is reached. Evans et. al. (10) used SSE and ISE to study solutions of decyltrimethylammonium bromide (the C10 *n*-alkyl analog of the TAB surfactants studied here). They demonstrate, with very significant data (Figure 1.8), for the SSE measurement of surfactant monomer and ISE measurement of the counterion that although the surfactant monomer activity does decrease, there is a concomitant increase in counterion activity. They conclude that the surfactant activity, $a_{surfactant} = \gamma_{\pm}^2$ [surfactant][counterion], expressed in terms of the mean activity coefficient ($\gamma_{\pm}$), is nearly constant above the CMC. This evidence shows that the decrease in surfactant monomer activity is a result of most of the surfactant being used to form micelles with a diffuse layer of counterion around the micelle. Ion repulsion prevents the diffuse layer from completely balancing the charge of the cations. Therefore, the "free" bromide ion activity should be increasing as the cationic surfactant monomer activity decreases. Evans et. al. also demonstrated the same micellar effect on sodium counterion measurements for the anionic surfactant sodium dodecylsulfate.

Table 1.2. CMC Determination of CTAB.

[CTAB] mM	mV
0.005	-60.0
0.01	-50.0
0.05	-25.0
0.1	-11.0
0.25	7.0
0.5	22.0
0.75	29.0
1	31.5
1.5	30.5
2	29.5
2.5	28.5
3	27.5
5	24.5

Table 1.3. CMC Determination of MTAB.

[MTAB] mM	mV
0.196	-32.0
0.389	-21.8
0.578	-15.2
0.763	-10.8
0.945	-7.2
1.124	-4.5
1.299	-2.2
1.470	-0.2
1.639	1.5
1.805	3.0
2.128	5.7
2.439	8.0
2.740	10.0
3.030	11.9
3.311	13.6
3.846	14.5
4.348	14.4
4.819	14.3
5.263	14.1
5.681	14.0
6.631	13.6
7.462	13.3

Table 1.4. CMC Determination of DDTAB.

[DDTAB] mM	mV
10.735	-5.1
11.633	-4.0
12.373	-2.9
12.992	-2.1
13.518	-1.5
13.971	-0.9
14.365	-0.5
14.710	-0.4
15.016	-0.4
15.288	-0.5

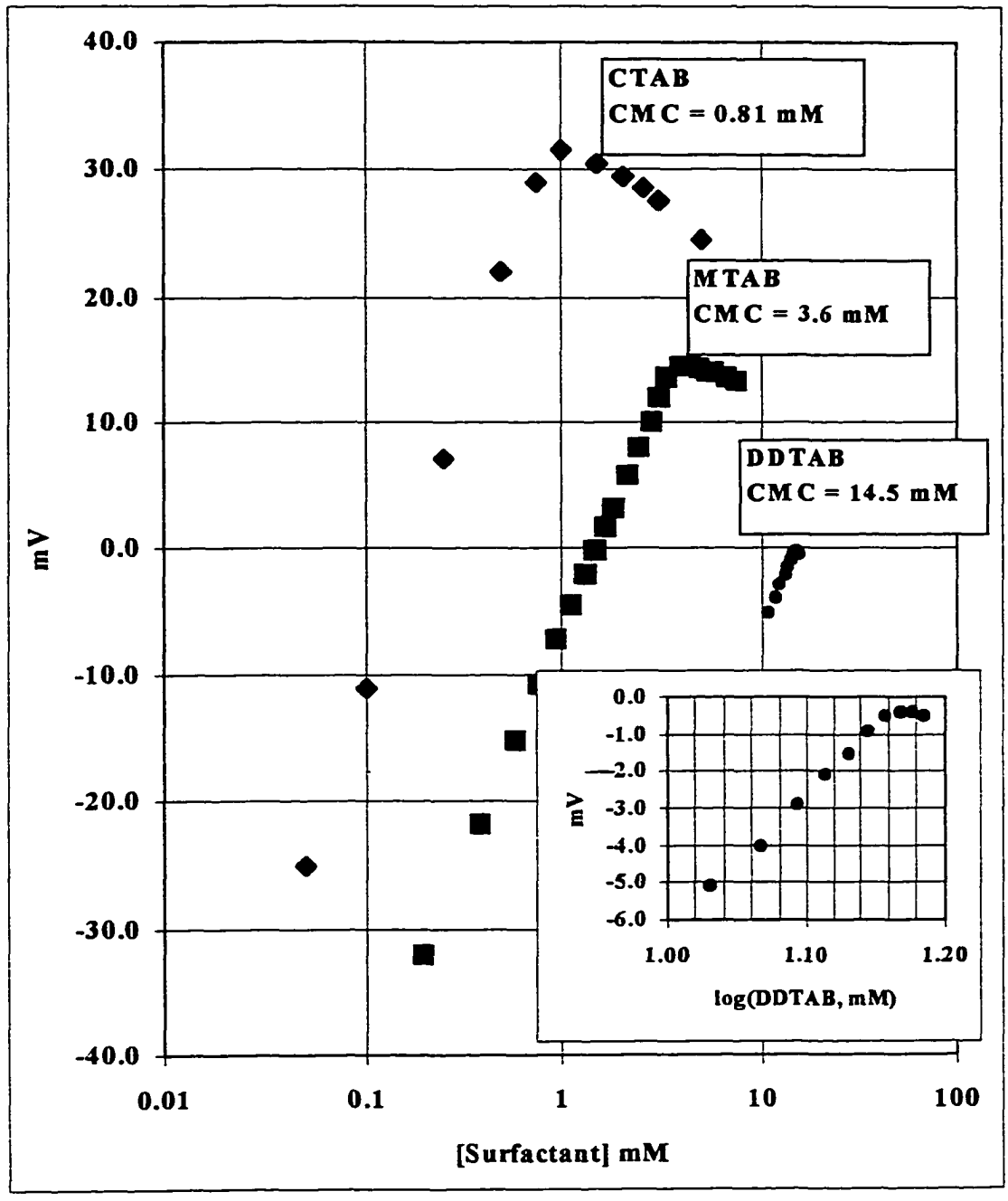

Figure 1.7. CMC determination of CTAB, MTAB and DDTAB. Measurements were made without added NaCl. The inset graph is a scale expansion of the DDTAB plot (on a linear scale).

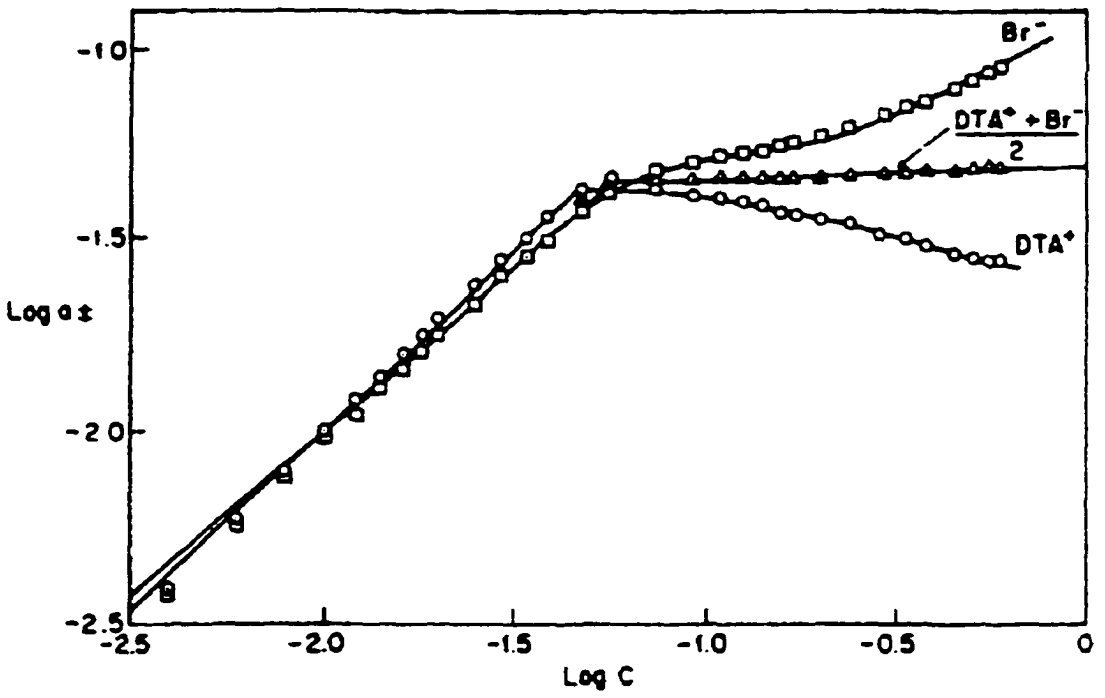

Figure 1.8. Surfactant counterion activity relative to surfactant activity. Data from Evans et. al. demonstrates the concomitant increase in counterion activity as the decyltrimethylammonium monomer is taken up in the micelles after the CMC is reached at ~50 mM total surfactant (10).

Cyclodextrin-Surfactant Binding Determination

The following equilibria were considered for the binding of the surfactants with cyclodextrin. The model includes the formation of complexes with 1:1, 1:2 and 2:1 CD:surfactant stoichiometries.

$$CD + S \Leftrightarrow CDS \qquad K_1 = \frac{[CDS]}{[CD][S]} \qquad \text{Equation 1.4a}$$

$$CDS + S \Leftrightarrow CDS_2 \qquad K_2 = \frac{[CDS_2]}{[CDS][S]} \qquad \text{Equation 1.4b}$$

$$CD + CDS \Leftrightarrow CD_2S \qquad K_3 = \frac{[CD_2S]}{[CD][CDS]} \qquad \text{Equation 1.4c}$$

Here, [S] and [CD] represent the equilibrium concentration of the unbound surfactant and cyclodextrin, respectively. Combining the appropriate equilibrium and the mass balance for total cyclodextrin and total surfactant leads to the following expressions,

$$CD_{total} = [CD] + [CDS] + [CDS_2] + 2[CD_2S]$$

$$CD_{total} = [CD] + K_1[CD][S] + K_1K_2[CD][S]^2 + 2K_1K_3[CD]^2[S] \qquad \text{Equation 1.5}$$

and

$$S_{total} = [S] + [CDS] + 2[CDS_2] + [CD_2S]$$

$$S_{total} = [S] + K_1[CD][S] + 2K_1K_2[CD][S]^2 + K_1K_3[CD]^2[S] \qquad \text{Equation 1.6}$$

Two assumptions are made to apply this equilibrium model: (a) there is no association between CD molecules, and (b) the salt does not interfere with electrode

measurements. Evidence for (b) is given by experiments involving varying β-CD concentration and varying NaCl concentration while making electrode measurements without surfactant present. There was no systematic change in electrode response when these concentrations were varied. Wyn-Jones (81-84) has made similar observations concerning electrode measurements of CD solutions. (Nonionic surfactants, while not expected to be directly measurable by the SSE, did cause significant change in the electrode response in the presence of cationic surfactant. For this reason, the SSE could not be used to measure cationoic/nonionic mixed micelle formation discussed in Chapter 2.)

Solution of the mass balance equations above was accomplished using a least-squares program with K_1, K_2 and K_3, together or independently, as adjustable parameters. For each experiment, the total cyclodextrin concentration was always known, as was the total surfactant concentration since the concentration of the stock solutions was known (as prepared) and dilution was accounted for by keeping track of volume added. The surfactant monomer concentration (free surfactant) was determined from a calibration curve of the SSE, and continuous measurement of the EMF.

The calibration curve for the SSE was determined in the course of each experiment. The linear portion of the titration curve, during the addition of surfactant, was fitted to a "Nernstian" equation of the following form:

$$E = E_{ref} + 2.303\frac{RT}{nF}\log[\text{surfactant}] \qquad \text{Equation 1.7}$$

This equation is similar to equation 1.3. The reference voltage, E_{ref}, was the intercept of the calibration curve of the measured potential, E, plotted against log[surfactant]. The magnitude and sign of E_{ref} is dependent on the concentration of surfactant in the filling solution used in the PVC electrode and the ionic strength of the solution. For a true Nernst response, the electrode calibration should yield a slope of $2.303\frac{RT}{nF}$ or approximately 59 mV at 25°C. However, in practice this value was not achieved. The slope depended on the membrane thickness and possibly the amount of and type of active complex used to make the membrane. Typical calibrations provided slopes in the range of 35 to 45 millivolts (Table 1.5). Figure 1.9 shows the calibration curves used for each experiment. Since the slope and intercept were different, even for the same surfactant, a calibration is required at the beginning of each experiment. This presented no difficulty since some initial surfactant concentration below the CMC was required before adding cyclodextrin. To achieve this, a relatively high known concentration of surfactant (10-20 mM, e.g.) was added in aliquots and the resulting linear data provided the calibration. (This built up the surfactant concentration in the test solution at the beginning of each CD binding experiment.) Cyclodextrin aliquots were added and the resulting millivolt response was recorded. Figures 1.10 - 1.12 are the response curves showing the effect of added cyclodextrin. As cyclodextrin was added, the electrode response (mV) decreases since the free surfactant is gradually taken up by the cyclodextrin cavity.

Fitting experimental data to the equilibrium model was carried out on a personal computer with the least squares program (LLSQ, developed by Professor

Christian) written and compiled in True BASIC. The program permits the inclusion or removal of any step of the equilibria from the model. Thus, fitting was carried out for each permutation of the model (different combinations of K_1, K_2 and K_3). The combination of equilibria that provided the best fit, based on the root mean square deviation (RMSD), was determined to be the best model. Values of K_1-K_3 could not be found which would provide an acceptable fit of data for most of the systems. Typically, the best-fit line was determined to fall consistently below the experimental data, especially at lower cyclodextrin concentrations (higher free surfactant concentrations). It became apparent that the linear fit of E(mV) vs. log[free surfactant] could not apply in the presence of added CD, where one or more CD:surfactant complexes may form which might interfere with electrode response. An additional dimensionless parameter, K_4, was introduced due to the inability, initially, of the K_1-K_3 model to adequately fit the data. Therefore, equation 1.7 would take the following form:

$$E = E_{ref} + 2.303\frac{RT}{nF}\log\{[\text{surfactant}] \times K_4\} \qquad \text{Equation 1.8}$$

In the form of equation 1.8, the fitting parameter K_4 acts as a multiplicative constant in the log[surfactant] term. Equation 1.8 can easily be rearranged to make it obvious that K_4 simply acts as a linear offset for the intercept of the calibration curves. A value of K_4 greater than 1 will result in a positive offset of the intercept; a value less than 1 will result in a negative offset; and a value equal to 1 results in zero offset. Since the values determined for K_4 are greater than one (or equal to one within the standard error) this parameter accounts for an additional response of the electrode,

probably due to a CD:surfactant complex at the membrane surface. This additional response may reach a near-saturation effect at low CD concentration and then level off at larger CD concentration. The calibrations curves were of course determined in absence of cyclodextrin and therefore only represent the response of the electrode to the surfactant. It is conceivable, and apparent from the necessity for the K_4 parameter, that a CD:surfactant complex similar to the one illustrated in Figure 1.2 could also cause a response in the electrode signal.

Evidence for the interference of CD:surfactant complexes may also be drawn from consideration of the values of the intercepts of the calibration curves. From the results in Table 1.5 it is apparent that the intercepts of the calibrations depend on the relative size (tail length or mobility) of the cationic surfactant. The intercepts of the calibration curves are larger (more positive) as the tail length of the surfactant increases from the C12 tail (average DDTAB intercept = –43.9 mV) to C14 tail (average MTAB intercept = -1 mV) to C16 tail (average CTAB intercept = 42mV). Since the K_4 values determined for each system (Table 1.15) are generally greater than or 1.0 the formation of a complex also corresponds to a larger or more positive intercept, in accordance with equation 1.8.

Table 1.15 gives the resulting values of the fitted constants corresponding to each system. Data was only fitted over the [Surfactant] range that had a linear response (constant slope) in the calibration curves in Figure 1.9. Fitted results are shown as solid lines in Figures 1.10-1.12. Although, as shown in Figures 1.10-1.12 (data in Tables 1.6-1.14), electrode response values were usually available outside the

linear response region, the fitted lines in those Figures only cover the mV range of the linear response region.

CD	CTAB		MTAB		DDTAB	
	Slope (mV/decade)	Intercept (mV)	Slope (mV/decade)	Intercept (mV)	Slope (mV/decade)	Intercept (mV)
α	33.385	37.938	36.653	-5.0148	25.639	-45.323
β	40.452	39.615	40.355	1.6487	40.684	-43.477
γ	39.888	49.585	39.982	1.1268	30.546	-42.832

Table 1.5. Calibration curves for CTAB, MTAB and DDTAB determined before each binding experiment. All solutions were prepared with 0.01 M NaCl. Each calibration curve was determined by linear least squares fit to the equation Measured potential = Intercept + slope x log[surfactant].

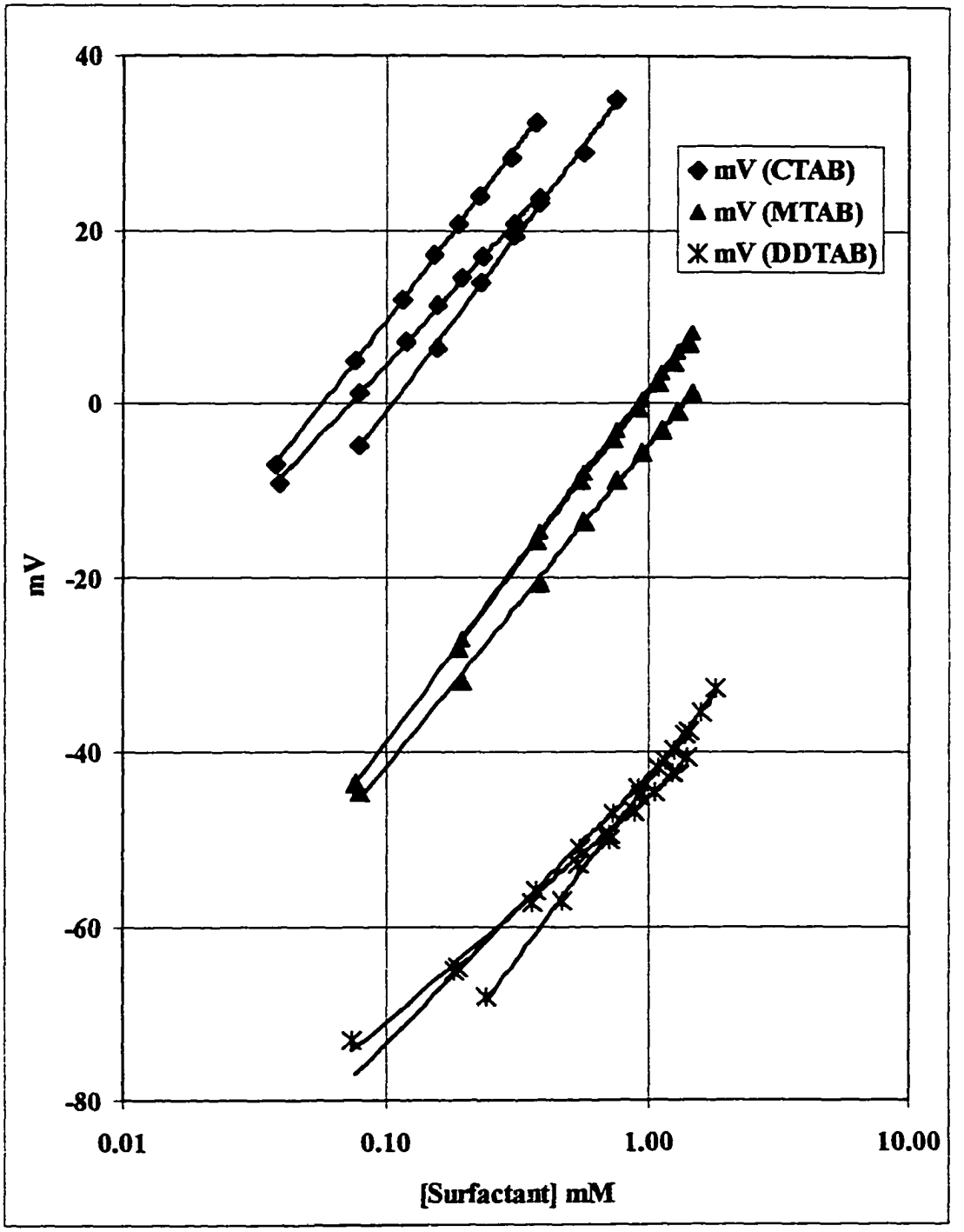

Figure 1.9. Calibration curves used at the beginning of each binding measurement to determine free surfactant concentration. These curves show the linear working range of the electrode with each cationic surfactant used.

Table 1.6. Titration of DDTAB with α-CD.

$[DDTAB]_{tot}$ mM	$[\alpha\text{-CD}]_{tot}$ mM	mV	$[DDTAB]_{free}$ mM
1.374	0.086	-41.6	1.34E+00
1.362	0.170	-42.5	1.25E+00
1.351	0.253	-43.8	1.12E+00
1.339	0.335	-45.1	1.00E+00
1.328	0.415	-46.1	9.23E-01
1.317	0.494	-47.5	8.21E-01
1.307	0.572	-49.1	7.19E-01
1.296	0.648	-50.3	6.51E-01
1.275	0.797	-53.9	4.82E-01
1.255	0.941	-57.7	3.51E-01
1.236	1.081	-61.9	2.48E-01
1.217	1.217	-66.9	1.63E-01
1.199	1.349	-72.0	1.07E-01
1.181	1.476	-77.2	6.92E-02
1.147	1.721	-86.7	3.14E-02
1.115	1.952	-94.2	1.68E-02
1.085	2.170	-100.1	1.03E-02
1.056	2.377	-105.1	6.78E-03
1.029	2.573	-109.3	4.78E-03
0.979	2.936	-116.3	2.67E-03
0.912	3.420	-124.4	1.36E-03
0.819	4.093	-134.1	6.05E-04
0.743	4.641	-140.8	3.46E-04
0.680	5.096	-145.9	2.26E-04
0.626	5.480	-149.9	1.62E-04
0.581	5.808	-153	1.25E-04

Table 1.7. Titration of MTAB with α-CD.

$[MTAB]_{tot}$ mM	$[\alpha\text{-CD}]_{tot}$ mM	mV	$[MTAB]_{free}$ mM
1.455	0.091	0.2	1.39E+00
1.441	0.180	-0.8	1.30E+00
1.429	0.268	-1.9	1.22E+00
1.416	0.354	-3.0	1.13E+00
1.403	0.439	-4.3	1.05E+00
1.391	0.522	-5.6	9.64E-01
1.368	0.684	-8.4	8.08E-01
1.345	0.840	-11.4	6.70E-01
1.322	0.992	-15.0	5.34E-01
1.301	1.138	-19.0	4.15E-01
1.280	1.280	-23.6	3.11E-01
1.260	1.417	-28.6	2.27E-01
1.240	1.550	-33.9	1.63E-01
1.203	1.804	-44.4	8.42E-02
1.168	2.044	-53.7	4.70E-02
1.135	2.269	-61.9	2.81E-02
1.103	2.483	-68.9	1.81E-02
1.074	2.685	-74.9	1.24E-02
1.046	2.876	-80.1	8.94E-03
1.019	3.057	-84.7	6.70E-03
0.994	3.230	-88.9	5.15E-03
0.970	3.394	-92.5	4.10E-03
0.947	3.550	-95.6	3.38E-03
0.904	3.842	-100.9	2.42E-03
0.865	4.108	-105.4	1.82E-03
0.829	4.352	-109.1	1.45E-03
0.796	4.577	-112.3	1.18E-03
0.766	4.785	-115.1	9.92E-04

Table 1.8. Titration of CTAB with α-CD.

$[CTAB]_{tot}$ mM	$[\alpha\text{-CD}]_{tot}$ mM	mV	$[CTAB]_{free}$ mM
0.387	0.039	22.4	3.42E-01
0.385	0.077	20.9	3.09E-01
0.384	0.115	19.3	2.77E-01
0.382	0.153	17.5	2.44E-01
0.381	0.190	15.7	2.16E-01
0.377	0.283	10.5	1.51E-01
0.374	0.374	4.2	9.76E-02
0.370	0.463	-2.7	6.06E-02
0.367	0.550	-9.8	3.72E-02
0.364	0.636	-16.6	2.32E-02
0.360	0.721	-23.0	1.50E-02
0.354	0.885	-33.6	7.20E-03
0.348	1.043	-42.2	3.98E-03
0.342	1.197	-49.3	2.44E-03
0.336	1.345	-55.2	1.62E-03
0.331	1.488	-60.2	1.15E-03
0.325	1.626	-64.5	8.54E-04
0.315	1.890	-71.6	5.24E-04
0.305	2.137	-77.4	3.51E-04
0.296	2.370	-82.1	2.54E-04
0.288	2.590	-86.1	1.93E-04
0.280	2.797	-89.5	1.52E-04
0.265	3.179	-95.2	1.03E-04
0.252	3.522	-99.7	7.54E-05
0.240	3.832	-103.5	5.80E-05
0.229	4.114	-105.2	5.16E-05
0.219	4.372	-108.1	4.22E-05

Table 1.9. Titration of DDTAB with β-CD.

$[DDTAB]_{tot}$ mM	$[\beta\text{–}CD]_{tot}$ mM	mV	$[DDTAB]_{free}$ mM
1.773	0.039	-32.5	1.86E+00
1.766	0.077	-32.8	1.83E+00
1.758	0.115	-33.3	1.78E+00
1.750	0.152	-33.6	1.75E+00
1.742	0.190	-34.1	1.70E+00
1.724	0.282	-35.0	1.62E+00
1.705	0.371	-36.1	1.52E+00
1.670	0.545	-38.4	1.33E+00
1.636	0.712	-40.8	1.16E+00
1.603	0.873	-43.4	1.00E+00
1.571	1.026	-46.3	8.52E-01
1.512	1.317	-53.2	5.77E-01
1.457	1.586	-61.2	3.67E-01
1.406	1.837	-69.3	2.32E-01
1.358	2.070	-76.7	1.53E-01
1.313	2.288	-82.5	1.10E-01
1.272	2.492	-87.2	8.42E-02
1.232	2.684	-90.8	6.87E-02
1.161	3.033	-96.3	5.03E-02
1.097	3.345	-100.5	3.97E-02
1.040	3.624	-103.9	3.27E-02
0.989	3.875	-106.2	2.87E-02
0.942	4.103	-108.3	2.55E-02
0.843	4.588	-112.8	1.98E-02
0.763	4.981	-116.2	1.63E-02

Table 1.10. Titration of MTAB with β-CD.

$[MTAB]_{tot}$ mM	$[\beta\text{–}CD]_{tot}$ mM	mV	$[MTAB]_{free}$ mM
1.455	0.032	7.9	1.43E+00
1.450	0.063	7.6	1.40E+00
1.445	0.094	7.1	1.36E+00
1.440	0.125	6.8	1.34E+00
1.434	0.156	6.4	1.31E+00
1.422	0.232	5.3	1.23E+00
1.409	0.307	4.3	1.16E+00
1.385	0.452	2.0	1.02E+00
1.361	0.593	-0.6	8.80E-01
1.338	0.729	-3.4	7.50E-01
1.316	0.860	-6.4	6.32E-01
1.274	1.110	-14.2	4.05E-01
1.235	1.345	-24.6	2.24E-01
1.198	1.565	-36.6	1.13E-01
1.163	1.773	-46.5	6.41E-02
1.130	1.969	-53.5	4.30E-02
1.099	2.154	-57.4	3.44E-02
1.070	2.330	-61.3	2.76E-02
1.016	2.654	-67.7	1.91E-02
0.967	2.946	-72.6	1.45E-02
0.922	3.212	-76.3	1.17E-02
0.881	3.454	-79.4	9.81E-03
0.844	3.676	-82.1	8.41E-03
0.764	4.157	-87.5	6.18E-03
0.697	4.553	-91.6	4.89E-03

Table 1.11. Titration of CTAB with β-CD.

$[CTAB]_{tot}$ mM	$[\beta\text{–}CD]_{tot}$ mM	mV	$[CTAB]_{free}$ mM
0.749	0.082	34.0	7.26E-01
0.742	0.162	32.6	6.71E-01
0.736	0.240	30.5	5.95E-01
0.729	0.317	28.5	5.31E-01
0.716	0.468	22.7	3.82E-01
0.703	0.613	16.3	2.65E-01
0.691	0.752	6.2	1.49E-01
0.679	0.888	-4.0	8.35E-02
0.668	1.018	-12.6	5.12E-02
0.657	1.145	-18.7	3.62E-02
0.646	1.267	-23.2	2.80E-02
0.636	1.385	-27.0	2.26E-02
0.617	1.611	-32.2	1.68E-02
0.598	1.823	-36.4	1.32E-02
0.581	2.023	-39.8	1.09E-02
0.549	2.390	-45.3	7.96E-03
0.520	2.719	-49.2	6.37E-03
0.495	3.015	-50.5	5.92E-03
0.471	3.284	-53.5	4.99E-03
0.450	3.528	-56.1	4.30E-03
0.431	3.751	-58.4	3.78E-03

Table 1.12. Titration of DDTAB with γ-CD.

$[DDTAB]_{tot}$ mM	$[\gamma\text{-CD}]_{tot}$ mM	mV	$[DDTAB]_{free}$ mM
1.455	0.091	-40.3	1.42E+00
1.442	0.180	-41.1	1.35E+00
1.429	0.268	-41.7	1.29E+00
1.416	0.354	-42.5	1.23E+00
1.391	0.522	-43.7	1.13E+00
1.368	0.684	-44.8	1.05E+00
1.345	0.840	-45.9	9.73E-01
1.322	0.992	-46.9	9.09E-01
1.280	1.280	-48.7	8.04E-01
1.240	1.550	-50.3	7.21E-01
1.203	1.805	-51.6	6.60E-01
1.135	2.270	-39.1	1.55E+00
1.074	2.685	-40.1	1.44E+00
1.019	3.057	-41.2	1.34E+00
0.970	3.394	-42.2	1.25E+00
0.925	3.700	-43.1	1.18E+00
0.884	3.978	-43.9	1.11E+00
0.847	4.233	-44.7	1.06E+00
0.812	4.467	-45.3	1.01E+00
0.766	4.785	-46.3	9.47E-01
0.724	5.068	-47.0	9.03E-01
0.687	5.322	-47.7	8.61E-01

Table 1.13. Titration of MTAB with γ-CD.

$[MTAB]_{tot}$ mM	$[\gamma\text{-CD}]_{tot}$ mM	mV	$[MTAB]_{free}$ mM
1.402	0.088	5.7	1.30E+00
1.390	0.174	4.3	1.20E+00
1.378	0.258	2.9	1.11E+00
1.366	0.342	1.6	1.03E+00
1.343	0.504	-1.0	8.85E-01
1.321	0.661	-3.3	7.75E-01
1.300	0.812	-5.3	6.91E-01
1.279	0.959	-7.1	6.23E-01
1.239	1.239	-10.3	5.18E-01
1.202	1.502	-12.9	4.46E-01
1.167	1.750	-15.1	3.93E-01
1.103	2.205	-18.6	3.21E-01
1.045	2.612	-21.4	2.73E-01
0.993	2.979	-23.6	2.41E-01
0.946	3.311	-25.6	2.15E-01
0.903	3.614	-27.2	1.96E-01
0.864	3.890	-28.7	1.79E-01
0.829	4.143	-30.0	1.67E-01
0.796	4.376	-31.1	1.56E-01
0.751	4.692	-32.7	1.43E-01
0.711	4.975	-34.1	1.32E-01
0.675	5.230	-35.3	1.23E-01
0.642	5.459	-36.4	1.15E-01
0.613	5.668	-37.4	1.09E-01
0.586	5.858	-38.4	1.03E-01

Table 1.14. Titration of CTAB with γ-CD.

$[CTAB]_{tot}$ mM	$[\gamma\text{-CD}]_{tot}$ mM	mV	$[CTAB]_{free}$ mM
0.372	0.093	22.4	2.08E-01
0.368	0.184	20.9	1.91E-01
0.365	0.274	19.3	1.74E-01
0.361	0.361	17.5	1.57E-01
0.355	0.533	15.7	1.41E-01
0.349	0.698	10.5	1.05E-01
0.343	0.857	4.2	7.28E-02
0.337	1.011	-2.7	4.89E-02
0.326	1.305	-9.8	3.24E-02
0.316	1.579	-16.6	2.19E-02
0.306	1.837	-23.0	1.51E-02
0.288	2.308	-33.6	8.21E-03
0.273	2.728	-42.2	5.00E-03
0.259	3.104	-49.3	3.32E-03
0.246	3.443	-55.2	2.36E-03
0.234	3.750	-60.2	1.77E-03
0.224	4.030	-64.5	1.38E-03
0.214	4.286	-71.6	9.16E-04
0.194	4.839	-77.4	6.55E-04
0.176	5.294	-82.1	4.99E-04

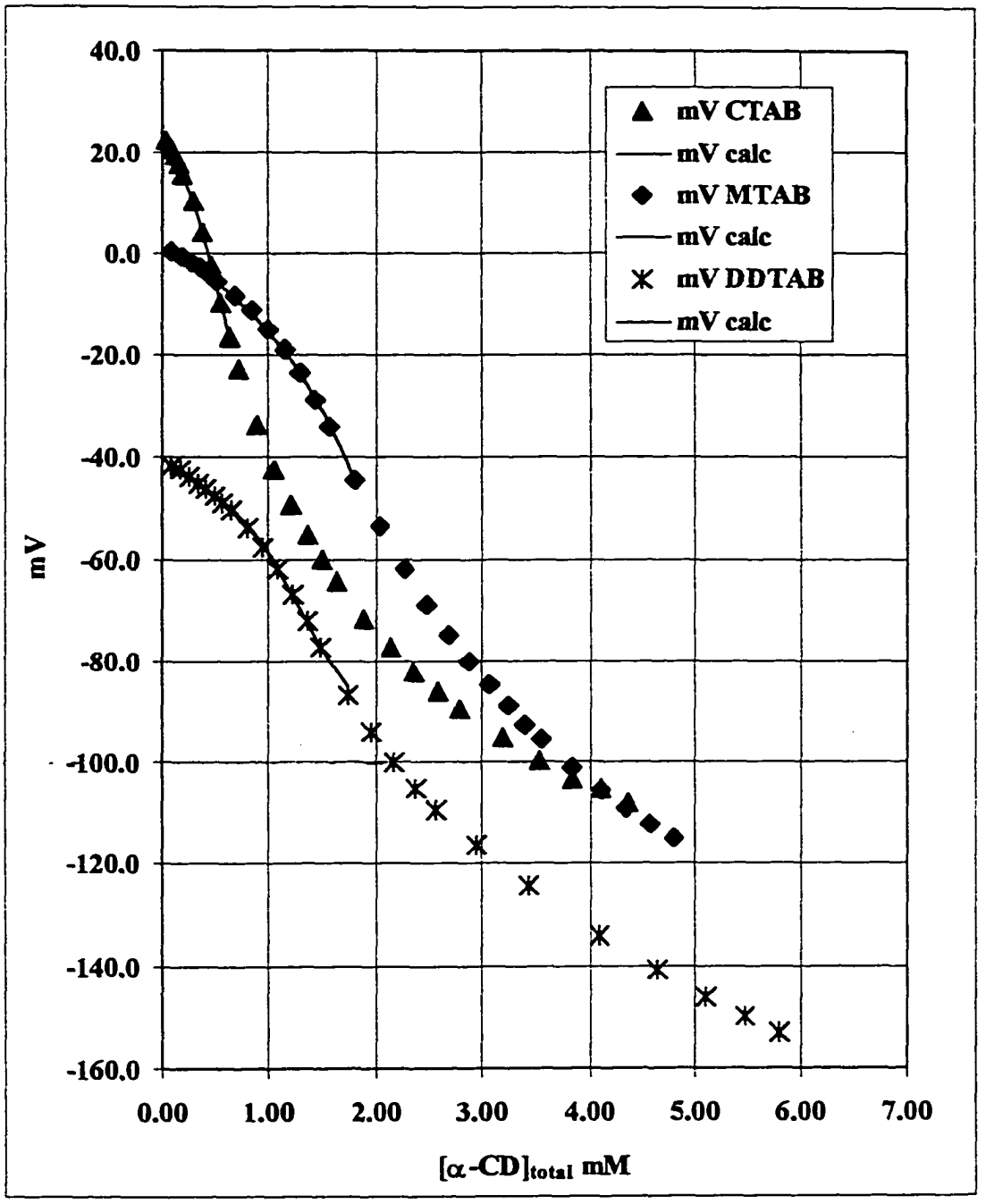

Figure 1.10. Millivolt response as a function of α-CD complexation. All measurements were made in 0.01M NaCl.

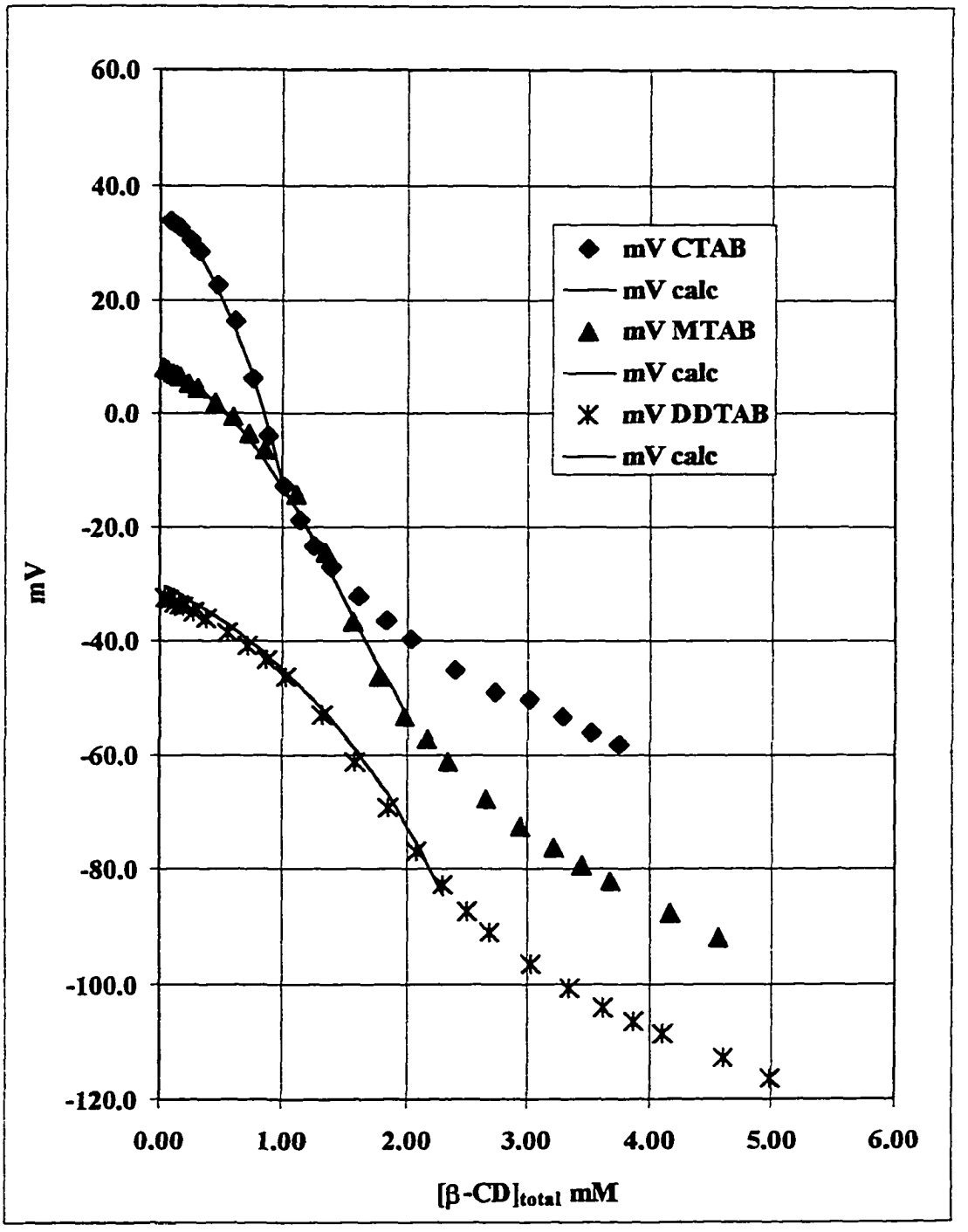

Figure 1.11. Millivolt response as a function of β-CD complexation. All measurements were made in 0.01M NaCl.

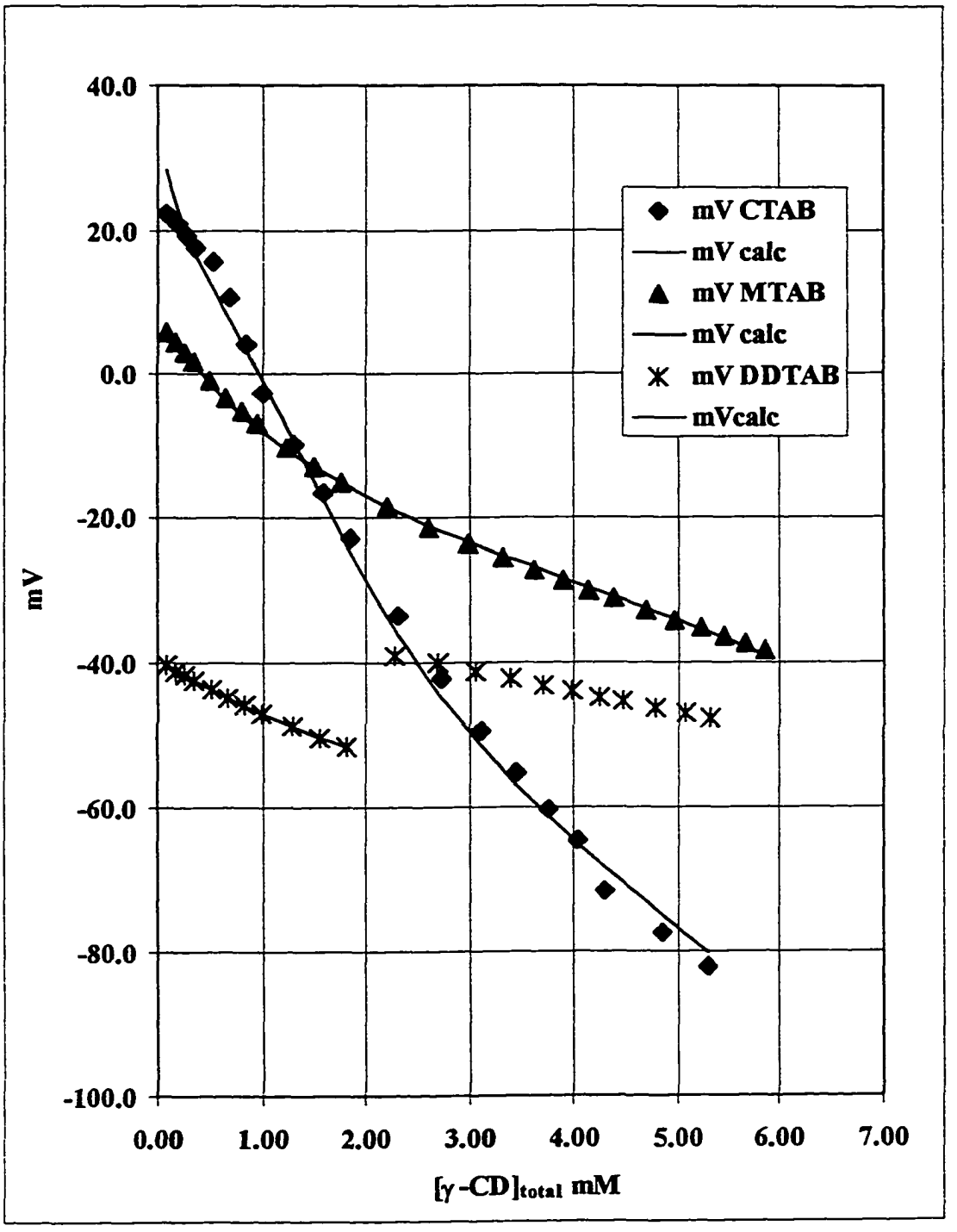

Figure 1.12. Millivolt response as a function of γ-CD complexation. All measurements were made in 0.01M NaCl.

		DDTAB	MTAB	CTAB
α-CD	K_1	64. ± 2.	58. ± 3.	56. ± 1.
	K_2	-	-	-
	K_3	1. ± 0.2	8. ± 4.	6.5 ± 0.4
	K_4	0.99 ± 0.01	1.05 ± 0.01	0.99 ± 0.01
	RMSD	0.4	0.4	0.2
β-CD	K_1	19. ± 3	43. ± 5.	83. ± 3.
	K_2	-	-	-
	K_3	4. ± 2.	3. ± 1.	10. ± 4.
	K_4	1.11 ± 0.01	1.06 ± 0.02	1.16 ± 0.04
	RMSD	0.6	1.1	1.1
γ-CD	K_1	0.39 ± 0.02	0.67 ± 0.02	-
	K_2	0.51 ± 0.03	2.1 ± 0.1	34. ± 4.‡
	K_3	-	-	15. ± 1.‡
	K_4	1.021 ± 0.003	1.04 ± 0.01	1.17
	RMSD	0.01	0.3	3.4

Table 1.15. Stepwise equilibrium constants for the inclusion complexes of DDTAB, MTAB, and CTAB with α–, β–, and γ–cyclodextrin. Concentrations are expressed in mM units; therefore, the equilibrium constants have units of mM^{-1}. The K_4 constant is dimensionless. RMSD is the root mean square deviation in mV units. All measurements were made in 0.01M NaCl. (‡Values for K_2 and K_3 constants cannot be determined independently for the γ-CD/CTAB system, see page 48 for discussion)

Figures 1.13 - 1.15 are plots of the surfactant concentration vs total CD concentration (Tables 1.6 - 1.14) for the α, β and γ cyclodextrins with each of the three cationic surfactants, dodecyltrimethylammonium bromide (DDTAB), tetradecyltrimethylammonium bromide (MTAB) and cetyltrimethylammonium bromide (CTAB). The fitted curve plotted for each data set was the result calculated based on the results of the least-squares fitting program. Total cyclodextrin concentration was known since the aliquot volume, total solution volume, and stock cyclodextrin concentration where known. The value of $[Surfactant]_{free}$ was calculated according to equation 1.8 using the value of K_4 returned by the least-squares program. The values of $[CD]_{total}$ and $[Surfactant]_{free}$ are given in Tables 1.6-1.14.

Although the fitting range may appear small, according to the fitted lines in Figures 1.10-1.12, the plots in the form of $[Surfactant]_{free}$ in Figures 1.13-1.15 make it clear that fitting always covers a region where there is a significant amount of free surfactant available for binding. For example, in Figure 1.12 the fitted line for mV vs. $[\beta\text{-CD}]_{total}$ for MTAB only goes to a $[\beta\text{-CD}]_{total}$ concentration of ~2 mM, although the data set obviously continues to show some type of response (decreasing mV reading) at higher $[\beta\text{-CD}]_{total}$ concentrations. Fitting did not include data at lower mV readings because the calibration curves for CTAB in Figure 1.9 show the linear calibration region for CTAB is between approximately -45mV tc 10 mV. Figure 1.14 shows that this mV region covers a $[CTAB]_{free}$ range from 1.35 to 0.04 mM or the region where 5% to 95% of the MTAB is been available for binding.

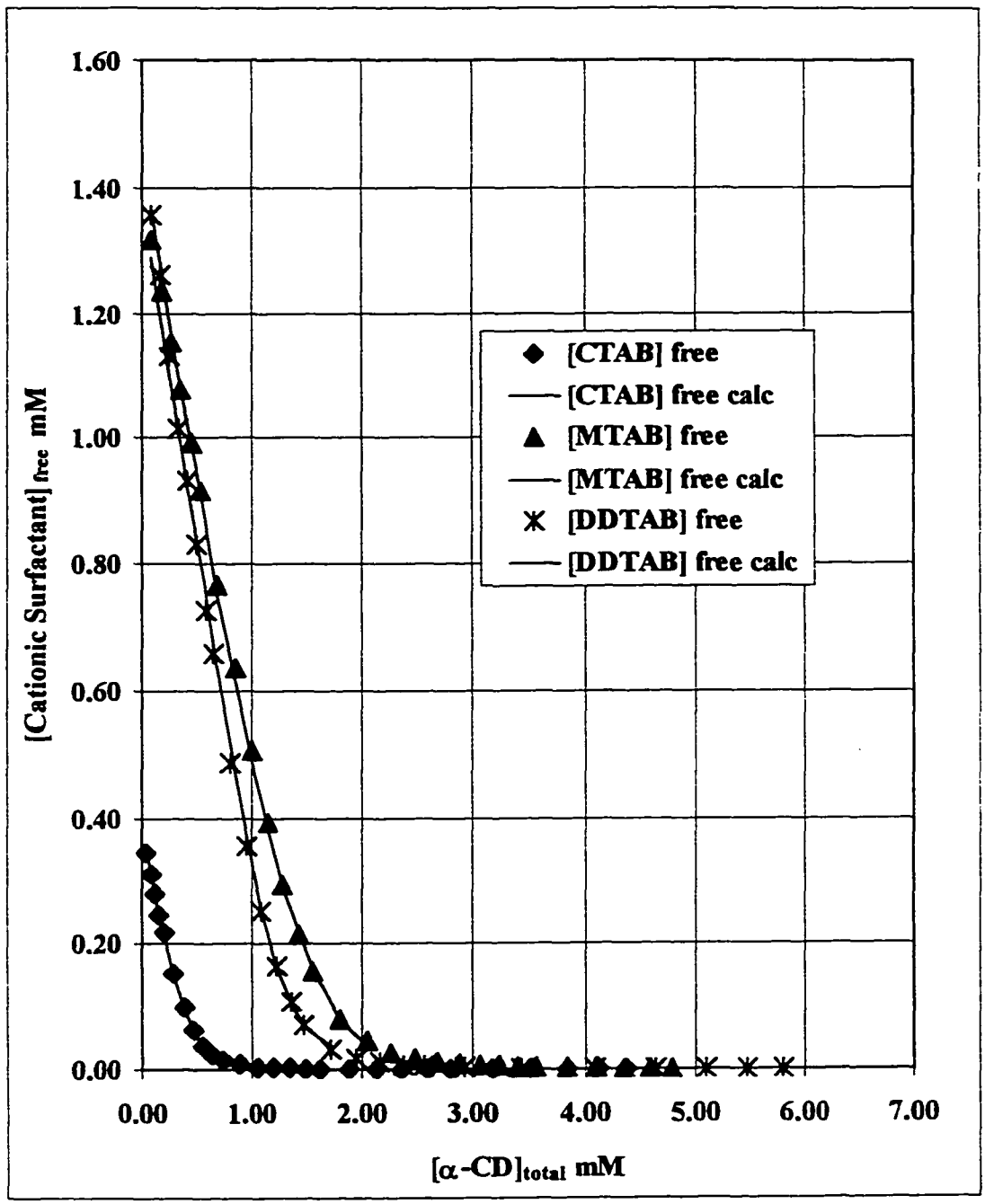

Figure 1.13. Free cationic surfactant concentration as a function of α-CD complexation. All measurements were made in 0.01M NaCl.

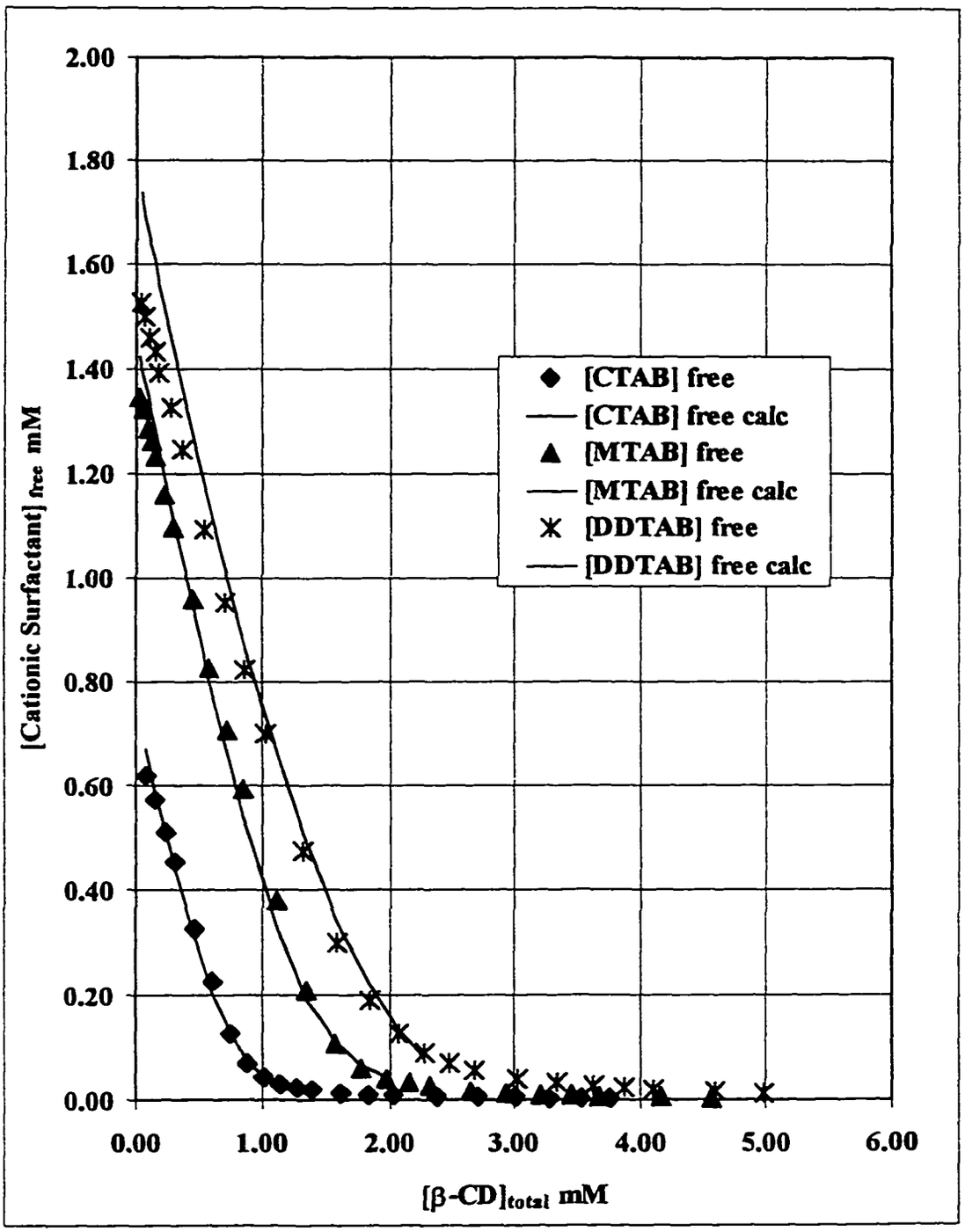

Figure 1.14. Free cationic surfactant concentration as a function of β-CD complexation. All measurements were made in 0.01M NaCl.

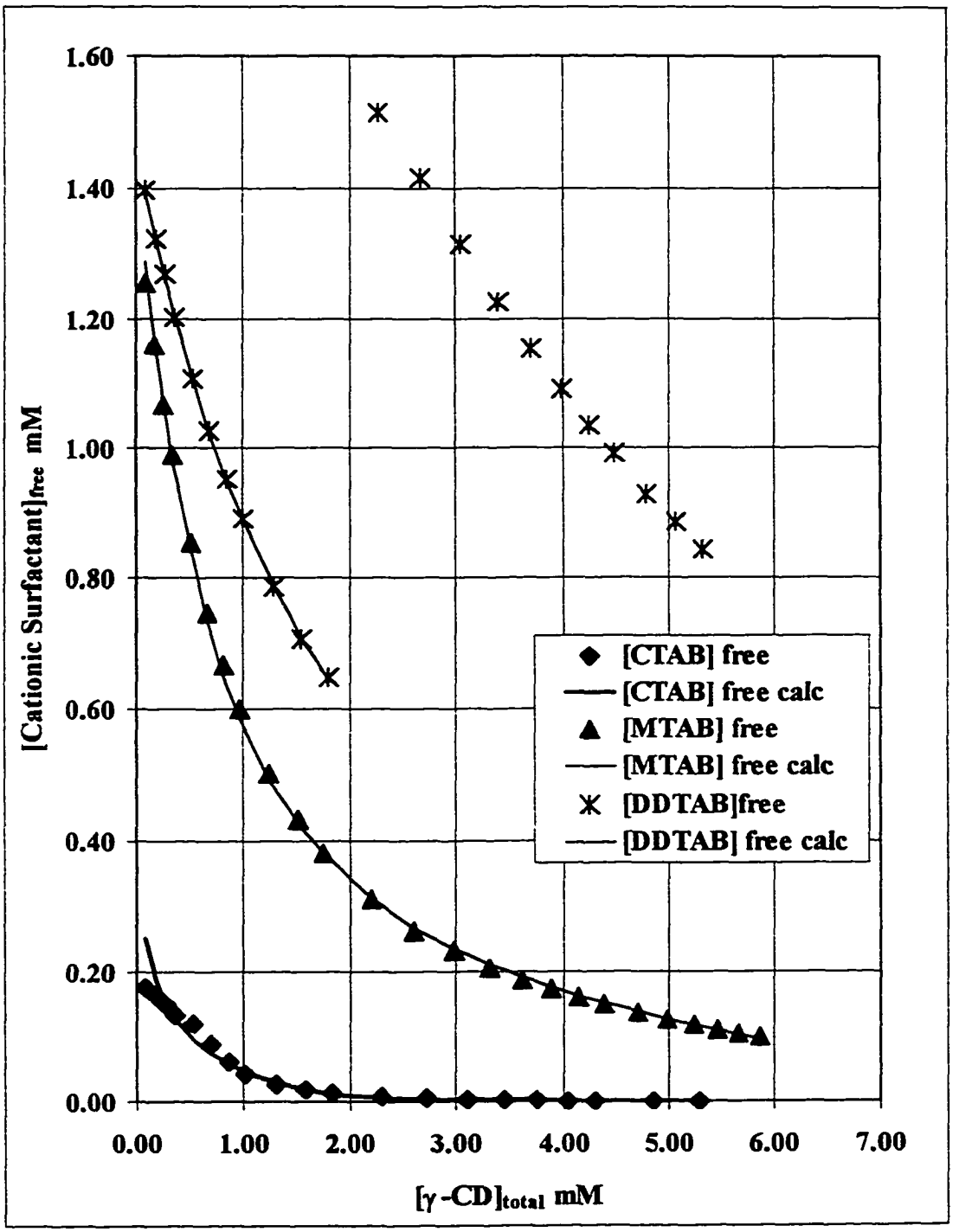

Figure 1.15. Free cationic surfactant concentration as a function of γ-CD complexation. All measurements were made in 0.01M NaCl.

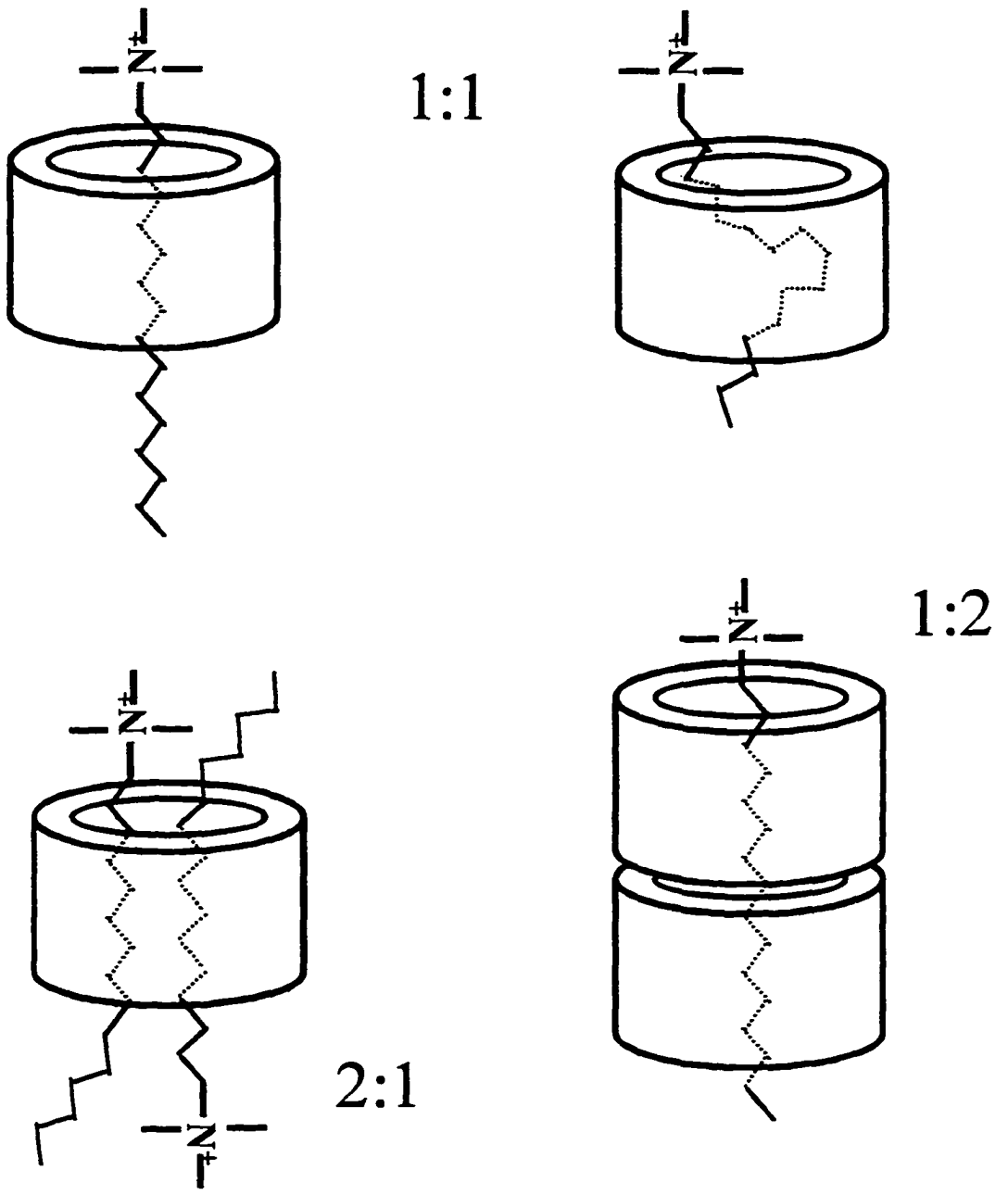

Figure 1.16. Simplified structures illustrating some possible binding configurations of surfactant:CD complexes.

A peculiar feature (see Figure 1.15) in the data is a jump in DDTAB electrode response, or $[DDTAB]_{free}$, in the γ-CD system. Since the jump occurred at a CD:Surfactant ratio of 2:1 it is possible that a precipitation phenomenon is responsible for this electrode response. However, no cloudiness was noted during the course of the experiment and due to the low concentrations being used, it is unlikely that a precipitation would be easily observed. Very little data is published pertaining to γ-cyclodextrin and no information on similar behavior has been found.

Results presented in Table 1.15 show that the strength of the inclusion complex with β-CD increases as the length of the surfactant tail increases. The length of the completely extended hydrocarbon chains can be estimated to be approximately 15.5, 17.9 and 20.5 Å respectively for C12, C14 and C16 tails. Based only on the lengths of the surfactant tails relative to the height of the cyclodextrin molecule (~7.9 Å) it is plausible that a 1:2 complex could also be formed in which the 2 cyclodextrin molecules are "stacked" onto a single surfactant as illustrated in Figure 1.16. If the cross sectional diameter of a straight chain hydrocarbon tail may be estimated as approximately 4.8 Å it is easy to see that geometrically the hydrocarbon tail can be accommodated by the α-CD cavity. Evidence that the tail length is an important factor in the formation of 1:2 complex with α-CD is the increasing value of K_3 as the length of the surfactant tail increases. A similar observation was made by Park and Song (76) in a study of anionic surfactants with α-cyclodextrin. These results are important in understanding the cyclodextrin binding model because it demonstrates

that tail length is the dominant factor in stoichiometry of the complex relative to the CD-headgroup interaction.

The results indicate the formation of a weak 1:2 complex with β-CD. Park and Song (76) suggested that the larger cavity of the β-CD, relative to α-CD, permits the hydrocarbon tail to kink up in order to minimize energetic interactions in the cavity. This result is expected since the interior of the cyclodextrin cavity is a hydrophobic environment with only C-H bonds directed inwards. Due to the smaller diameter of the α-CD cavity, the hydrocarbon tail is unable to kink up and a longer portion of the tail protrudes from the end of the CD, making itself available for further binding. Figure 1.16 illustrates how some of the complexes may be formed. The most important complex formed for β-CD is the 1:1 CD:surfactant complex.

Palepu, et. al. (86-87) investigated the binding of MTAB with α-, β- and γ-cyclodextrin by conductance measurements. However, in their model only the 1:1 complex was considered and K_1 was calculated directly from one or two individual concentrations of surfactant in the presence of CD. Thus comparison of results, especially for α- and γ-cyclodextrin is unreliable. The β-CD:MTAB constant was approximately 10.7 mM^{-1}.

Tominaga, et. al. (88) investigated the binding of MTAB with α-, β- and γ-cyclodextrin with a SSE and calculated equilibrium constants for individual concentrations similar to Palepu, et al (86-87). However, they did consider the 1:2 and 2:1 binding constants for their model. For α-CD, K_1 and K_3 were 43 and 3 mM^{-1}; for β-CD, K_1 was 51 mM^{-1}; for γ-CD K_1 and K_2 were 0.6 and 3.4 mM^{-1}. In cases

where one of the three constants was zero, quadratic solution to the mass balance equations (similar to those on page 19) permitted calculation of the equilibrium constants directly. One other group to investigate surfactant binding with SSE, Wyn-Jones, et al (82-85), measured the binding constants for α- and β-cyclodextrin with alkylpyridinium bromides (compounds similar in structure to the trimethyl ammonium bromides). The trends for binding constants of α-CD and β-CD with the alkyl tail series C10, C12, C14, C16 are similar to those observed in the present work. The K_1 values generally increase as the hydrocarbon tail length increases, the K_2 values for the α-CD are more important than for β-CD, and K_3 values are not important at all. Wyn-Jones did publish results for MTAB and CTAB binding with α- and β-CD using SSEs. The results are presented in Table 1.15 because they should be directly comparable with those in the present work. Although the trend for binding constant with tail length and CD cavity size are the same as the present work, the values differ considerably. Further, the K_2 values are much higher than for the present work. Indeed the K_2 values determined by the SSE work of Wyn-Jones (see Table 1.16) are much higher than values determined by any other method also.

		MTAB	CTAB
α-CD	K_1	61.	99.2
	K_2	7.0	20.4
β-CD	K_1	39.8	67.7
	K_2	20.4	9.6

Table 1.16. Results of SSE studies by Wyn-Jones (115). Units of K_1 and K_2 are mM^{-1}.

Dharmawardana, et. al. (89) determined K_1 and K_2 of 65.5 mM^{-1} and 0.4 mM^{-1} by surface tension measurement for CTAB with β-CD. Park et. al. (76) determined K_1 and K_2 of 59.8 mM^{-1} and 0.4 mM^{-1} for β-CD with CTAB. Other workers using SSE also give similar, smaller values for K_2 for β-CD with CTAB (89).

Relatively few studies have been published on the binding of γ-CD with surfactants (or other compounds for that matter) owing to its comparatively weak binding ability and high cost. Note that in Table 1.15 the binding constants are extraordinarily weak compared with the α- or β- cyclodextrin. Binding with γ-CD might only be thoroughly investigated with compounds more compatible with the relatively large size of the cavity. The equilibrium constants determined for γ-CD binding with CTAB in Table 1.15 should not be compared absolutely to other values in the table. The least squares fit actually determines values for K_2 and K_3 as dependent combinations with K_1 (as K_1K_2 and K_1K_3). Because a value of K_1 is not determined for this system, K_2 and K_3 cannot be determined independently and comparison can only be made on a relative basis (e.g., K_2/K_3). On that basis it is apparent that for the γ-CD:CTAB system a 1:2 complex is more important in the binding model than the 2:1 complex.

The only certain way to determine the binding stoichiometry is by structural studies. One possible technique is x-ray diffraction, although the crystal state and the dramatic change in concentration required to form crystals may result in structures not representative of the dilute aqueous conditions of interest.

Conclusions

A surfactant sensitive electrode was developed to permit quantitative measurement of the activity of "free" surfactant monomer in aqueous solution. In titrations of given concentrations of cationic surfactants with the three different cyclodextrins, the surfactant activity was measured and used to calculate binding constants with the cyclodextrins. The ionic strength of the solutions was held relatively constant by always maintaining a constant NaCl concentration.

Results indicate that the binding strength depends dramatically on the size of the cyclodextrin cavity and the length of the hydrocarbon tail of the surfactant. A trend of increasing strength for the 1:1 complex is observed for β-cyclodextrin with the series of cationic surfactants (with increasing tail length from C12, C14 and C16). There is not a significant amount of 1:2 or 2:1 complex formed with β-cyclodextrin. However, for α-cyclodextrin a strong K_3 binding constant indicates that the formation of a 2:1 (CD:surfactant) complex is important. Binding (1:1) with γ-cyclodextrin is very weak relative to α- or β- because of the poor fit of these surfactants in the larger γ-cyclodextrin cavity.

Following the work with cationic surfactants, cursory experiments with the anionic surfactant sodium dodecylsulfate (SDS) have shown that linear response is exhibited with the same SSE. This was expected since the active complex used in making the electrode membrane had equal amounts of cationic surfactant with SDS. Future work could be useful in elucidating the binding of anionic surfactants with

CD's. The binding of β-cyclodextrin with bile salts, which has been studied by the surface tension method (91) might be adaptable to a surfactant sensitive electrode study since the salts are basically an anionic surfactant.

Future investigations might also be directed towards development of a more selective electrode. It has been proposed in this work that an additional parameter, K_4, is required to aid fitting data to the standard equilibria described by 1:1, 1:2 and 2:1 surfactant:CD binding. If this parameter does indeed account for response of the electrode to surfactant:CD complexes at the membrane surface, then a more selective electrode could eliminate that interference. It is also possible that by altering the electrode composition a more Nernstian response could be obtained. However, in their present form the electrodes developed here are very useful for ionic surfactant measurements in single surfactant solutions, such as the conditions normally encountered when determining critical micelle concentrations with or without the presence of added salt.

The equilibrium constants determined for the cationic surfactant/CD systems in the present study compare reasonably well with values determined from a variety of other methods. Qualitatively, the results show the same trends as other studies and strengths of binding constants are explained by considerations of relative sizes of the CD cavity and the lengths of surfactant tails.

References

1) Cremer, M., Z. Biol., **1906**, 47, 562.
2) Haber, F; Klemensiewiez, Z. "Über Electriche Phasengrenkräfte", Z. Physik. Chem., **1909**, 67, 385.
3) Haber, F. "Uber Electriche Pasengrenkrafte", Z. Physik. Chem. **1909**, 67, 385.
4) Skoog, D.A.; West, D. M. *Analytical Chemistry: an Introduction*, 4th Ed., Saunders College Publishing, **1985**, p 342.
5) Scholer, R.; Simon, W. "Membranelekrode zur selektiven, potentiometrischen Erfassung organischer Kationen", Helv. Chim. Acta. **1972**, 55(5), 1801-1809.
6) Kakiuchi, T.; Obi, I.; Senda, M. "Tetraalkylammonium Ion-selective Electrodes with Supporting Electrolytes. An Experimental Test of the Theory of Liquid Ion-exchange Memebrane Ion-selective Electrodes Based on the Concept of the Mixed Ion-transfer Potential", Bull. CHem. Soc. Jpn. **1985**, 58, 1636-1641.
7) Davis, S. S.; Olejnik, O. "An Ion-Selective Electrode for the Determination of the Activity of Quaternary Ammonium Salts in Formulated Products", J. Pharm. **1979**, 31, 191.
8) Gloton, M. P.; Turmine, M.; Mayaffre, A. Letellier, P. "Électrodes á Membrane Indicatrices de Surfactifs Cationiques. Variation des Propertiétés Électriques de la Membrane en Fonction de sa Composition", Can. J. Chem. **1993**, 71, 371-376.
9) Maeda, T.; Ikeda, M.; Shibahara, M.; Haruta, T.; Satake, I. "Study of Cationic Surfactant Ion Selective Poly(vinyl chloride) Membrane Electrode Containing Dibenzo-18-crown-6", Bull. Chem. Soc. Jpn. **1981**, 54, 94-98.
10) Kale, K. M.; Cussler, E. L.; Evans, D. F. "Characterization of Micellar Solutions Using Surfactant Ion Electrodes", J. Phys. Chem. **1980**, 84, 593-598.
11) Koshinuma, M. "Dissociation of Micelles and Intermicellar Concentrations of Aqueous Solutions of Calcium and Sodium Decyl Sulfates", Bull. Chem. Soc. Jpn. **1981**, 54, 3128-3132.
12) Zana, R. "Micellaneous Methods" In *Surfactant Solutions: New Methods of Investigations*, Raoul Zana, Ed., Marcel Dekker, Inc., New York, **1987**, Chap. 9, pp. 463-469.
13) Evans, F.F.; Wennerstrum, H., *The Colloidal Domain*, VCH Publ., Inc., NY, **1994**, pp. 146-147.
14) Botré C.; Crescenzi, V.; Mele, A. "Studies on Complex Formation by Means of Eon Selective Membranes", J. Inorg. Nucl. Chem. **1958**, 8, 369-384.
15) Abuin, E. B.; Lissi, E. A.; Núñez, R.; Olea, A. "Study of Aqueous Tetradecyltrimethylammonium Bromide-Brij 35 Solutions by Ion Activity Measurements", Langmuir, **1989**, 5, 753-757.
16) Gharibi, H.; Takisawa, N.; Brown, P.; Thomason, M. A.; Painter, D. M.; Bloor, D. M.; Hall, D. G.; Wyn-Jones, E. "Analysis of the Fast Relaxation

Times for Micelle Kinetics Taking into Account New EMF Data", J. Chem. Soc. Far. Trans. **1991**, 87(5), 707-710.

17) Wan-Badhi, W. A.; Palepu, R.; Bloor, D. M.; Hall, D. G.; Wyn-Jones, E. "Ultrasonic Relaxation and Electrochemical Measurements on Monomer/ Micelle Exchange in Dodecylpyridinium Bromide Solutions Containing Added Sodium Bromide", J. Phys. Chem. **1991**, 95, 6642-6647.

18) Kale, K. M.; Cussler, E. L.; Evans, D. F. "Surfactant Ion Electrode Measurements of Sodium Alkylsulfate and Alkyltrimethylammonium Bromide Micellar Solutions", J. Sol. Chem **1982**, 11(8), 581-592.

19) Palepu, R.; Hall, D. G.; Wyn-Jones, E. "The use of Ion-selective Electrodes to determine the Effective Degree of Micelle Dissociation in Tetradecylpyridinium Bormide Solutions", J. Chem. Soc. Far. Trans. **1990**, 86(9), 1535-1538.

20) Tyagi, V.; Jain, A. K. "Estimation of Cationic Surfactants Using Liquid Membrane Electrodes", Ind. J. Chem. **1991**, 30A, 844-848.

21) Davis, S. S.; Olejnik, O. "The Determination of Free Long-Chain Quaternary Ammonium Species With an Ion-Selective Electrode Based on a Cetyltrimethylammonium Ion Pair", Anal. Chim. Acta. **1981**, 132, 51-58.

22) Maeda, T.; Satake, I. "The Micellar Properties of 1-Dodecylpyridinium Chloride as Studied by the Ion-selective Electrodes", Bull. Chem. Soc. Jpn. **1984**, 57, 2396-2399.

23) Gharibi, H.; W. A.; Palepu, R.; Bloor, D. M.; Hall, D. G.; Wyn-Jones, E. "Electrochemical Studies Associated with Micellization of Cationic Surfactants in Ethylene Glycol", Langmuir **1992**, 8, 782-787.

24) Garibi, H.; Palepu, R.; Tiddy, G. J. T.; Hall, D. G.; Wyn-Jones, E. "The Use of Surfactant Selective Electrodes in Non-aqueous Solvents", J. Chem Soc., Chem Communic. **1990**, 115-116.

25) Botré, C.; Crescenzi, V. L.; Mele. A. "A Study on Micelle Formation in Colloidal Electrolyte Solutions", J. Phys. Chem. **1959**, 63, 650-653.

26) Botré, C.; Hall, D. G.; Scowen, R. V. "EMF Measurements in the Cells Containing Ion Exchange Membranes as a Means of Determining Activities of Ionic Surfactants in Solution", Kolloid-Z. U. Z. Polymere **1972**, 250, 900-903.

27) Vikingstad, E. "The Effect of Solubilizates on the Activity of Sodium Decanoate above the Critical Micelle Concentration at 25°C.", J. Coll. Int. Sci. **1980**, 73(1), 261-262.

28) Vikingstad, E. "The Mean Activity and the Activities of the Separate Ions of Sodium Decanoate above and below the CMC Determined by a Surfactant Selective Silver/Silver Decanoate Electrode", J. Coll. Int. Sci. **1979**, 72, 68-75.

29) Burn, T.; Hoiland, H.; Vikingstad, E. "The Fraction of Associated Counterions and Singly Dispersed Amphiphiles in Micellar Systems from Ion Exchange Membrane Electrode Measurements", J. Coll. Int. Sci. **1978**, 63(3), 591-592.

30) Yamauchi, A.; Kunisake, T.; Minematsu, T.; Tomokiyo, Y.; Yamaguichi, T.; Kimizuka, H. "A Study of Surfactant Solutions Using the Liquid Membrane Electrode Selective to Alkyl Sulfate Ions", Bull. Chem. Soc. Jpn. **1978**, 51(10), 2791-2794

31) Cutler, S. G.; Meares, P., Hall, D. G. "Ionic Activities in Sodium Dodecyl Sulphate Solutions from Electromotive Force Measurements", J. Chem. Soc. Far. Trans. **1974**, 74, 1758-1767.

32) Cutler, S. G.; Meares, P. "Surfactants-Sensitive Polymeric Membrane Electrodes", J. Electroanal. Chem **1977**, 85, 145-161.

33) Birch B. J.; Clarke, D. E. "An Electrode Selective to the Dodecyl Sulphate Anion: Comments on the Application of Direct Potentiometry to C.M.C. Measurements", Anal. Chim. Acta **1972**, 61, 159-162.

34) Birch, B. J.; Clarke, D. E. "Surfactant-selective electrodes: Part I. An Improved Liquid Ion-Exchanger", Anal. Chim. Acta. **1973**, 67, 387-393.

35) Birch, B. J.; Clarke, D. E. "Surfactant-selective electrodes: Part II. The use of perm-selective membranes", Anal. Chim. Acta. **1974**, 69, 473-477.

36) Birch, B. J.; Clarke, D. E.; Lee, R. S.; Oakes, J. "Part III. Evaluation of a Dodecyl Sulphate Electrode in Surfactant Solutions Containing Polymers and A Protein", Anal. Chim. Acta. **1974**, 70, 417-423.

37) Newberry, J. E.; Smith, V. "Measurement of the critical micelle concentration by ion-selective electrodes", Coll. Poly. Sci. **1978**, 686, 494-495.

38) Shedlovsky, L.; Jakob, C. W.; Epstein, M. B. "Study of pNa of Aqeuous Solutions Solutions of Sodium Decyl , Dodecyl, and Tetradecyl Sulfates by E.M.F. Measurements", J. Phys. Chem **1963**, 67,2075-2079.

39) Satake, I.; Tahara, T.; Matuura, R. "The pNa Study of Sodium Alkyl Sulfates in Aqueous Solutions", Bull Chem. Soc. Jpn. **1969**, 42, 319-322.

40) Sasaki, T.; Hattori, M.; Sasaki, J.; Nukina, K. "Studies of Aqueous Sodium Dodecyl Sulfate Solutions by Activity Measurements", Bull Chem. Soc. Jpn. **1975**, (5), 1397-1403.

41) Koshinuma, M.; Sasaki, T. "Activity Measurements and Colloid Chemical Studies of Aqueous Sodium Tetradecyl Sulfate Solutions", Bull. Chem. Soc. Jpn. **1975**, 48(10), 2755-2759.

42) Dilley, G. C. "Determination of Anionic-active Matter in Detergents by Potentiometric Titration", Analyst, **1980**, 105, 713-719.

43) Gavach, C.; Bertrand, C. "Electrodes Specifiques D'anions a Longue Chaine Hydrocarbonee", Anal. Chim. Acta. **1971**, 55, 385-393.

44) Gilligan, T. J.; Cussler, E. L.; Evans, D. F. "Liquid Membrane Electrodes for Bile Salts", BBA Report **1977**, 497, 627-629.

45) Fujinaga, T.; Okazaki, S.; Freiser, H. "Ion Selective Electrodes Responsive to Anionic Detergents", Anal. Chem. **1974**, 46(12), 1842-1844.

46) Ciocan, N.; Anghel, D.F. "An Ion-Extractive Liquid-Membrane Anionic Surfactant Sensitive Electrode and Its Analytical Applications", Fresenius Z. Anal. Chem, **1978**, 290, 237-240.

47) Ciocan, N.; Anghel, D. "Liquid Membrane Electrodes for Potentiometric Determination of Anionic Detergents on Their Own and in Mixtures", Tenside Det., **1976**, 13(4), 188-192.
48) Buschmann, N. "Determination of Cationic and Zwitterionic Surfactants Using Ion Selective Electrodes", Tenside Surf. Det. **1992**, 29, 128-130.
49) Rippin, R.; Laskowski, J. "PVC-surfactant-selective electrode responsive to primary amines", Coll. Surf. **1985**, 15, 277-283.
50) Carnali, J. O. "(Polymer/Polymer)-Like Phase Behavior in the System Tetradecyltrimethylammonium Bromide/Sodium Polyacrylate/Water", Langmuir **1993**, 9, 2933-2941.
51) Kiefer, J. J.; Somasundaran, P.; Ananthapadmanabhan, K. P. "Interaction of Tetradecyltrimethylammonium Bromide with Poly(acrylic acid) and Poly(methacrylic acid). Effect of Charge Density", Langmuir **1993**, 9, 1187-1192.
52) Shirahama, K.; Tashiro, M. "Binding of 1-Decylpyridinium Bromide to Poly(vinyl sulfate)", Bull. Chem. Soc. Jpn. **1984**, 57, 377-380.
53) Shirahama, K.; Yuasa, H.; Sugimoto, S. "Binding of Sodium Decyl Sulfate to a Cationic Polymer", Bull. Chem. Soc. Jpn. **1981**, 54, 375-377.
54) Hayakawa, K.; Santerre, J. P.; Kwak, C. T. "Study of Surfactant-Polyelectrolyte Interactions. Binding of Dodecyl- and Tetradecyl-trimethylammonium Bromide by Some Carboxylic Polyelectrolytes", Macromolecules **1983**, 16, 1642-1645.
55) Hayakawa, K.; Kwak, J. C. T. "Surfactant-Polyelectrolyte Interactions. 1. Binding of Dodecyltrimethylammonium Ions by Sodium Dextran Sulfate and Sodium Poly(styrenesulfonate) in Aqueous Solution in the Presence of Sodium Chloride", J. Phys. Chem. **1982**, 86, 3866-3870.
56) Hayakawa, K.; Kwak, J. C. T. "Study of Surfactant-Polyelectrolyte Interactions. 2. Effect of Multivalent Counterions on the Binding of Dodecyltrimethylammonium Ions by Sodium Dextran Sulfate and Sodium Poly(styrenesulfonate) in Aqueous Sulution", J. Phys. Chem. **1983**, 87, 506-509.
57) Malovikova, A.; Hayakawa, K.; Kwak, J. C. T. "Surfactant-Polyelectrolyte Interactions. 4. Surfactant Chain Length Dependence of the Binding of Alkylpyridinium Cations to Dextran Sulfate", J. Phys. Chem. **1984**, 88, 1930-1933.
58) Satake, I.; Yang, J. T. "Interaction of Sodium Decyl Sulfate with Poly(L-ornithine) and Poly(L-lysine) in Aqueous Solution", Biopolymers **1976**, 15, 2263-2275.
59) Satake, I.; Gondo, T.; Kimizuka, H. "Conformational Transition of Poly(L-glutamic acid) in Aqueous Decylammonium Chloride Solution", Bull. Chem. Soc. Jpn. **1979**, 52(2), 361-364.
60) Hoffmann, H. Huber, G. "Electric Birefringence and EMF Measurements on Polymer/Surfactant Complexes", Colloids and Surfaces **1989**, 40, 181-193.

61) Shirahama, K.; Takashima, K.; Takisawa, N. "Interaction between Dodecyltrimethylammonium Chloride and DNA", Bull. Chem. Soc. Jpn. **1987**, 60, 43-47.
62) Hayakawa, K.; Santerre, J. P.; Kwak, J. C. T. "The Binding of Cationic Surfactants by DNA", Biophys. Chem. **1983**, 17, 185-181.
63) Shirahama, K.; Himuro, A.; Takisawa, N. "Binding of Hexadecylammonium Surfactants to Water-Soluble Neutral Polymers", Coll. Pol. Sci. **1987**, 265, 96-100.
64) Carlsson, A.; Lindman, B.; Watanabe, T.; Shirahama, K. "Polymer-Surfactant Interactions. Binding of *n*-Tetradecylpyridinium Bromide to Ethyl(hydroxy-ethyl)cellulose", Langmuir **1989**, 5, 1250-1252.
65) Shirahama, K.; Nishiyama, Y.; Takisawa, N. "Binding of *n*-Alkylpyridinium Chlorides to Nonionic Micelles", J. Phys. Chem. **1987**, 91, 5928-5930.
66) Tominaga, T.; Stem, T. B.; Evans, D. F. "The Study of Surfactant-Alcohol Mixed Micelles Using Conductance Viscosity, and Electromotive Force Measurements", Bull. Chem. Soc. Jpn. **1980**, 53, 795-799.
67) Gloton, M. P.; Mayaffre, A.; Turmine, M.; Letellier, P.; Suquet, H. "Use of Surfactant-Specific Electrodes in the Study of Adsorption of Cationic Amphiphilic Ions onto Clays", J. Coll. Int. Sci. **1995**, 172, 56-62.
68) Hayakawa, K.; Ayub, A. L.; Kwak, J. C. T. "The Application of Surfactant-Selective Electrodes to the Study of Surfactant Adsorption in Collodial Suspension", Colloids and Surfaces **1982**, 4, 389-396.
69) Szejtli, J. *Cyclodextrin Technology*; Kluwer Academic Publishers: Boston, **1988**.
70) Fromming, K.; Szejtli, J. *Cyclodextrins in Pharmacy*, Kluwer Academic Publishers: Boston, **1988**.
71) Szejtli, J.; Zsadon, B.; Cserhati, T. "Cyclodextrin Use in Separations"; In *Ordered Media in Chemical Separations*, Hinze, W.L.;Armstrong, D.W., Eds.; American Chemial society: Washington, DC, **1987**; Chapter 11, p 200.
72) Bender, M.L.; Komiyama, M. *Cyclodextrin Chemistry*, Springer-Verlag: New York, **1978**.
73) Connors, K. A., "The Stability of Cyclodextrin Complexes in Solution", Chem. Rev., **1997**, 97, 1325-1357.
74) VanEtten,R.L.; Sebastian, J.F.; Clowes, G.A.; Bender, M.L. "Acceleration of Phenyl Ester Clevage by Cycloamyloses. A Model for Enzymatic Specificity", J.A.C.S., **1967**, 89(13), 3242-3253.
75) Paulson, A.; Connors, K.A. In *5th Internat. Sympos. Cyclodextrins*, Duchêne, Ed. Editions de Santé: Pais, **1990**, p. 71.
76) Park, J. W.; Song, H. J. "Association of Anionic Surfactants with β-Cyclodextrin. Fluorescence-Probed Studies on the 1:1 and 1:2 Complexation", J. Phys. Chem. **1989**, 93, 6454-6458.
77) Lin, L.; Jiang, Y.; Du, X. Huang, X.; Chen, G. "A Study of the Properties of the 1:1 Inclusion Complex of β-Cyclodextrin with Cetyltrimethylammonium Bromide", Chem. Phys. Lett. **1997**, 266, 358-362.

78) Armstrong, R.D.; Horvai, G. "Properties of PVC Based Membranes Used in Ion-Selective Electrodes", Elect. Acta., **1990**, 35(1), 1-7.
79) Hórvai, G.; Toth, K.; Pungor, E. "Theoretical Models of Ion-Selective Membranes", Anal. Chim. Acta, **1989**, 216, 163-176.
80) McCallum, C.; Meares, P. "Some Observations on Membrane Potentials Measured With Surfactant Solutions", Elect. Acta. **1974**, 19, 537-539.
81) Mukerjee, P. Mysells, K.J. *Natl. Stand. Ref. Data Ser., Nat. Bur. Stand.*, **1971**, 36, 105-107.
82) Wan Yunus, W. M. Z.; Taylor, J., Bloor, D. M.; Hall, D. G.; Wyn-Jones, E.; "Electrochemical Measurements on the Binding of Sodium Dodecyl Sulfate and Dodecyltrimethylammonium Bromide with α- and β-Cyclodextrins", J. Phys. Chem., **1992**, 96, 8979-8982.
83) Mwakibete, H.; Bloor, D. M.; Wyn-Jones, E. "Determination of the Complexation Constants between Alkylpyridinium Bromide and α- and β-Cyclodextrins Using Electromotive Force Methods", Langmuir **1994**, 10, 3328-3331.
84) Takisawa, N., Hall, D.G.; Wyn-Jones, E.; Brown, P. "The Construction and Characteristics of Drug-selective Electrodes: Applications for the Determination of Complexation Constants of Inclusion Complexes with α- and β-Cyclodextrins Including a Kinetic Study", J. Chem. Soc., Faraday Trans. I, **1988**, 84(9), 3059-3070.
85) Mwakibete, H.; Cristantino, R.; Bloor, B. M.; Wyn-Jones, E.; Holzwarth, J. F. "Reliability of the Experimental Methods To Determine Equilibrium Constants for Surfactant/Cyclodextrin Inclusion Complexes", Langmuir **1995**, 11, 57-60
86) Palepu, R.; Reinsborough, V. C. "Surfactant-Cyclodextrin Interactions by Conductance Measurements", Can. J. Chem **1988**, 66, 325-328.
87) Palepu, R.; Richardson, J. E.; Reinsborough V. C. "Binding Constants of β-Cyclodextrin/Surfactant Inclusion by Conductivity Measurements", Langmuir **1989**, 5, 218-221.
88) Tominaga, T.; Hachisu, D.; Kamado, M. "Interactions Between the Tetradecyltrimethylammonium Ion and α-, β-, and γ-Cyclodextrin in Water as Studied by a Surfactant-Selective Electrode", Langmuir **1994**, 10, 4676-4680.
89) Dharmawardana, U. R.; Christian, S. D.; Tucker, E. E.; Taylor, R. W.; Scamehorn, J. F. "A Surface Tension Method for Determining Binding Constants for Cyclodextrin Inclusion Complexes of Ionic Surfactants", Langmuir **1993**, 9, 2258-2263.
90) Jezequel, D.; Mayaffreet, A.; Letellier, P. "Etude Potentiometrique de la Stabilite de Complexes Tensioactif-β-Cyclodextrine", Can. J. Chem. **1991**, 69, 1865-1871.
91) Dunaway, C.S. Ph.D. Dissertation, University of Oklahoma, Chapter 3, **1998**.

Chapter 2

Synergism in Nonionic/Cationic Mixed Micelle Systems

Introduction

Aqueous mixtures of surfactants are able to exhibit dramatic differences in physical properties compared to the behavior of the individual components (1-3). When the property of interest is enhanced, the term synergism is often applied to describe the effect. Understanding mixed surfactant properties is important because in applications, especially where large quantities of surfactant are required, pure single component surfactants are seldom available. High cost prohibits purification of bulk quantities of surfactant and the nature of surfactant production results in mixtures. In addition, the enhancement in a characteristic property may also mean that a mixture (formulation) can more efficiently accomplish an objective than a pure component.

In the present study, results are presented for the binary mixtures of a series of monodisperse polyethyleneoxide (PEOs) nonionic surfactants with the cationic surfactant cetylpyridinium chloride (CPC). Most commercially available PEOs are polydisperse mixtures of surfactant due to the method of synthesizing the materials. Nikko Corporation has produced an array of monodisperse PEOs with varying

ethylene oxide subunits and varying alkyl chain length. The cost of the chemicals will prevent their use for large scale commercial or industrial applications, but these pure surfactants are ideal for fundamental investigations of the behavior of mixtures. Surprisingly few researchers (6-10) have published results on the monodisperse PEOs similar to those studied in the present work.

The critical micelle concentration (CMC) of a given surfactant is the highest concentration that can be reached before micelles begin to form. Once the CMC is reached, surfactant monomers begin to associate in a way to form conglomerates, and the "free" surfactant monomer concentration is relatively constant after micelles begin to form. Because different types of molecules might interact differently (due to size, charge or polarity) to form micelles, the CMC of a (binary) surfactant mixture may be different from the CMC of either component. For example, two molecular properties that effect the formation of micelles in a cationic surfactant solution are the length of the surfactant tail and the charge of the head group. To alleviate the repulsive interaction between head groups in a cationic surfactant micelle, nonionic surfactant molecules may be inserted into the micelle, thus separating the charges of the head groups. Reducing the charge interaction makes it easier to form micelles and therefore lowers the critical micelle concentration. Since surface activity is proportional to the amount of free surfactant monomer in solution the synergistic effect of lowering the critical micelle concentration is readily monitored by measuring the surface tension of series of surfactant mixtures.

Results will be modeled based on a single parameter model. This model is sometimes derived, erroneously, with reference to regular solution theory (4-6). However, strong evidence exists showing that regular solution theory does not apply to most mixed surfactant systems, as indicated by the temperature dependence of the enthalpy of interaction (1-2, 7). Instead, by consideration of a simple one-parameter empirical Margules equation, it will be shown that the same model can be derived without the thermodynamic restrictions of regular solution theory. The single parameter, β, will be determined by fitting measured CMC values of surfactant mixtures of known composition (mole fraction, y). The values of β are a measure of the degree of synergism for the surfactant mixtures..

Experimental

The polyethyleneoxide (PEO) nonionic surfactants heptaethyleneglycol mono *n*-dodecylether (BL7SY), octaethyleneglycol mono *n*-decylether (BD8SY), octaethyleneglycol mono *n*-dodecylether (BL8SY), and octaethyleneglycol mono *n*-tetradecylether (BM8SY) were each 99.9%+ purity from Nikko Chemicals Co., Ltd., Japan, and were used as provided. Cetylpyridinium chloride (CPC) from Hexcel Corp, USA was recrystallized from 90% ethanol/water, rinsed with cold ethanol, and dried for two days at 65 °C before use. The structures for the surfactants are illustrated in Figure 2.1. The probable reason for the lack of literature related to mixed surfactants

systems studied here is the very high cost of the nonionic surfactants in monodisperse form. The nonionic surfactants used for the present work were graciously donated by Professor Yoshihiro Saito of Nihon University College of Pharmacy, Chiba, Japan.

All solutions were made using 0.01 M NaCl solutions, which were prepared with 18 Megaohm distilled and deionized water. Mixed surfactant solutions at specific mole fractions (y_A, y_B) were prepared by combining appropriate volumes of stock solutions of the individual surfactants. Surface tension measurements were made at room temperature (23.0 ± 0.5 °C).

The CMC_{mix} of each mixture was determined from the bend in the surface tension vs $[Surfactant]_{total}$ in plots like those in Figures 2.2-2.5. Straight lines were drawn through the data before and after the bend and the CMC_{mix} determined visually at the intersection of the two lines. Data for the plots (Tables 2.1-2.4) were collected by measuring the surface tension as surfactant concentration was increased sequentially, at fixed mole fractions (y_B). Each surface tension, y_B data set collected this way is referred to as a titration.

An initial intent in this study was to utilize the surfactant sensitive electrodes developed as described in Chapter 1 to measure critical micelle concentrations of the surfactant mixtures. However, it was determined that the nonionic PEO surfactant significantly dampened the response of the electrodes for the cationic surfactant, most probably by adsorbing to the PVC sensing membrane.

All surface tensions were measured using a Central Scientific Co, Inc., (CSC) du Noüy Tensiometer (Catalog # 70535) and a single Pt-Ir (platinum-iridium) du

Noüy Ring (mean circumference: 5.992 cm, R/r: 53.6). Accurate surface tension values were determined (in units mN/m) by correcting the instrument reading according to the following equation, determined by fitting the factory-provided correction table values for this ring.

$$\text{Surface Tension} = 0.7364(\text{Instrument Reading})^{1.056} \qquad \text{Equation 2.1}$$

The common and recommended procedure for using the CSC tensiometer is to pull the ring from a liquid surface (after initially contacting and submerging the ring) until the ring breaks free for the surface. The horizontal position of the ring is maintained by simultaneously lowering the stage on which the sample rests, while upward force is applied as if to raise the ring. This procedure was followed although, as will be pointed out in Chapter 3, the maximum force is actually reached slightly before the ring breaks free from the liquid.

At low surfactant concentrations (especially with nonionic surfactant) long equilibration times were required before making a reading with the du Noüy ring tensiometer. Since the du Noüy ring creates new surface area as the ring is pulled up, some time is required for surfactant to diffuse from the bulk solution to the newly created surface to reestablish equilibrium. At the lowest concentration conditions, like those used when measuring the surface tensions for the nonionic surfactants, longer equilibration times were required. Generally, a quick measurement was made to determine the approximate value of the surface tension. Afterwards, the procedure was repeated and the ring was pulled to within ~3 mN/m of the initial reading and

allowed to stand for up to 10 minutes before the maximum pull was determined. This time delay reading was repeated three times or until consistent readings were obtained.

The Pt-Ir ring was cleaned periodically by immersing in concentrated sulfuric acid, then rinsing with distilled deionized water and heating to red hot in the flame of a Fisher burner. Between measurements of a single surfactant system the ring was cleaned by rinsing it in distilled deionized water followed by holding it in the flame of a Fisher burner until it was red hot. The ring was always handled with forceps to avoid contamination by hand contact.



CPC: cetylpyridinium chloride
or *n*-hexadecylpyridinium chloride



BL7SY: heptaethyleneglycol mono *n*-dodecylether



BD8SY: octylethyleneglycol mono *n*-decylether



BL8SY: octylethyleneglycol mono *n*-dodecylether



BM8SY: octylethyleneglycol mono *n*-tetradecylether

Figure 2.1. Structures of compounds used in mixed micelle studies.

Results and Discussion

If mixed micelles follow ideal behavior, the critical micelle concentration could be calculated according to the following expression

$$CMC_{mix} = \frac{CMC^{o}_{A} CMC^{o}_{B}}{y_A CMC^{o}_{B} + y_B CMC^{o}_{A}} \qquad \text{Equation 2.2}$$

CMC_A° and CMC_B° represent the CMCs of the pure surfactants and y_A and y_B represent the monomer mole fraction of surfactant A and B, respectively (2, 8). The micellar mole fractions of one surfactant may be calculated according to

$$x_A = \frac{y_A CMC_{mix}}{CMC^{o}_{A}} \qquad \text{Equation 2.3}$$

The CMC for each binary surfactant system predicted by these ideal relationships are represented by the dashed lines in Figures 2.6-2.10. This model works well for ideal surfactant mixtures when the molecules are of like type. For example mixtures of decylmethyl sulfoxide, $C_{10}(CH_3)SO$ (CMC=1.7 mM) and decyldimethylphosphine oxide, $C_{10}(CH_3)_2PO$ (CMC=3.8 mM) have been shown to follow ideal behavior (8). This result was explained by the similarity in polarity of the surfactant head groups and the similar length of the hydrocarbon tails. Because of the similarities, there is no reason for the escaping tendency of components from mixed micelles to be different from that with micelles of the individual surfactants. For mixtures of dissimilar surfactants, as in the present study with mixtures of cationic and nonionic surfactants,

the ideal behavior modeled by equations 2.2 and 2.3 fails. A better representation for non-ideal mixtures has been found by using the following treatment (8).

First, under the condition of micellization equilibrium ($\mu_A^M = \mu_A^B$ and $\mu_B^M = \mu_B^B$, where μ_i^M and μ_i^B are the chemical potentials of a component in the micelle and bulk phases respectively) the monomer concentrations, C_i^m, of each surfactant may be represented as follows:

$$C_A^m = x_A f_A CMC_A^o \quad \text{and} \quad C_B^m = x_B f_B CMC_B^o \qquad \text{Equations 2.4}$$

In this treatment, f_A and f_B represent the activity coefficients of the surfactant monomers. The natural logarithms of the activity coefficients are expressed in terms of a single empirical parameter, β.

$$\ln(f_A) = \beta\, x_B^2 \quad \text{and} \quad \ln(f_B) = \beta\,(1 - x_B)^2 \qquad \text{Equations 2.5}$$

Equations like 2.5 may be referred to as one-parameter Margules equations.

Equations 2.4, at the CMC of the mixture (CMC_{mix}), become:

$$y_A CMC_{mix} = x_A f_A CMC_A^o \quad \text{and}$$

$$(1 - y_A) CMC_{mix} = (1 - x_A) f_B CMC_B^o \qquad \text{Equation 2.6}$$

Combining equations 2.5 and 2.6 the following expression can be obtained.

$$x_A^2 \ln\left(\frac{CMC_{mix} y_A}{CMC_A^o x_A}\right) = (1 - x_A)^2 \ln\left(\frac{CMC_{mix}(1 - y_A)}{CMC_B^o (1 - x_A)}\right) \qquad \text{Equation 2.7}$$

The new variable introduced in equations 2.5, β, is an empirical parameter used to fit experimental data to the model. For the present work, the CMC_{mix} was measured for

a series of mixtures at known monomer mole fractions (y_A and y_B). Since the concentrations were known quite accurately it was assumed, for the least squares analysis, that y_A and y_B are free from error. The value of β was determined by least-squares fit of equation 2.8.

$$CMC_{mix} = x_A CMC_A^o e^{\beta x_B^2} + x_B CMC_B^o e^{\beta x_A^2} \qquad \text{Equation 2.8}$$

The strategy in obtaining the best value of β from the sets of CMC, y_B data involved choosing an initial trial value of β and solving equation 2.8 to obtain a calculated value for the CMC. The program calculated the sum of the squares of deviations for a given provisional value of β: $s(\beta) = \Sigma\ (CMC_{calc,i} - CMC_i)^2$. The best value of β was found in an iterative manner by stepping it systematically until the value of $s(\beta)$ was minimized. At each iterative value of β, for each y_A value, it was also necessary to determine the value of x_A (or x_B) which satisfied equation 2.9.

$$y_A = \frac{f_B x_B CMC_B^o}{f_A(1-x_B)CMC_A^o + f_B x_B CMC_B^o} \qquad \text{Equation 2.9}$$

Equation 2.9 is analogous to an equation used to treat liquid vapor pressures, which relates partial pressures to total pressure. This equation does not depend on the experimentally determined CMC_{mix}.

The program used to fit CMC vs $y_{\text{nonionic surfactant}}$ data and obtain the best value of the β parameter is provided the appendix to this chapter. The program is written in True BASIC; however it is short enough to be easily re-written in any programming language. CMC and mole fraction values are entered as DATA statements near the

end of the code. Upon executing the program the user is prompted for the number of data sets (7 in this program listing) and an initial estimate of β. Since the program is written to approach the value of β from below, a value smaller than the expected result should be initially estimated. An initial estimate of -3 is reasonable for each of the surfactant systems studied.

Surface tensions were measured for surfactant mixtures with mole fractions varying from pure cationic (y = 0) to pure nonionic (y = 1). Generally, 7 to 10 solutions with mole fractions (of PEO) from 0 to 1 were prepared. Figures 2.2 - 2.5 show the combined results of the CMC data for each binary system investigated. The plots are presented here as combined graphs to conserve space. To actually determine the CMC from the data, it was necessary to plot each CMC curve separately. Also, if required, it was sometimes necessary to zoom in on the graph region where the CMC break occurs. Experimentally determined surface tensions are presented in Tables 2.1 through 2.4 and critical micelle concentrations for each mole fraction are given in Tables 2.5 through 2.8.

After each CMC was determined, a plot of CMC vs y (total mole fraction of nonionic surfactant) was made. Using the least-squares fitting program described above, the value of β was determined, and a fitted line was calculated and graphed with the experimental data. A corresponding line was calculated based on the ideal mixing model (equations 2.2 and 2.3) to demonstrate the deviation from ideality. Figure 2.6 shows the resulting data and calculated lines for BL7SY. The S-shaped

curve in Figure 2.7 shows the relationship between the total mole fraction of BL7SY and the mole fraction of BL7SY in the micelle. Two characteristic features are revealed from the data shown in Figure 2.7. First, the apparent existence of an azeotrope is observed in solutions that show a synergistic minimum in the CMC curve like that shown in Figure 2.6. By definition, the micellar mole fraction of surfactant (x_B) at the azeotrope is observed where the y = x line intersects the experimental (fitted) line. This azeotrope corresponds to a point at which the mole fractions of surfactants in the micellar phase is the same as the mole fractions in the monomer phase. Second, the model for ideal behavior does not cross the y = x line. Graciaa et al., (11) point out that a phase separation model can be used to show that the existence of an azeotrope corresponds to a minimum (or maximum in the case of negative synergism) in the CMC curve at the same mole fraction. No rigorous proof is given, but it is observed that the mole fraction y_{BL7SY}=0.65 from Figure 2.7 does correspond to the minimum in the CMC curve of Figure 2.6. Figures 2.8 - 2.10 show the CMC vs y_{Bx8SY} (where x= D for C10, L for C12, and M for C14) curves for the alkyl tail analogs of the nonionic surfactant with 8 EO subunits. Plots of the characteristic S-shaped curve like that in Figure 2.7 are not given for the remaining surfactant systems since the purpose of the present work is to determine the interaction parameter, β, which is obtained only with regard to the CMC curves and the non-ideal model described by equations 2.5 – 2.9. Table 2.9 presents the resulting β values.

[BL7SY] mM	S.T. y=1	[BL7SY] mM	[CPC] mM	S.T. y= 0.842	[BL7SY] mM	[CPC] mM	S.T. y= 0.744	[BL7SY] mM	[CPC] mM	S.T. y= 0.658	[BL7SY] mM	[CPC] mM	S.T. y= 0.480
	71.78			70.87			72.11			71.81			72.54
1.71E-03	53.42	5.08E-03	9.56E-04	47.68	2.96E-03	1.02E-03	51.11	1.79E-03	9.33E-04	52.71	9.21E-04	1.00E-03	57.36
3.42E-03	51.96	1.02E-02	1.91E-03	43.04	5.92E-03	2.03E-03	47.04	3.59E-03	1.86E-03	49.46	1.84E-03	2.00E-03	53.32
5.12E-03	49.92	1.52E-02	2.87E-03	40.97	8.87E-03	3.05E-03	44.58	5.38E-03	2.80E-03	47.13	2.76E-03	3.00E-03	50.73
8.53E-03	47.59	2.03E-02	3.82E-03	39.19	1.18E-02	4.06E-03	43.26	7.17E-03	3.73E-03	45.39	3.68E-03	4.00E-03	49.01
1.28E-02	45.45	2.54E-02	4.78E-03	38.81	1.48E-02	5.07E-03	41.37	8.97E-03	4.66E-03	43.52	4.60E-03	5.00E-03	47.97
1.71E-02	43.47	3.81E-02	7.16E-03	36.22	2.22E-02	7.61E-03	39.10	1.34E-02	6.99E-03	41.75	6.90E-03	7.49E-03	46.19
2.56E-02	41.11	5.07E-02	9.54E-03	34.69	2.95E-02	1.01E-02	37.05	1.79E-02	9.31E-03	39.86	9.20E-03	9.98E-03	44.39
3.40E-02	39.83	7.60E-02	1.43E-02	34.84	4.43E-02	1.52E-02	35.62	2.68E-02	1.40E-02	37.47	1.38E-02	1.50E-02	41.85
5.10E-02	37.18	1.01E-01	1.90E-02	34.79	5.89E-02	2.02E-02	35.36	3.58E-02	1.86E-02	35.74	1.84E-02	1.99E-02	40.01
8.47E-02	34.60	1.52E-01	2.85E-02	35.17	8.82E-02	3.03E-02	35.55	5.36E-02	2.78E-02	35.46	2.75E-02	2.98E-02	37.27
1.26E-01	34.65	2.02E-01	3.80E-02	35.08	1.17E-01	4.03E-02	35.65	8.89E-02	4.62E-02	35.36	4.56E-02	4.95E-02	36.99
1.68E-01	34.69	2.52E-01	4.74E-02	34.98	1.46E-01	5.03E-02	35.65	1.76E-01	9.16E-02	36.09	6.81E-02	7.39E-02	36.99
3.30E-01	34.74	3.76E-01	7.07E-02	35.03	2.19E-01	7.51E-02	35.62	3.46E-01	1.80E-01	36.22	9.04E-02	9.81E-02	37.08
		4.99E-01	9.38E-02	35.03	2.90E-01	9.96E-02	35.74				1.77E-01	1.92E-01	37.08

Table 2.1. S.T. (Surface Tension, mN/m) data for BL7SY. Surfactant concentration is given in mM units and surface tension measurements were made at nine different mole fractions (y) of BL7SY. All solutions were made with 0.01 M NaCl.

[BL7SY] mM	[CPC] mM	S.T. y= 0.322	[BL7SY] mM	[CPC] mM	S.T. y= 0.159	[BL7SY] mM	[CPC] mM	S.T. y= 0.046	[CPC] mM	S.T. y= 0
		71.85			72.28			72.41		72.37
4.33E-04	9.11E-04	57.82	1.59E-04	8.39E-04	62.70	2.40E-04	5.04E-03	57.20	9.20E-03	58.80
8.65E-04	1.82E-03	54.14	3.17E-04	1.68E-03	59.23	4.80E-04	1.01E-02	53.45	2.75E-02	52.64
1.30E-03	2.73E-03	52.25	4.76E-04	2.52E-03	56.78	7.20E-04	1.51E-02	51.13	4.57E-02	49.17
2.16E-03	4.55E-03	49.84	7.93E-04	4.19E-03	55.18	9.59E-04	2.01E-02	49.62	6.82E-02	46.42
3.24E-03	6.82E-03	48.17	1.19E-03	6.28E-03	52.84	1.44E-03	3.01E-02	47.29	9.05E-02	44.39
4.32E-03	9.09E-03	46.39	1.58E-03	8.38E-03	51.42	2.38E-03	4.99E-02	44.10	1.13E-01	42.56
6.47E-03	1.36E-02	44.29	2.38E-03	1.26E-02	47.49	3.56E-03	7.45E-02	41.50	1.35E-01	40.95
8.62E-03	1.82E-02	42.70	3.16E-03	1.67E-02	44.87	4.72E-03	9.89E-02	39.48	1.78E-01	39.58
1.29E-02	2.72E-02	40.09	4.74E-03	2.50E-02	44.78	7.01E-03	1.47E-01	38.47	2.20E-01	39.58
2.14E-02	4.51E-02	37.18	7.87E-03	4.16E-02	41.50	9.26E-03	1.94E-01	38.52	2.62E-01	39.67
3.20E-02	6.74E-02	37.15	1.18E-02	6.22E-02	38.90	1.36E-02	2.85E-01	38.94	4.22E-01	39.61
4.25E-02	8.95E-02	37.18	1.56E-02	8.25E-02	38.04	2.19E-02	4.59E-01	39.00		
6.32E-02	1.33E-01	37.18	2.32E-02	1.23E-01	37.94					
8.36E-02	1.76E-01	37.18	3.07E-02	1.62E-01	38.04					
			4.54E-02	2.40E-01	38.09					
			7.33E-02	3.87E-01	38.28					

Table 2.1. Continued.

[BD8SY] mM	S.T. y= 1	[BD8SY] mM	[CPC] mM	S.T. y= 0.838	[BD8SY] mM	[CPC] mM	S.T. y= 0.748	[BD8SY] mM	[CPC] mM	S.T. y= 0.666	[BD8SY] mM	[CPC] mM	S.T. y= 0.508	[BD8SY] mM	[CPC] mM	S.T. y= 0.443
	70.62			72.11			71.02			69.93			72.41			71.52
2.44E-03	62.34	6.22E-03	1.20E-03	57.92	3.54E-03	1.19E-03	59.00	2.33E-03	1.17E-03	57.72	1.23E-03	1.19E-03	59.68	9.09E-04	1.14E-03	61.35
4.89E-03	60.57	1.24E-02	2.40E-03	55.37	7.09E-03	2.38E-03	56.25	4.65E-03	2.33E-03	55.28	2.47E-03	2.39E-03	57.43	1.82E-03	2.28E-03	59.19
7.33E-03	59.49	1.86E-02	3.59E-03	53.42	1.06E-02	3.58E-03	54.40	6.97E-03	3.50E-03	53.91	3.70E-03	3.58E-03	55.86	2.73E-03	3.42E-03	57.62
1.22E-02	57.92	3.11E-02	5.99E-03	50.79	1.77E-02	5.96E-03	52.25	1.16E-02	5.83E-03	52.06	6.16E-03	5.97E-03	53.23	4.54E-03	5.71E-03	55.37
1.83E-02	56.06	4.66E-02	8.97E-03	48.56	2.65E-02	8.93E-03	50.21	1.74E-02	8.74E-03	49.62	9.23E-03	8.95E-03	52.06	6.81E-03	8.55E-03	53.42
2.44E-02	54.98	6.20E-02	1.20E-02	46.81	3.54E-02	1.19E-02	48.65	2.32E-02	1.16E-02	48.36	1.23E-02	1.19E-02	50.30	9.07E-03	1.14E-02	51.86
3.65E-02	53.32	9.30E-02	1.79E-02	44.39	5.30E-02	1.78E-02	46.42	3.48E-02	1.74E-02	46.33	2.46E-02	2.38E-02	47.20	1.81E-02	2.27E-02	48.36
4.87E-02	52.15	1.24E-01	2.39E-02	43.33	7.06E-02	2.37E-02	44.78	4.63E-02	2.32E-02	43.72	3.67E-02	3.56E-02	44.97	2.71E-02	3.40E-02	46.23
7.28E-02	50.21	1.85E-01	3.57E-02	40.82	1.06E-01	3.55E-02	42.46	6.93E-02	3.48E-02	42.08	6.09E-02	5.91E-02	41.98	4.50E-02	5.65E-02	43.43
1.21E-01	47.78	3.07E-01	5.92E-02	39.00	1.75E-01	5.89E-02	39.58	1.15E-01	5.77E-02	39.58	9.09E-02	8.81E-02	39.58	6.71E-02	8.42E-02	40.92
1.80E-01	45.55	4.58E-01	8.83E-02	38.90	2.61E-01	8.79E-02	39.19	1.71E-01	8.60E-02	39.10	1.20E-01	1.17E-01	39.00	8.89E-02	1.12E-01	39.38
2.39E-01	44.00	6.07E-01	1.17E-01	38.71	3.46E-01	1.17E-01	39.10	2.27E-01	1.14E-01	38.90	2.35E-01	2.28E-01	38.90	1.74E-01	2.18E-01	38.90
3.54E-01	42.46	9.00E-01	1.74E-01	38.33	5.13E-01	1.73E-01	38.90	4.45E-01	2.23E-01	38.90	3.45E-01	3.35E-01	38.81	2.55E-01	3.21E-01	38.90
4.67E-01	40.82	1.19E+00	2.29E-01	38.33	6.77E-01	2.28E-01	38.90	6.52E-01	3.27E-01	38.71	5.51E-01	5.34E-01	38.81	4.08E-01	5.13E-01	38.90
6.85E-01	39.10	1.74E+00	3.35E-01	38.04	9.93E-01	3.34E-01	38.81	1.04E+00	5.22E-01	38.62	7.40E-01	7.17E-01	38.71	5.49E-01	6.89E-01	38.90
1.09E+00	37.18	2.78E+00	5.35E-01	37.75	1.58E+00	5.33E-01	38.62	1.40E+00	7.02E-01	38.52	9.95E-01	9.65E-01	38.62	7.40E-01	9.30E-01	38.71
1.47E+00	37.18	3.73E+00	7.19E-01	37.75	2.13E+00	7.16E-01	38.42	1.89E+00	9.46E-01	38.52						
1.98E+00	37.18	5.02E+00	9.67E-01	37.56	2.86E+00	9.63E-01	38.23									

Table 2.2. S.T. (Surface Tension, mN/m) data for BD8SY. Surfactant concentration is given in mM units and surface tension measurements were made at nine different mole fractions (y) of BD8SY. All solutions were made with 0.01 M NaCl.

[BD8SY] mM	[CPC] mM	S.T. y= 0.369	[BD8SY] mM	[CPC] mM	S.T. y= 0.288	[BD8SY] mM	[CPC] mM	S.T. y= 0.179	[BD8SY] mM	[CPC] mM	S.T. y= 0.106	[CPC] mM	S.T. y= 0
		71.81			70.62			70.92			70.53		71.42
6.69E-04	1.14E-03	63.02	4.89E-04	1.21E-03	62.43	2.60E-04	1.19E-03	63.12	1.41E-04	1.20E-03	63.32	1.17E-03	67.07
1.34E-03	2.28E-03	60.96	9.78E-04	2.42E-03	59.88	5.21E-04	2.39E-03	60.96	4.23E-04	3.59E-03	59.68	2.34E-03	65.09
2.01E-03	3.43E-03	59.39	1.47E-03	3.63E-03	58.31	7.81E-04	3.58E-03	59.39	7.05E-04	5.97E-03	57.72	3.51E-03	63.71
3.34E-03	5.71E-03	57.13	2.44E-03	6.05E-03	56.65	1.30E-03	5.97E-03	57.72	1.06E-03	8.96E-03	55.86	5.84E-03	61.45
5.01E-03	8.56E-03	54.89	3.66E-03	9.07E-03	54.40	1.95E-03	8.95E-03	55.37	1.41E-03	1.19E-02	54.20	8.76E-03	59.49
6.68E-03	1.14E-02	53.13	4.88E-03	1.21E-02	52.84	2.60E-03	1.19E-02	53.91	2.81E-03	2.38E-02	50.89	1.17E-02	57.92
1.33E-02	2.28E-02	49.53	9.74E-03	2.41E-02	49.14	5.19E-03	2.38E-02	50.40	4.20E-03	3.56E-02	48.46	1.75E-02	55.86
2.00E-02	3.40E-02	47.10	1.46E-02	3.61E-02	47.00	7.76E-03	3.56E-02	48.26	6.97E-03	5.91E-02	45.65	2.33E-02	54.10
3.31E-02	5.65E-02	44.10	2.42E-02	5.98E-02	44.10	1.29E-02	5.90E-02	45.55	1.04E-02	8.81E-02	43.43	3.49E-02	51.67
4.94E-02	8.43E-02	41.50	3.60E-02	8.92E-02	41.40	1.92E-02	8.80E-02	42.94	1.38E-02	1.17E-01	41.59	5.78E-02	48.26
6.55E-02	1.12E-01	39.48	4.78E-02	1.18E-01	39.77	2.54E-02	1.17E-01	40.63	2.69E-02	2.28E-01	39.48	8.63E-02	45.65
1.28E-01	2.19E-01	39.10	9.34E-02	2.31E-01	39.10	4.97E-02	2.28E-01	39.00	3.95E-02	3.35E-01	39.48	1.14E-01	43.33
1.88E-01	3.21E-01	39.00	1.37E-01	3.39E-01	39.00	7.29E-02	3.34E-01	39.10	6.30E-02	5.34E-01	39.19	1.70E-01	40.54
3.00E-01	5.13E-01	39.00	2.18E-01	5.40E-01	38.90	1.16E-01	5.34E-01	39.00	8.46E-02	7.17E-01	39.19	2.24E-01	40.34
4.04E-01	6.90E-01	39.00	2.93E-01	7.25E-01	38.90	1.56E-01	7.17E-01	39.00				3.28E-01	40.44
5.45E-01	9.30E-01	38.71	3.94E-01	9.75E-01	38.90							5.24E-01	40.44
												7.04E-01	40.15

Table 2.2. Continued.

[BL8SY] mM	S.T. y=1	[BL8SY] mM	[CPC] mM	S.T. y= 0.857	[BL8SY] mM	[CPC] mM	S.T. y= 0.748	[BL8SY] mM	[CPC] mM	S.T. y= 0.667	[BL8SY] mM	[CPC] mM	S.T. y= 0.498	[BL8SY] mM	[CPC] mM	S.T. y= 0.443
	70.82			71.61			70.82			71.02			70.82			70.82
7.34E-03	49.72	7.44E-03	1.24E-03	48.75	3.49E-03	1.17E-03	51.86	2.48E-03	1.24E-03	52.54	1.19E-03	1.20E-03	54.98	9.07E-04	1.14E-03	55.96
1.47E-02	47.10	1.49E-02	2.48E-03	44.87	6.97E-03	2.35E-03	48.36	4.95E-03	2.48E-03	48.65	2.38E-03	2.40E-03	52.25	1.81E-03	2.28E-03	52.93
2.20E-02	44.87	2.23E-02	3.72E-03	42.56	1.05E-02	3.52E-03	46.04	7.42E-03	3.71E-03	46.62	3.57E-03	3.60E-03	50.40	2.72E-03	3.42E-03	50.99
2.94E-02	43.43	2.97E-02	4.96E-03	41.02	1.39E-02	4.69E-03	44.39	9.89E-03	4.95E-03	45.07	4.75E-03	4.79E-03	48.94	3.63E-03	4.56E-03	49.43
3.67E-02	42.37	3.72E-02	6.19E-03	39.77	1.74E-02	5.86E-03	43.23	1.24E-02	6.18E-03	43.62	5.94E-03	5.99E-03	47.88	4.53E-03	5.70E-03	48.56
5.50E-02	39.29	7.42E-02	1.24E-02	36.99	2.61E-02	8.78E-03	40.73	1.85E-02	9.27E-03	41.31	8.91E-03	8.98E-03	45.36	6.79E-03	8.55E-03	46.13
7.33E-02	37.37	1.48E-01	2.47E-02	36.51	3.48E-02	1.17E-02	39.00	2.47E-02	1.24E-02	39.67	1.19E-02	1.20E-02	43.62	9.05E-03	1.14E-02	44.20
1.10E-01	35.94	3.68E-01	6.13E-02	36.32	5.21E-02	1.75E-02	37.37	3.70E-02	1.85E-02	37.56	1.78E-02	1.79E-02	41.21	1.36E-02	1.71E-02	41.98
1.46E-01	35.84	7.26E-01	1.21E-01	36.32	6.95E-02	2.34E-02	37.18	4.93E-02	2.46E-02	36.99	2.37E-02	2.39E-02	39.58	1.81E-02	2.27E-02	40.54
2.19E-01	35.65	1.08E+00	1.79E-01	36.22	1.04E-01	3.49E-02	37.08	7.37E-02	3.69E-02	36.99	3.54E-02	3.57E-02	37.94	2.70E-02	3.40E-02	38.23
3.63E-01	35.65	1.42E+00	2.36E-01	36.22	1.38E-01	4.65E-02	37.08	1.22E-01	6.12E-02	37.08	5.88E-02	5.93E-02	37.85	4.49E-02	5.64E-02	37.47
7.17E-01	35.65				1.72E-01	5.80E-02	37.08	2.42E-01	1.21E-01	37.08	1.16E-01	1.17E-01	37.75	8.87E-02	1.12E-01	37.56
1.06E+00	35.55				3.41E-01	1.15E-01	37.08	3.58E-01	1.79E-01	37.08	1.72E-01	1.74E-01	37.66	1.74E-01	2.18E-01	37.85
1.40E+00	35.55				5.06E-01	1.70E-01	36.99	4.72E-01	2.36E-01	37.08	2.27E-01	2.29E-01	37.66	2.55E-01	3.21E-01	37.94
2.05E+00	35.55				6.66E-01	2.24E-01	36.99	6.91E-01	3.46E-01	37.08	3.33E-01	3.36E-01	37.66	4.07E-01	5.12E-01	37.94
3.27E+00	35.46				9.78E-01	3.29E-01	36.89	1.10E+00	5.51E-01	37.08	5.31E-01	5.35E-01	37.66			
					1.28E+00	4.29E-01	36.80									

Table 2.3. S.T. (Surface Tension, mN/m) data for BL8SY. Surfactant concentration is given in mM units and surface tension measurements were made at nine different mole fractions (y) of BL8SY. All solutions were made with 0.01 M NaCl.

[BL8SY] mM	[CPC] mM	S.T. y= 0.380	[BL8SY] mM	[CPC] mM	S.T. y= 0.278	[BL8SY] mM	[CPC] mM	S.T. y= 0.169	[BL8SY] mM	[CPC] mM	S.T. y= 0.058	[CPC] mM	S.T. y=0
		70.82			71.52			71.81			71.02		70.82
7.25E-04	1.18E-03	57.62	4.47E-04	1.16E-03	59.19	2.26E-04	1.11E-03	62.04	7.21E-05	1.17E-03	65.88	6.11E-03	58.21
1.45E-03	2.37E-03	53.91	8.94E-04	2.33E-03	56.55	4.51E-04	2.21E-03	59.00	1.44E-04	2.34E-03	63.81	1.22E-02	55.18
2.17E-03	3.55E-03	52.06	1.34E-03	3.49E-03	54.01	6.77E-04	3.32E-03	57.72	2.16E-04	3.51E-03	60.27	2.44E-02	51.18
2.90E-03	4.73E-03	50.69	1.79E-03	4.65E-03	53.03	9.03E-04	4.43E-03	54.79	2.88E-04	4.68E-03	58.11	3.65E-02	49.14
3.62E-03	5.91E-03	49.62	2.23E-03	5.82E-03	51.96	1.13E-03	5.53E-03	53.71	3.60E-04	5.85E-03	56.55	4.85E-02	47.49
5.43E-03	8.86E-03	47.29	3.35E-03	8.72E-03	49.72	1.69E-03	8.29E-03	51.47	5.40E-04	8.77E-03	54.30	6.05E-02	46.13
7.23E-03	1.18E-02	45.45	4.46E-03	1.16E-02	48.07	2.25E-03	1.11E-02	49.62	7.20E-04	1.17E-02	52.54	7.24E-02	44.87
1.08E-02	1.77E-02	43.33	6.69E-03	1.74E-02	45.36	3.38E-03	1.66E-02	47.49	1.44E-03	2.33E-02	49.24	9.61E-02	42.94
1.44E-02	2.36E-02	41.79	8.90E-03	2.32E-02	43.62	4.50E-03	2.21E-02	45.84	2.15E-03	3.49E-02	46.13	1.20E-01	42.08
2.16E-02	3.53E-02	39.48	1.33E-02	3.47E-02	41.11	6.73E-03	3.30E-02	43.23	3.56E-03	5.79E-02	43.23	1.48E-01	40.15
3.58E-02	5.85E-02	38.04	2.21E-02	5.75E-02	38.04	1.12E-02	5.48E-02	40.44	7.05E-03	1.14E-01	38.90	1.77E-01	39.58
7.08E-02	1.16E-01	38.04	4.37E-02	1.14E-01	37.94	2.21E-02	1.08E-01	38.42	1.38E-02	2.24E-01	39.00	2.33E-01	39.48
1.38E-01	2.26E-01	37.94	8.55E-02	2.23E-01	38.14	3.28E-02	1.61E-01	38.33	2.02E-02	3.28E-01	38.90	2.88E-01	39.19
2.03E-01	3.32E-01	37.94	1.25E-01	3.27E-01	38.04	4.33E-02	2.12E-01	38.33	3.23E-02	5.24E-01	38.90	3.42E-01	39.19
3.24E-01	5.29E-01	37.94	2.00E-01	5.21E-01	38.04	6.35E-02	3.12E-01	38.42				4.46E-01	39.58
			2.69E-01	7.01E-01	38.04	1.02E-01	4.99E-01	38.42				5.45E-01	39.48
						1.37E-01	6.71E-01	38.42				7.32E-01	39.58
												9.84E-01	39.58

Table 2.3. Continued.

[BM8SY] mM	S.T. y=1	[BM8SY] mM	[CPC] mM	S.T. y= 0.834	[BM8SY] mM	[CPC] mM	S.T. y= 0.749	[BM8SY] mM	[CPC] mM	S.T. y= 0.664	[BM8SY] mM	[CPC] mM	S.T. y= 0.505	[BM8SY] mM	[CPC] mM	S.T. y= 0.458
	71.02			69.93			71.91			70.92			69.73			71.52
9.45E-04	50.30	1.47E-03	2.92E-04	44.58	8.88E-04	2.98E-04	49.24	6.01E-04	3.04E-04	49.62	3.09E-04	3.02E-04	52.15	2.54E-04	3.01E-04	0.00
1.89E-03	44.87	2.94E-03	5.84E-04	40.54	1.78E-03	5.96E-04	44.10	1.20E-03	6.09E-04	45.16	6.18E-04	6.05E-04	52.15	5.08E-04	6.02E-04	56.06
2.83E-03	41.79	4.40E-03	8.77E-04	37.56	2.66E-03	8.93E-04	41.21	1.80E-03	9.13E-04	42.08	1.24E-03	1.21E-03	44.39	1.02E-03	1.20E-03	48.94
4.72E-03	37.66	5.87E-03	1.17E-03	35.94	3.55E-03	1.19E-03	39.19	2.40E-03	1.22E-03	40.44	1.85E-03	1.81E-03	42.17	2.03E-03	2.41E-03	44.49
7.07E-03	35.27	8.81E-03	1.75E-03	35.36	5.33E-03	1.79E-03	36.60	3.60E-03	1.83E-03	38.81	2.47E-03	2.42E-03	41.98	3.05E-03	3.61E-03	41.02
9.43E-03	33.93	1.17E-02	2.34E-03	34.79	7.10E-03	2.38E-03	35.55	4.80E-03	2.43E-03	36.60	3.71E-03	3.63E-03	39.19	5.08E-03	6.02E-03	37.27
1.88E-02	33.74	1.76E-02	3.50E-03	34.50	1.06E-02	3.57E-03	35.08	7.20E-03	3.65E-03	34.50	6.17E-03	6.04E-03	36.32	2.02E-02	2.40E-02	36.32
2.82E-02	33.55	2.93E-02	5.84E-03	34.79	1.77E-02	5.95E-03	34.60	1.20E-02	6.08E-03	34.41	1.23E-02	1.21E-02	35.65	5.02E-02	5.95E-02	36.41
4.67E-02	33.65	5.86E-02	1.17E-02	34.79	3.54E-02	1.19E-02	34.50	2.40E-02	1.21E-02	34.60	2.46E-02	2.41E-02	35.74	9.93E-02	1.18E-01	36.32
6.97E-02	33.46	1.17E-01	2.33E-02	34.31	7.07E-02	2.37E-02	34.50	4.78E-02	2.42E-02	34.50	6.11E-02	5.97E-02	35.65			
9.25E-02	33.36	2.90E-01	5.78E-02	34.22	1.76E-01	5.89E-02	34.50	1.19E-01	6.01E-02	34.60						
1.81E-01	33.27				3.47E-01	1.16E-01	34.50									
2.66E-01	33.17															

Table 2.4. S.T. (Surface Tension, mN/m) data for BM8SY. Surfactant concentration is given in mM units and surface tension measurements were made at nine different mole fractions (y) of BM8SY. All solutions were made with 0.01 M NaCl.

[BM8SY] mM	[CPC] mM	S.T. y= 0.377	[BM8SY] mM	[CPC] mM	S.T. y= 0.291	[BM8SY] mM	[CPC] mM	S.T. y= 0.172	[BM8SY] mM	[CPC] mM	S.T. y= 0.051	[CPC] mM	S.T. y=0
		71.91			72.11			70.33			71.42		70.62
1.78E-04	2.93E-04	66.37	1.18E-04	2.88E-04	67.95	6.06E-05	2.91E-04	64.50	6.35E-05	1.18E-03	66.37	1.19E-03	67.26
3.56E-04	5.87E-04	59.39	2.36E-04	5.77E-04	65.39	1.21E-04	5.83E-04	61.45	1.27E-04	2.35E-03	59.39	2.37E-03	64.40
5.33E-04	8.80E-04	54.30	3.55E-04	8.65E-04	55.28	1.82E-04	8.74E-04	57.72	1.90E-04	3.53E-03	56.25	3.55E-03	63.02
7.11E-04	1.17E-03	52.54	4.73E-04	1.15E-03	52.45	2.42E-04	1.17E-03	56.06	3.17E-04	5.87E-03	52.35	5.92E-03	61.16
1.07E-03	1.76E-03	47.59	7.09E-04	1.73E-03	49.24	3.63E-04	1.75E-03	54.30	4.75E-04	8.80E-03	48.94	1.18E-02	57.13
1.42E-03	2.35E-03	45.94	9.45E-04	2.31E-03	47.88	4.85E-04	2.33E-03	50.99	6.33E-04	1.17E-02	46.71	2.36E-02	53.13
2.13E-03	3.52E-03	42.75	1.42E-03	3.46E-03	45.16	7.27E-04	3.49E-03	48.07	1.26E-03	2.34E-02	41.50	3.53E-02	50.69
3.55E-03	5.86E-03	39.38	2.36E-03	5.76E-03	41.50	1.21E-03	5.82E-03	44.10	1.89E-03	3.50E-02	38.90	5.86E-02	47.39
7.10E-03	1.17E-02	36.32	4.72E-03	1.15E-02	36.51	2.42E-03	1.16E-02	39.19	3.14E-03	5.81E-02	36.70	8.74E-02	44.29
1.42E-02	2.34E-02	36.22	9.41E-03	2.30E-02	36.32	4.83E-03	2.32E-02	35.74	4.68E-03	8.67E-02	36.70	1.16E-01	42.46
3.51E-02	5.80E-02	36.22	2.34E-02	5.70E-02	36.32	1.67E-02	8.03E-02	36.13	6.20E-03	1.15E-01	36.70	2.26E-01	39.10
6.95E-02	1.15E-01	36.22	4.62E-02	1.13E-01	36.32	3.06E-02	1.47E-01	36.22	1.21E-02	2.25E-01	37.18	3.32E-01	39.10
									2.84E-02	-2.56E-01	37.66	5.30E-01	39.10

Table 2.4. Continued.

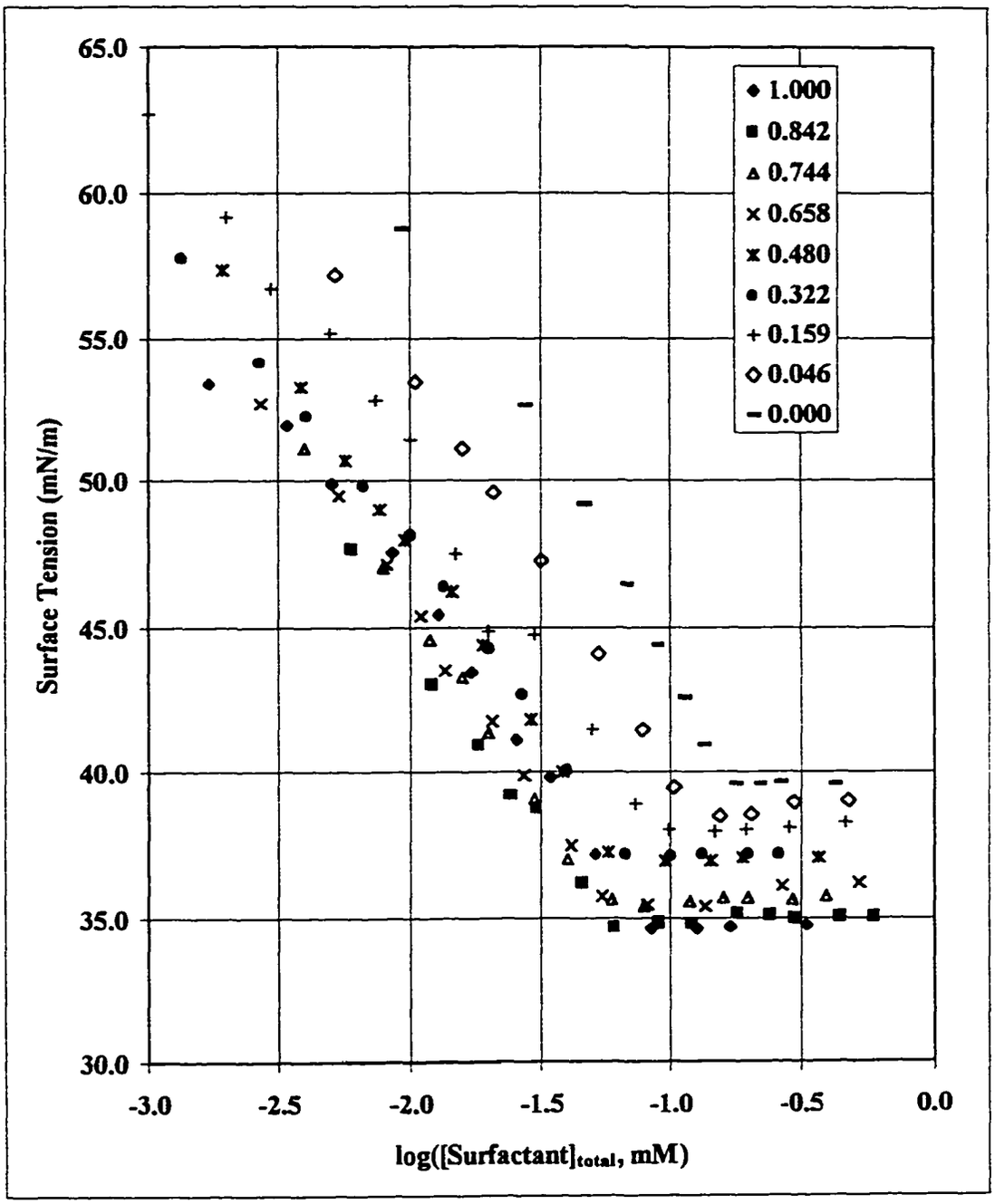

Figure 2.2. Log(total surfactant concentration) vs surface tension used to determine CMC for BL7SY/CPC mixtures in 0.01 M NaCl. The values in the legend are the mole fractions of nonionic surfactant.

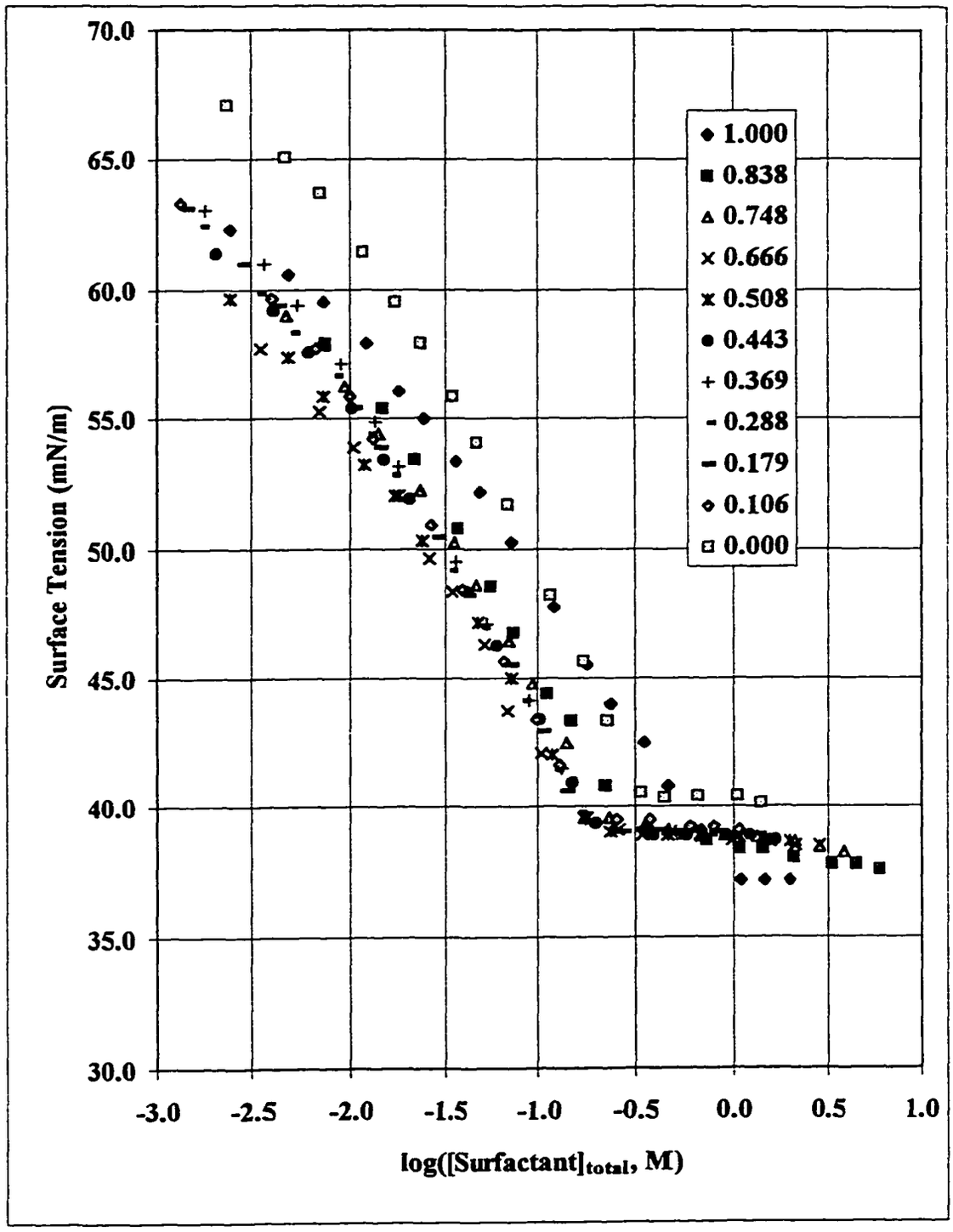

Figure 2.3. Log(total surfactant concentration) vs surface tension used to determine CMC for BD8SY/CPC mixtures in 0.01 M NaCl. The values in the legend are the mole fractions of nonionic surfactant.

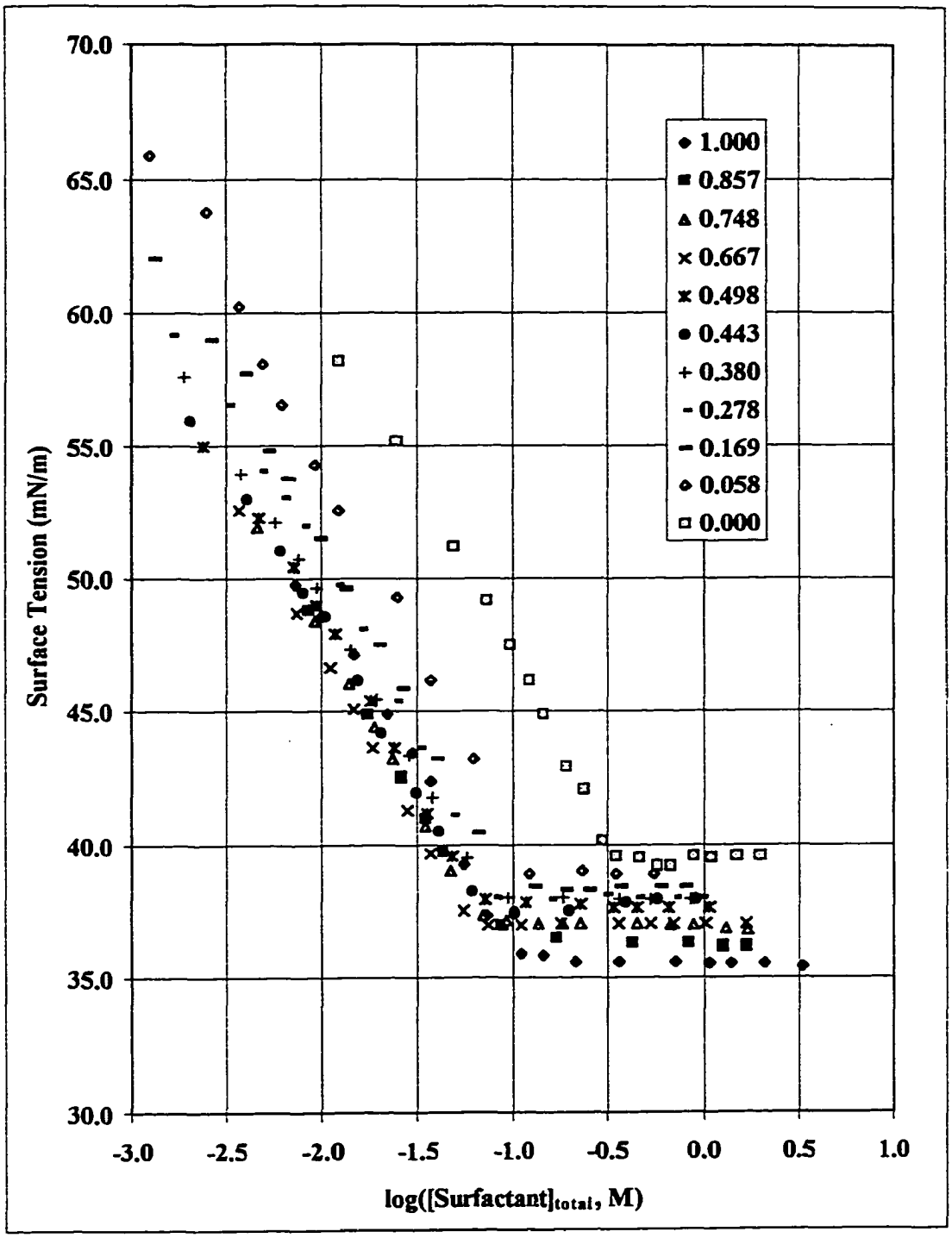

Figure 2.4. Log(total surfactant concentration) vs surface tension used to determine CMC for BL8SY/CPC mixtures in 0.01 M NaCl. The values in the legend are the mole fractions of nonionic surfactant.

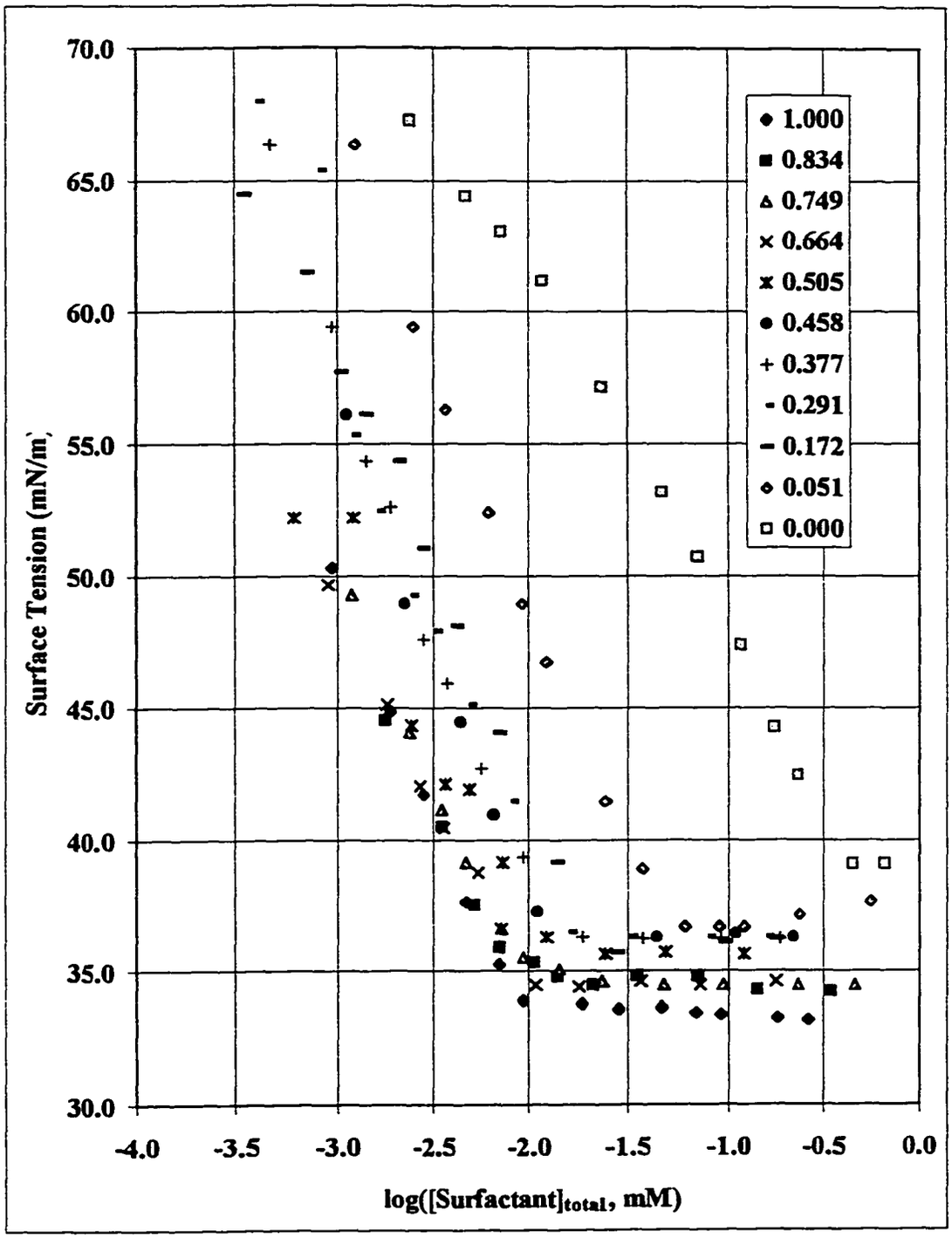

Figure 2.5. Log(total surfactant concentration) vs surface tension used to determine CMC for BM8SY/CPC mixtures in 0.01 M NaCl. The values in the legend are the mole fractions of nonionic surfactant.

Table 2.5

y_{BL7SY}	CMC_{mix}
0.000	1.57E-01
0.046	1.14E-01
0.159	8.46E-02
0.322	6.08E-02
0.480	5.90E-02
0.658	5.50E-02
0.744	5.34E-02
0.842	5.90E-02
1.000	8.21E-02

Table 2.6

y_{BD8SY}	CMC_{mix}
0.000	1.74E-01
0.105	1.92E-01
0.179	1.83E-01
0.288	1.92E-01
0.369	1.92E-01
0.443	2.17E-01
0.508	2.02E-01
0.748	2.54E-01
0.838	3.17E-01
1.000	9.70E-01

Table 2.7

y_{BL8SY}	CMC_{mix}
0.000	1.65E-01
0.058	1.22E-01
0.169	9.07E-02
0.278	8.05E-02
0.380	7.43E-02
0.443	6.39E-02
0.498	6.08E-02
0.667	5.84E-02
0.748	6.39E-02
0.857	7.81E-02
1.000	9.35E-02

Table 2.8

y_{BM8SY}	CMC_{mix}
0.000	1.83E-01
0.051	4.98E-02
0.172	2.02E-02
0.290	1.58E-02
0.377	1.29E-02
0.458	1.23E-02
0.505	1.17E-02
0.664	1.01E-02
0.749	9.10E-03
0.834	7.83E-03
1.000	7.45E-03

Tables 2.5-2.8. The critical micelle concentrations for mixtures of different mole fractions (y) of nonionic surfactant. CMC values were determined by inspection of individual plots of log([total surfactant concentration]) vs surface tension similar to those shown in Figures 2.2-2.5. All measurements were made in 0.01 M NaCl.

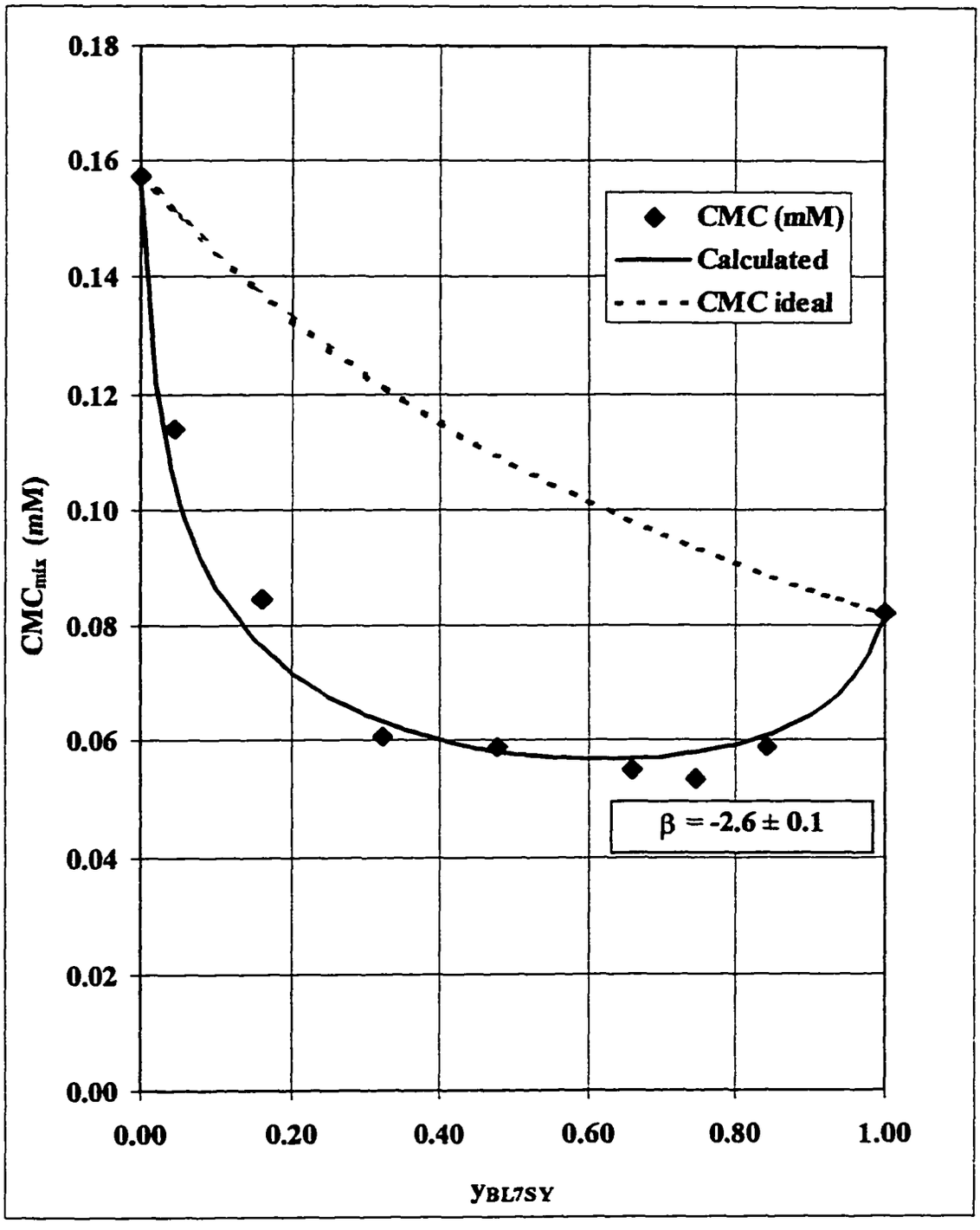

Figure 2.6. CMC vs mole fraction BL7SY with a line representing the fit of the one parameter model for BL7SY/CPC mixtures in 0.01 M NaCl.

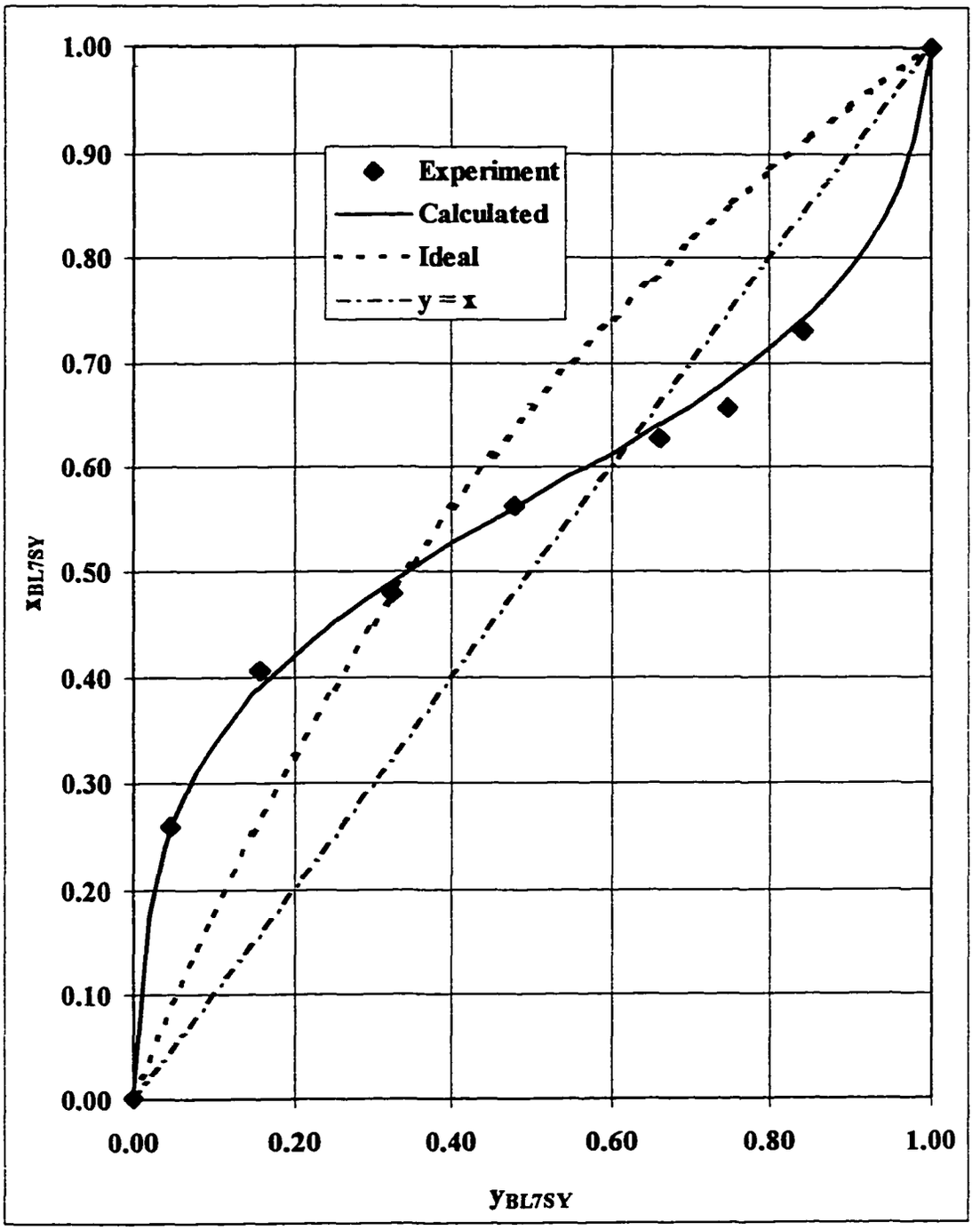

Figure 2.7. Mole fraction of BL7SY in the micelle vs total mole fraction with a line representing the fit of the one parameter model in 0.01 M NaCl.

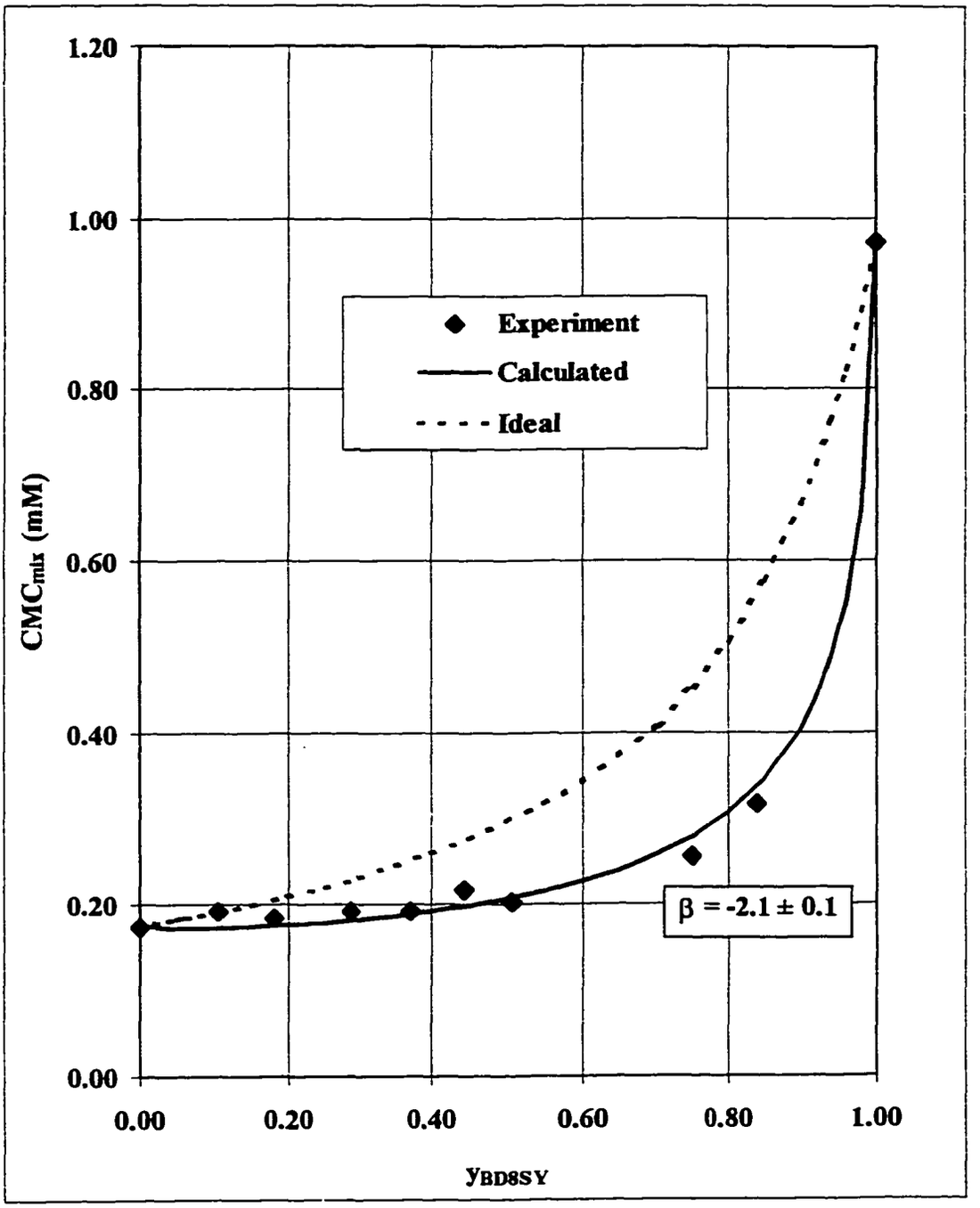

Figure 2.8. CMC vs mole fraction BD8SY with a line representing the fit of the one parameter model for BD8SY/CPC mixtures in 0.01 M NaCl.

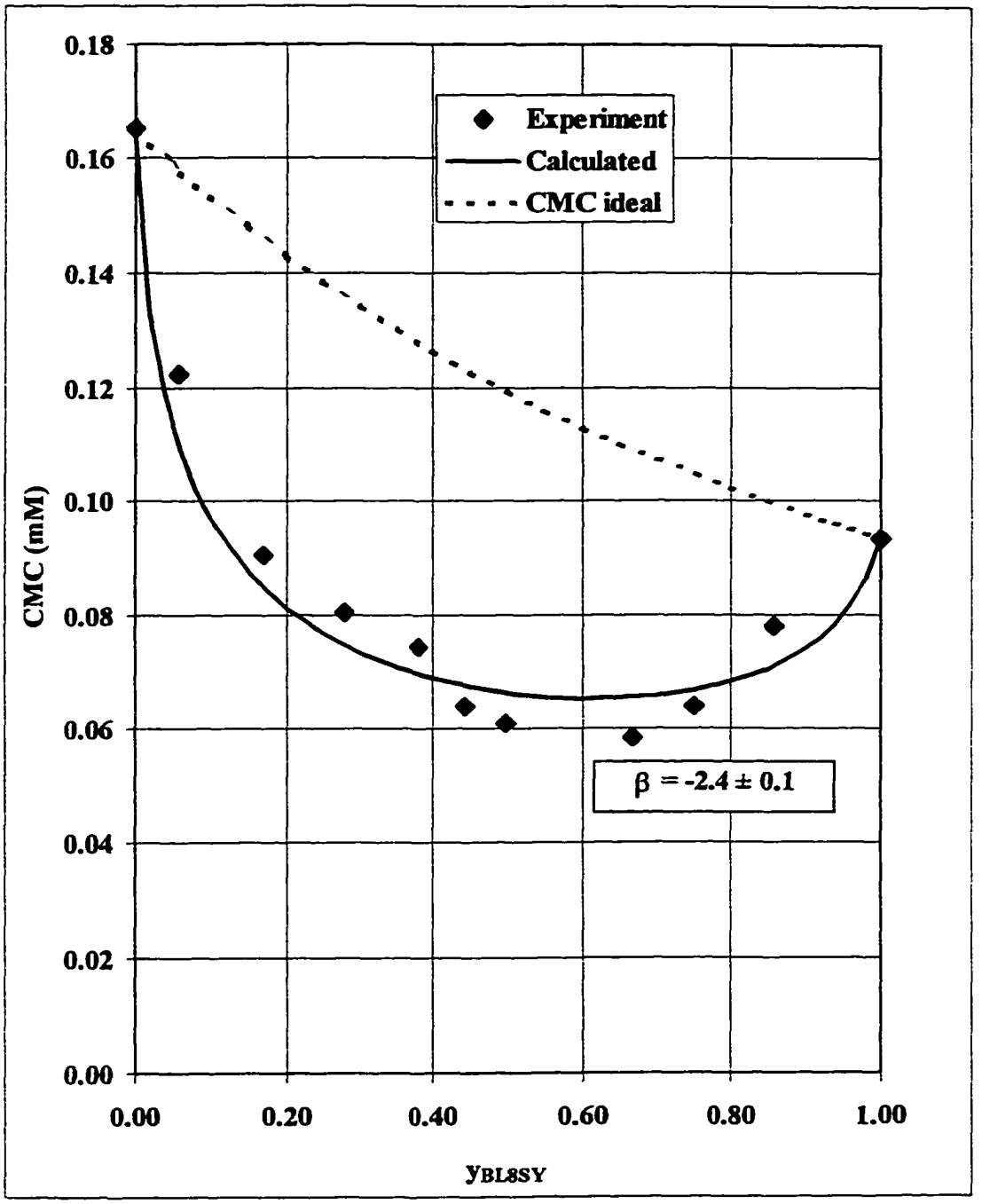

Figure 2.9. CMC vs mole fraction BL8SY with a line representing the fit of the one parameter model for BL8SY/CPC mixtures in 0.01 M NaCl.

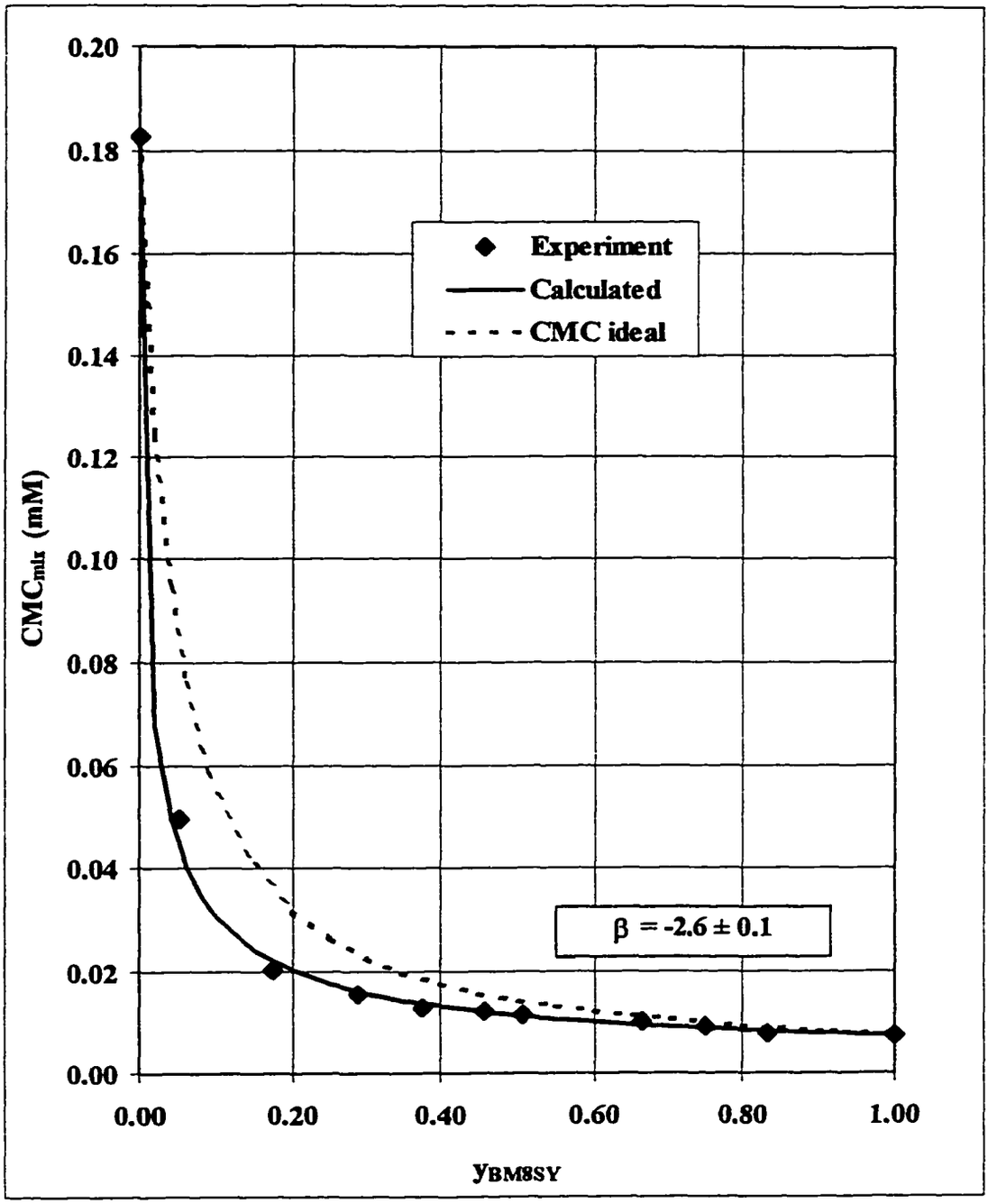

Figure 2.10. CMC vs mole fraction BM8SY with a line representing the fit of the one parameter model for BM8SY/CPC mixtures in 0.01 M NaCl.

Nonionic Surfactant	Ethylene oxide subunits	Carbon Tail Length	β parameter
BL7SY	7	12	-2.6 ± 0.1
BD8SY	8	10	-2.1 ± 0.1
BL8SY	8	12	-2.4 ± 0.1
BM8SY	8	14	-2.6 ± 0.1

Table 2.9. β parameters calculated based on the one parameter model for *nonionic ethylene oxides in mixed micelles with CPC.* All measurements were made in 0.01 M NaCl.

In Figures 2.7 – 2.10 the experimental and fitted results are always below the curve calculated from ideality and, in Table 1.9, the magnitude of β increases as deviation from ideality increases. Thus, an enhanced interaction or synergism between the two types of surfactants results in a greater negative deviation from ideality. The results in Table 2.9 show that there is a trend towards increasing interaction with CPC (having a C16 hydrocarbon tail length) as the length of the hydrocarbon tail of the nonionic surfactant increases from 10 to 14 carbons. In addition, the interaction appears to increase in strength, as the number of ethylene oxide (EO) subunits decreases from 8 to 7. A major conclusion, however, is that the β values are all in the range –2.1 to –2.6 for the systems studied here.

The model used to determine the fitting parameter has been applied by other workers to cationic/nonionic (6-10), anionic/nonionic (1-13, 15-18) and

nonionic/nonionic (7) surfactant systems. Most of the published work involves anionic/nonionic mixtures and very few data have been published on cationic/nonionic systems (6-10) similar to the surfactants used here. None of the results specifically matches the systems studied here. Holland and Rubingh (8) made an interesting comparison between a C10-anionic/EO4 mixture and C10-cationic/EO4 mixture showing that the anionic/nonionic interaction parameter was much greater (β = -4.81 vs β = –1.8).

In the reported studies of cationic/nonionic systems (6-10) there were no systematic attempts to characterize a series of cationic surfactant tail lengths or EO chain length. To confuse the matter, some of the work is done using pure water and some is done with salt solutions ranging from 0.05 – 2.4 M NaCl to 0.05 M NaBr. However, some generalizations can be made by comparing results. Rosen (17) showed by measuring C12PyrCl/C12EO8 (Pyr represents a pyridinium head group) in water, 0.1 M NaCl and 0.5 M NaCl that the interaction enhancement decreases as salt concentration increases (β = -2.7, β = -1.4, and β = -1.0 respectively).

Scamehorn et al. (7) showed that the synergism increases from β = -1.3 to β = -1.7 when the chain length of the hydrocarbon tail of the cationic surfactant is increased from C12 to C16 for the two systems C12PyrCl/NPE10 and C16PyrCl/NPE10 (both at 0.03 M NaCl; NPE represents nonyl phenol ethoxylates). Although the polyethylene oxide surfactant was polydisperse, the results demonstrate that the enhancement increases with carbon tail length of the cationic surfactant.

These results agree with the results in Table 2.9, which show that increasing the hydrocarbon tail length of the nonionic surfactant also increases the synergism of the mixture.

Most of the mixed micelle work published concerning nonionic polyethylene oxide surfactants has been mixtures with anionic surfactants (5). Lange and Beck (9) showed that increasing the ethylene oxide subunit from EO6 to EO12 for the systems C12SO4Na/C8EO6 C12SO4Na/C8EO12 (in water) increased the synergism from β = -3.4 to β = -4.1. This work appears to be contrary to the results in Table 2.9 where a decrease in EO subunit from 8 to 7 results in an increase in synergism from β = -2.4 to β = -2.6. However, it is important that for a relatively modest change in synergism ($\Delta\beta$ = 0.7) was observed in increasing the number of EO subunits from 6 to 12, while an even smaller change ($\Delta\beta$ = -0.2) was seen in increasing from EO7 to EO8. Thus in neither case is there a very large dependence on the number of EO subunits. Furthermore, the difference between the results for EO7 to EO8 in Table 2.9 is nearly covered by the error associated with each β value.

Conclusions

A series of nonionic polyethylene oxide surfactants has been studied in mixtures with the cationic surfactant cetylpyridinium chloride (CPC). It has been shown that the CMC behavior of mixtures of polyethylene oxide surfactants with

cetylpyridinium chloride deviates greatly from that of an ideal mixture. Binary mixtures of the surfactants were used to determine the β parameter, which is an indicator of the magnitude of the enhanced micelle formation. The more negative the value of the interaction parameter the stronger the interaction between the two surfactants. The results indicate that as the carbon chain length of the nonionic surfactant increases the interaction with CPC also increases. In addition, it is possible that the interaction increases as the number of ethylene oxide subunits decreases in the nonionic surfactant. The results are comparable to data for similar (cationic/nonionic) mixtures reported by other researchers.

References

1) ACS Symposium Series 311, *Phenomena in Mixed Surfactant Systems*, **1986**, Scamehorn, J.F., Ed., American Chemical Society, Washington, D.C., p 11.
2) Christian, S.D.; Tucker, E.E.; Scamehorn, J.F. In *ACS Symposium Series 501, Mixed Surfactant Systems*, **1992**, Holland, P.M. and Rubingh, D.N., Eds., American Chemical Society, Washington, D.C., pp 45-51.
3) Surfactant Science Series, Volume 46, *Mixed Surfactant Systems*, Ogino, K. and Abe, M., Eds., **1993**, Marcel Dekker, Inc.,New York.
4) Rosen, M.J. "Predicting Synergism in Binary Mixtures of Surfactants", Prog. Coll. Poly. Sci., **1994**, 95, 39-47.
5) Holland, P.M. In ACS Symposium Series 501, *Mixed Surfactant Systems*, **1992**, Holland, P.M. and Rubingh, D.N., Eds., American Chemical Society, Washington, D.C., pp 31-44.
6) Rubingh, D.N. In *Solution Chemistry of Surfactants*, Mittal, K.L., Ed.; Plenum Press, New York, NY, **1979**, Vol. 3, 96-97.
7) Nguyen, C.M.; Rathman, J.F.; Scamehorn, J.F. "Thermodynamics of Mixed Micelle Formation" J. Coll. Int. Sci., **1986**, 112(2), 438-446
8) Holland, P.M.; Rubingh, D.N. "Nonideal Multicomponent Mixed Micelle Model" J. Phys. Chem., **1983**, 87, 1984-1990.
9) Lange, H.; Beck, K.H. "Zur Mizellbildung in Mischlosungen homologer und nichtomologer Tenside", Kolloid-Z.u.Z. Polyere, **1973**, 251, 424-431.
10) Rosen, M.J. In ACS Symposium Series 311, *Phenomena in Mixed Surfactant Systems*, **1986**, Scamehorn, J.F., Ed., American Chemical Society, Washington, DC., p 11.
11) Graciaa, A.P.; Lachaise, J.; Schecter, R.S. In Surfactant Science Series, Volume 46, *Mixed Surfactant Systems*, Ogino, K. and Abe, M., Eds., **1993**, Marcel Dekker, Inc.,New York
12) Ingram, B.T.; Luckhurst, A.H.W. In *Surface Active Agents*; SCI Symposium Proceeding, SCI: London, **1979**, 89.
13) Christian, S.D.; Tucker, E.E.; Smith, G.A.; Bushong, D.S. "Calculation of Organic Solute and Surfactant Activities from Solubilization Data" J. Coll. Int. Sci., **1986**, 113, 439-448.
14) Smith, G.A.; Ph.D. Dissertation, University of Oklahoma, **1986**.
15) Hildebrand, J.H.; Scott, R.L. *Solubility of Nonelectrolytes*, 3rd. Ed, Reinhold: New York, **1950**.
16) Scamehorn, J.F.; Harwell, J.H. In Surfactant Science Series, Volume 46, *Mixed Surfactant Systems*, Ogino, K. and Abe, M., Eds., **1993**, Marcel Dekker, Inc.,New York.
17) Rosen, M.J.; Hua, X.Y. "Conditions for Synergism in Surface Tension Reduction Effectiveness in Binary Mixtures of Surfactants", J. Coll. Int. Sci., **1988**, 125(2), 730-732.

18) Rosen, M.J.; Hua, X.Y. "Synergism in Binary Mixtures of Surfactants", J. Coll. Int. Sci., **1982**, 90(1), 212-219.
19) Rosen, M.J.; Hua, X.Y. "Surface Concentrations and Molecular Interactions in Binary Mixtures of Surfactants", J. Coll. Int. Sci., **1982**, 86(1), 164-172.

Appendix to Chapter 2.

Following is a listing of the least-squares program used to calculate a value for β based on the model presented in the discussion section of this chapter. The program is coded in True BASIC. After the user provides an initial estimate for β, the program proceeds according to the following basic outline.

1) A value of xx (x_B) that corresponds to the β, y_B values is determined for each point in the CMC_{mix}, y_B data set.

2) A calculated CMC_{mix}, cmcpr(i), is determined for each point in the data set based on x_B, y_B, and β.

3) The sum of the squares of the relative difference between experimental and calculated CMCs is determined:

$$s = s + (cmc(i) - cmcpr(i))^2/cmc(i)^2.$$

4) If the value of s is lower than the prior value (sbest) then beta is incremented by betastep and the procedure continues back at step 1.

5) If the value of s is worse than the prior value then a minimum has been passed so β is de-incremented and final values are printed.

The increment values for beta and xx, betastep and xstep respectively, can be changed to control how quickly and how accurately the program can determine x_B and β.

Program Listing

```
! BL7SY.TRU
OPTION NOLET
DIM y(100), x(100), cmc(100),cmcpr(100),gamA(100),gamB(100)
x0 = 0
sbest = 10000
betastep = 0.01
xstep = 0.00001

CLEAR
INPUT prompt "Number of data sets? ": n
READ cmcA,cmcB                    ! read in CMC of pure A and pure B
FOR i = 1 TO n
   READ y(i),cmc(i)               ! read in CMC of mixtures
NEXT i
INPUT prompt "initial beta (choose lower than expected beta) " : beta

! DO loop to Find best beta
DO
  cycle = cycle + 1
  ! FOR-NEXT loop to determine the correct xB for each beta, yB
  FOR i = 1 TO N
      LET xx = 0
      DO
         xx = xx + xstep
         gamB(i) = exp(beta*(1-xx)*(1-xx))
         gamA(i) = exp(beta*xx*xx)
         yy = gamB(i)*xx*cmcB/(gamA(i)*(1-xx)*cmcA + gamB(i)*xx*cmcB)
      LOOP UNTIL yy >= y(i) OR xx >= 1
      IF yy >= y(i) THEN
         x(i) = xx
         x0 = xx
         ! PRINT yy,y(i)
      END IF
  NEXT i
  PRINT "CMC","y","cmcpr","x"
  ! calculate CMC, cmcpr(i), for each point
  FOR i = 1 TO N
      cmcpr(i) = cmcA*(1-x(i))*gamA(i) + cmcB*x(i)*gamB(i)
      PRINT cmc(i),y(i),cmcpr(i),x(i)
  NEXT i
  LET s = 0
  ! calculate the sum of the squares of the deviations between
  ! experimental cmc(i) and calculated cmcpr(i)
  FOR i = 1 TO N
      s = s + (cmc(i) - cmcpr(i))^2/cmc(i)^2
  NEXT i
  PRINT "After cycle ";cycle;"s=";s; " beta=";beta
  x0 = .00001
  IF s < sbest THEN sbest = s
  beta = beta + betastep
LOOP UNTIL s > sbest
```

```
PRINT "To PRINT results, press return "
GET KEY a
CLEAR
PRINT
PRINT
beta = beta - betastep
PRINT  "best s = ";sbest;" for beta = ";beta
FOR i = 1 TO N
   x(i) = x(i) - xstep
   gamB(i) = exp(beta*(1-x(i))*(1-x(i)))
   gamA(i) = exp(beta*x(i)*x(i))
   cmcpr(i) = cmcA*(1-x(i))*gamA(i) + cmcB*x(i)*gamB(i)
NEXT i
PRINT
PRINT  "dev","cmc calc","cmc",",y,","xcalc"
PRINT
FOR i = 1 TO N
   PRINT cmcpr(i) - cmc(i), cmcpr(i), cmc(i), y(i) , x(i)
NEXT i

DATA .157, .082       ! CMC of pure cationic, pure nonionic
DATA 0.842,  0.059    ! mole fraction of monomer, CMC
DATA 0.744,  0.053
DATA 0.658,  0.055
DATA 0.480,  0.059
DATA 0.322,  0.061
DATA 0.159,  0.085
DATA 0.046,  0.114

END
```

Chapter 3

The Inverted Vertical Pull

Surface Tension Method

Introduction

General Introduction

The du Noüy ring and Wilhelmy plate methods are the two most common techniques used to determine surface tension at a liquid-air interface, or interfacial tension at a liquid-liquid interface. Wilhelmy's 1863 publication (2) described measurement of capillary constants by measuring forces using a number of different probe shapes but did not attempt to discuss a detailed calculation of surface tension. In his 1919 paper (1), Lecomte du Noüy pointed out the large discrepancies in results obtained with methods that had been applied prior to that time in determining the surface tensions of pure liquids and presented his new technique. Some of the other techniques were oscillating jet (dynamic), hanging drop, spinning drop, sessile drop, capillary rise and maximum bubble pressure. The key to du Noüy's new apparatus was the use of a torsion wire, which could be twisted to apply torque to a lever arm, from which a ring was suspended in contact with the liquid of interest. In the original

design du Noüy proposed simply calibrating the instrument by measuring the force for maximum pull of pure liquids for which surface tension was known, making the technique useful but still relative. It was not until 1930 that Harkins and Jordan (4) and Freud and Freud (5) published work very carefully analyzing the theory associated with the du Noüy ring. They determined that the technique could be used as a very accurate absolute method. The total force acting on the ring, W_{tot}, can be calculated as

$$W_{tot} = W_{ring} + 4\pi R\gamma_{ideal} \qquad \text{Equation 3.1}$$

where W_{ring} is the weight of the ring, R is the radius of the ring, and γ_{ideal} the surface tension. Harkins and Jordan (4) determined that an empirical correction factor was required because the size (and shape) of the surface inside and outside the ring was not the same, therefore the vertical force components acting on the ring were not symmetrical. The correction factor, f, was determined as a function of the size of the ring, radius R, and the size of the wire of which the ring was made, radius r.

$$\gamma = \gamma_{ideal} \times f(R^3/V, R/r) \qquad \text{Equation 3.2}$$

In 1941 it was pointed out by Zuidema and Waters (6) that an additional correction factor was required in cases when the difference between the densities of the two phases making the interface was small or when the scale readings were relatively high. Zuidema and Waters were mainly investigating the interfacial tension between hydrocarbon and water phases. In these cases, the density difference, $\Delta\rho$, was much lower ($\rho_{water} = 1.00$ g cm^{-3}, $\rho_{decane} = 0.73$ g cm^{-3}, $\rho_{decane} = 0.75$ g cm^{-3}, $\rho_{hexadecane} = 0.77$

g cm^{-3}) than in surface tension measurements where one phase is air (ρ_{air} = 0.001 g cm^{-3}).

The Wilhelmy plate method does not require a correction factor. The force acting on the plate is simply the sum of the surface effect and the buoyant effect of a column of water pulled up under the plate (if the contact angle of the liquid with the plate is zero);

$$W_{tot} = W_{plate} + p\gamma_{ideal} \qquad \text{Equation 3.3}$$

where p is the horizontal perimeter (2 x length + 2 x thickness) of the plate. A buoyant force, $\Delta\rho ghA$ (where h is the height above or below the free liquid level and A is the cross-sectional area of the plate), is added or subtracted if the plate is above or below the level of the free liquid.

A necessary consequence of Newton's third law is that the Wilhelmy, du Noüy, or any force-pull technique can all be performed by weighing the liquid rather than the suspended object. In both the Wilhelmy and the du Noüy techniques (and any other which involves measuring the force acting on a suspended object of any shape) the only previous method used in determining the value of the force has been to measure it from above the liquid. The technique in the present work relies on measuring the force pulling downward on a rod, instead of a ring or plate, for which the radius (and therefore the circumference or perimeter) is accurately known. All previous work has been done by measuring the force acting on a rod (with a balance from above.) For the work presented here, the force is measured as acting on the sample by monitoring the weight change on a top-loading analytical balance.

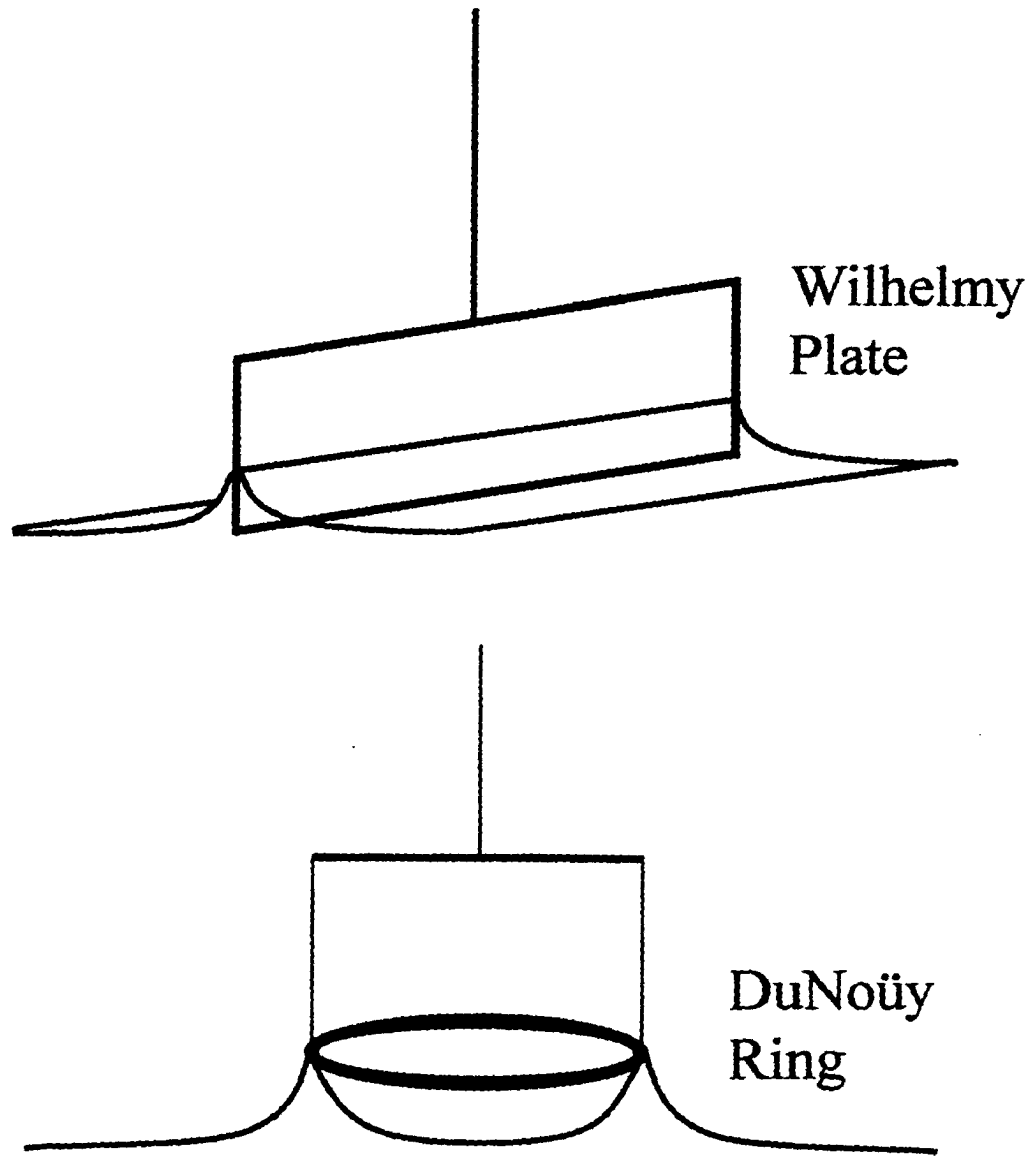

Figure 3.1. Illustrations of Wilhelmy plate and du Noüy ring methods.

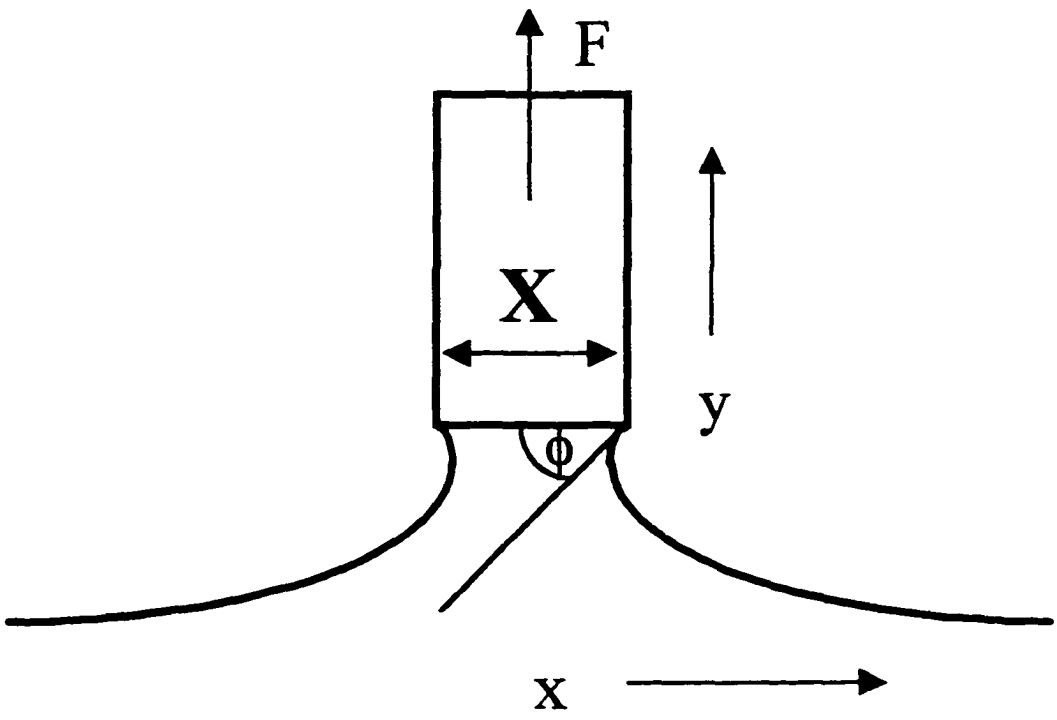

Figure 3.2. The important parameters needed to calculate force for the rod pull method.

$$F = \pi X^2 y \Delta\rho g + 2\pi X\gamma \sin\phi$$

$\Delta\rho$ = density difference (0.998 g cm^{-3})
g = accel. of gravity (980 cm s^{-2})
X = radius of rod (cm)
Y = height above free liquid (cm)
γ = surface tension of liquid (mN/m or dyne/cm)
ϕ = angle of meniscus/horizontal (radians)

The equation for calculating the total force, W_{tot}, acting on the rod is similar to the expressions of total force for the ring and plate,

$$W_{tot} = \pi X^2 Y \Delta\rho g + 2\pi X\gamma \sin\phi. \qquad \text{Equation 3.4}$$

The first term, $\pi X^2 Y \Delta\rho g$, represents the buoyant force due to the volume of water suspended under the rod as it is pulled away from the free surface. The second term, $2\pi X\gamma\sin\phi$, represents the downward force of the surface acting on the rod. The angle, ϕ, changes through the course of a measurement and the value corresponding to the maximum force is determined through numerical integration described in the next section (Theory of the Pull-Force Methods).

In the total weight expression the weight of the rod is not explicitly included, though it was in similar expressions of du Noüy and Wilhelmy methods. The weight of rod is not actually measured in this technique. The weight of the vessel and solution of interest are measured (or tared) on a top loading analytical balance accurate to 0.1 or 1 mg while the rod (or other probe such as a du Noüy Ring or Wilhelmy Plate) is contacted and pulled from above the liquid. When the probe is contacted with the liquid the resulting force on the balance is displayed as a loss of weight.

In the past, (7-11) before the development of top-loading analytical balances that automatically maintain the weighed object in the same vertical position, it was obvious that measuring the downward force on the plate, ring, or rod should be the method of choice. To that end a chainomatic, dialomatic, electro-balance, or the torsion wire used in du Noüy's method may have been the best choice at the time. In those devices the

probe (plate, ring or rod) is suspended from above a liquid surface on a balance lever arm so that the forces are measured as changes in the weight of the probe itself. But now, with accurate top-loading balances available in virtually every science laboratory, one can envision many situations in which weighing the liquid might make the determination of surface tension or interfacial tension more convenient without sacrificing accuracy. Precision of one milligram is sufficient to provide surface tensions to 0.01 mN/m.

Theory of the Pull-Force Methods

Ideally, the surface tension can be calculated by measuring the force and height of the column of water under the rod. The Laplace Equation

$$\Delta \mathbf{P} = \gamma \left(\frac{1}{R_h} + \frac{1}{R_v} \right) \qquad \text{Equation 3.5}$$

must apply continuously on the profiles depicted in Figure 3.2 as the rod is pulled upwards from the free surface. In Equation 3.5, $\Delta \mathbf{P}$ represents the difference in pressure between the liquid inside and outside the column of liquid, R_h and R_v are the principal radii of curvature, on horizontal and vertical planes, respectively, drawn symmetrically on the meniscus and γ is the surface tension of the liquid. From analytical geometry, the radii of curvature may be represented by the following equations in terms of Cartesian coordinates:

$$\frac{1}{R_h} = \frac{y''}{(1+y'^2)^{3/2}} \qquad \text{and} \qquad \frac{1}{R_v} = \frac{y'}{x(1+y'^2)^{1/2}} \qquad \text{Equation 3.6}$$

Here, x and y represent horizontal and vertical positions on the profile, and y' and y" denote the first and second derivatives with respect to x.

The pressure difference Δp may be replaced by $\Delta\rho gy$, where $\Delta\rho$ is the difference in density between the two phases and g is the acceleration of gravity. The symbol y represents the height above what would be the surface of the free liquid (plane liquid level away from the rod). Equation 3.5 may be written as

$$\frac{\Delta\rho gy}{\gamma} = \frac{y''}{(1+y'^2)^{3/2}} + \frac{y'}{x(1+y'^2)^{1/2}} \qquad \text{Equation 3.7}$$

This equation is applicable to any experiment in which the shape of the surface is described, by the radii of curvature, for symmetric figures of revolution. The value of $\sin\phi$ required for Equation 3.4, for the rod-pull method, is given by trigonometric considerations as

$$\sin\phi = \frac{y'}{\sqrt{1+y'^2}} \qquad \text{Equation 3.8}$$

However, for the rod pull method, Equation 3.7 cannot be integrated in closed form and therefore must be integrated numerically. The earliest solution of Equation 3.7 in this particular form was published in 1883 after Bashforth and Adams (3) calculated and tabulated solutions 'by hand' for capillary rise, bubble shape, and drop shapes. Padday (14, 15) used a computer program to integrate the equation and published the tables of data on microfiche form (Padday was employed by Kodak Ltd. in the UK). For the present work, programs (not published) written by Professor S. D. Christian and Dr.

Katsuhiko Fujio have been used and force curves like the one shown in Figure 3.4 will be compared with experimental results.

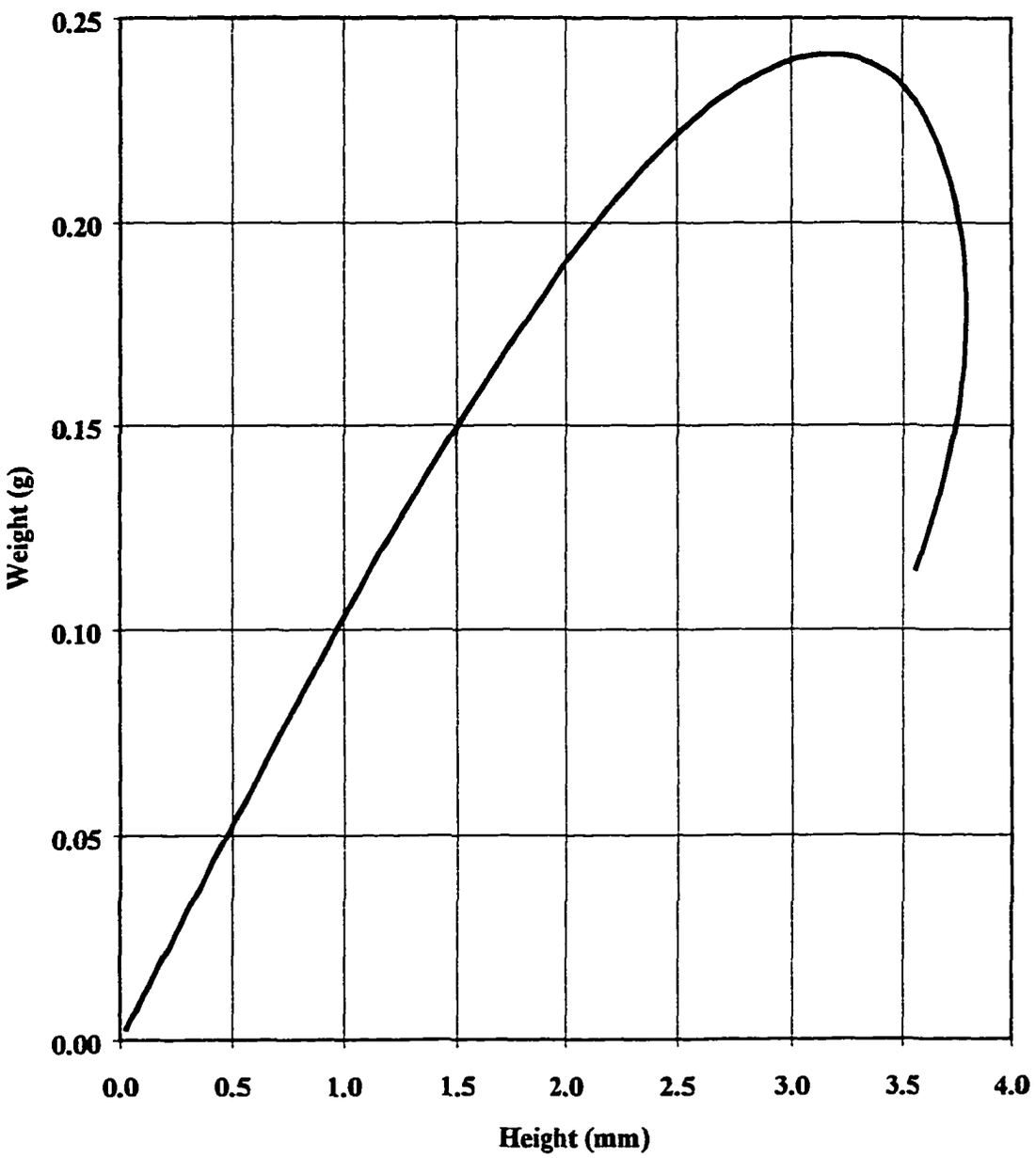

Figure 3.3. Force curve for water (72.3 mN/m @ 23 °C) as a function of rod height above the free surface.

In using the rod-pull method, it is not actually necessary to integrate the force curve each time a surface tension is to be measured. To calculate the surface tension, only the maximum pull (weight), the diameter of the rod, the density of the fluid and the gravitational constant are required. Padday et al. (16) developed a series of 18 polynomial equations to calculate X/k (where X is the radius of the rod and k is the meniscus constant) from measured values of X^3/V. The volume of liquid elevated above the plane surface at maximum pull V, is calculated by dividing the observed maximum weight (force in grams) by the liquid density (ρ in g/cm^3). Padday's equations are somewhat cumbersome to use so a fit was determined in the form of a single quasi polynomial. A single calibration curve for a given rod can be determined instead of the 18 equations of Padday. X/k is then calculated by the following equation.

$$X/k = 2.48573(X^3/V)^{1/2} + 0.70985(X^3/V) + 4.21654(X^3/V)^{3/2} \quad \text{Equation 3.9}$$
$$- 1.94468(X^3/V)^2 + 2.30285(X^3/V)^3 - 2.77894(X^3/V)^4$$
$$+ 1.65453(X^3/V)^5 - 0.420300(X^3/V)^6 + 0.0129372(X^3/V)^8$$

Although this equation has more terms than Padday's 3rd order polynomials this single expression can be easily programmed to facilitate quick determination of surface tensions. The meniscus (or capillary) constant is defined according to the following equation.

$$k = \left(\frac{\gamma}{\rho g}\right)^{1/2} \quad \text{Equation 3.10}$$

Therefore, the surface tension may be calculated easily once the meniscus constant is determined.

Experimental

Two different devices have been used to obtain vertical pull surface tension measurements with cylindrical rods. Figure 3.4 shows the first device, referred to as Inverted Rod Pull (IRP) Tensiometer. The second device, Directional Converted IRP (DCIRP) in Figure 3.5, was constructed to simplify the measurement of small samples, as will be described, but was also determined to be just as useful for measurements in large samples.

Our procedure is a modification of the technique introduced by Padday and others (14,16,21) that we will call the rod-pull method. The steel rod, having a known radius (3.175-mm in this work), is attached to the metal spindle of a high-quality micrometer, allowing reproducible positioning in a vertical direction to within a few microns. In operation, liquid is placed in the specially constructed glass cell, which has an opening large enough to allow unrestricted passage of the rod but small enough to reduce the rate of evaporation of the liquid. The rod is slowly lowered until it contacts the surface, at which point it is raised until the maximum pull is reached. The position corresponding to maximum force can be determined quite accurately by approaching it both from below and above. Figure 3.6 shows the configuration of the meniscus during several phases of the pull. It should be emphasized that there is no ambiguity in determining the position of maximum pull; this weight is determined repetitively on the same sample, without breaking the meniscus.

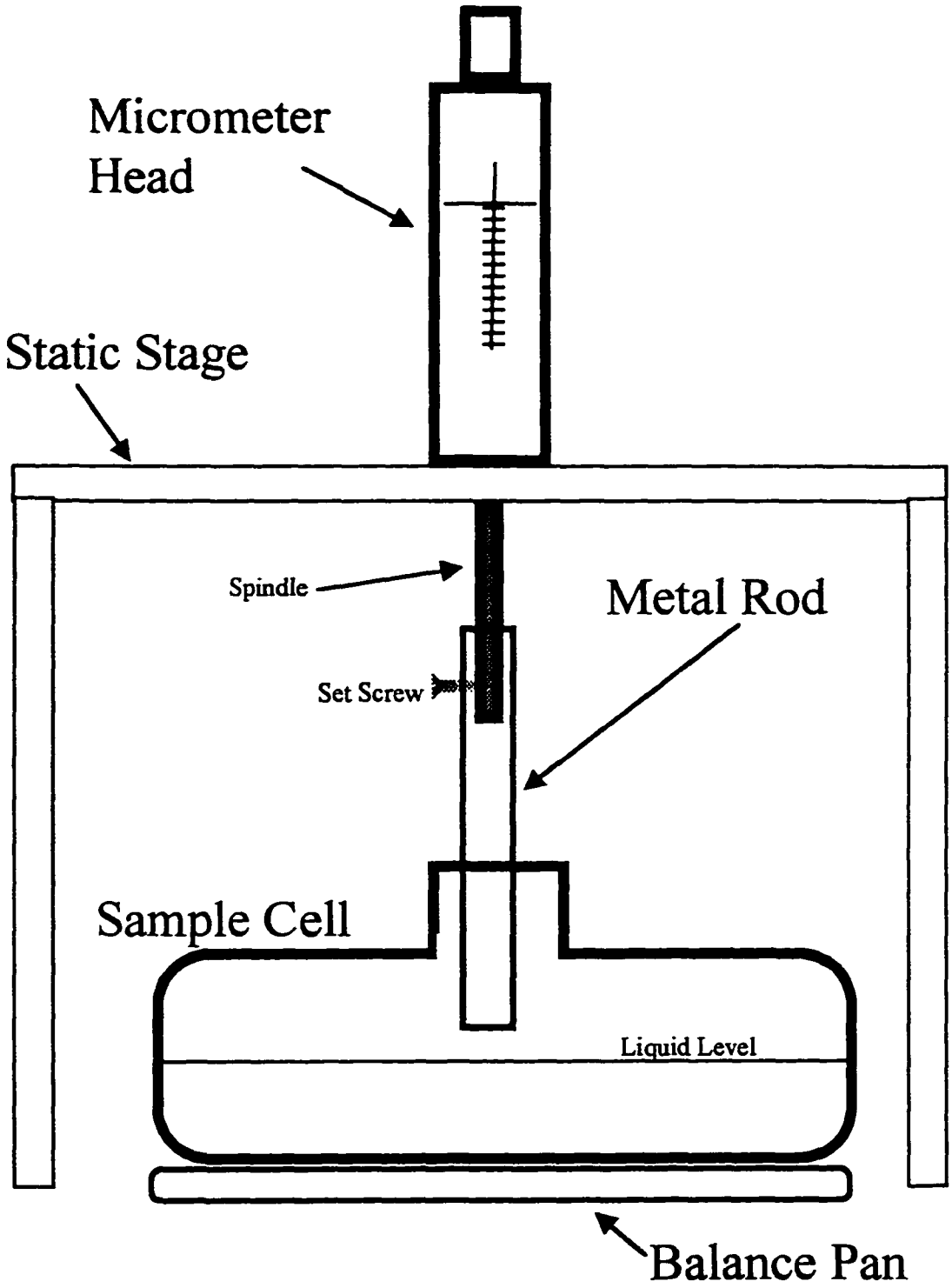

Figure 3.4. Inverse Rod Pull (IRP) Tensiometer: Micrometer and liquid cell arrangement for vertical pull measurement.

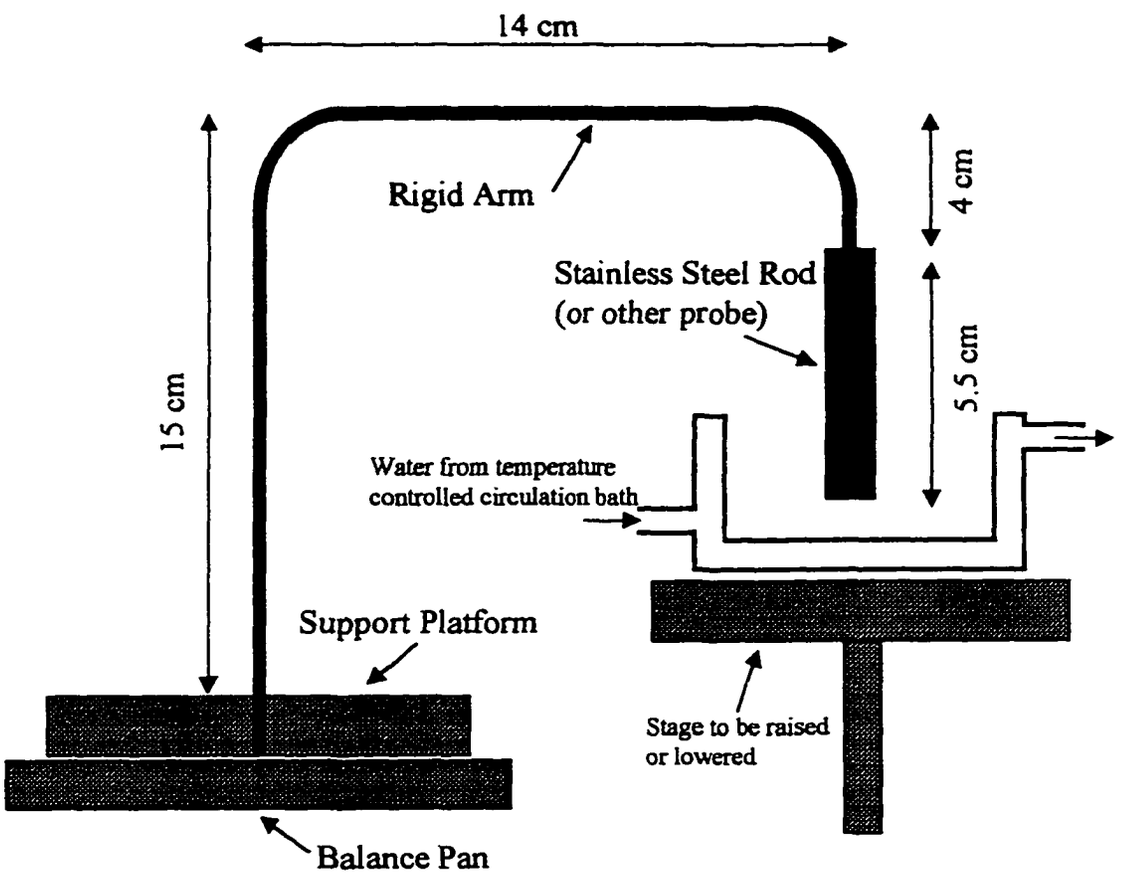

Figure 3.5. Directional Converted Inverse Rod Pull (DCIRP) Tensiometer: Directional force conversion tensiometer.

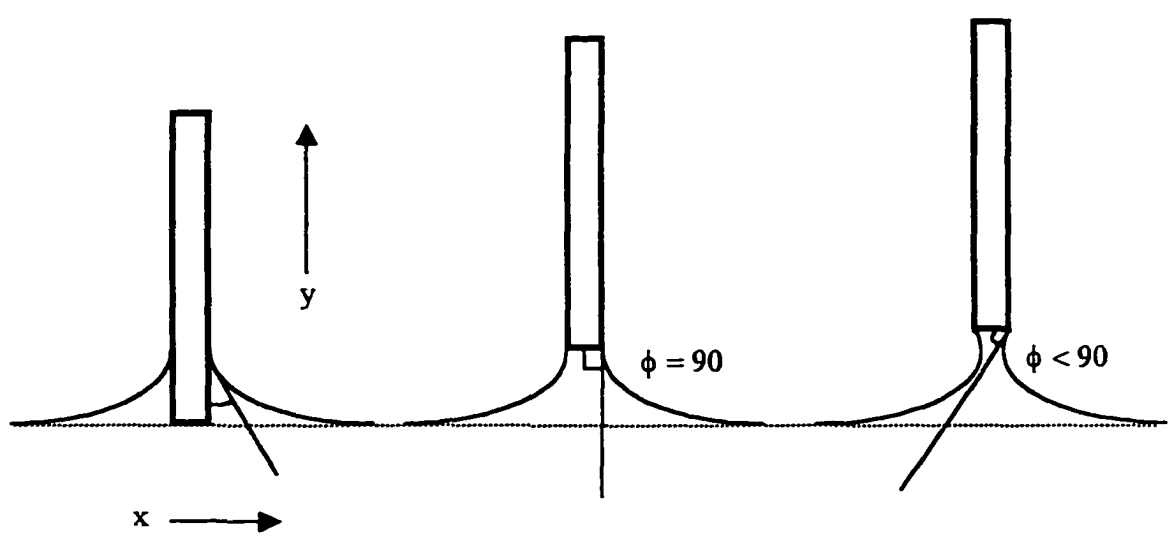

Figure 3.6. Depiction of rod pulling liquid surface.

One critical factor in the rod-pull method is that the sample position remains fixed. To verify that the balance pan did not change its vertical position a cathetometer was used to monitor a mark on the sample flask while the weight was increased by addition of water. The sample flask weighed 65.26 grams and water was added to increase the weight incrementally up to a total mass of water of 50 grams. The mark on the flask was viewed through the cathotometer at a height of 674.38 cm and this position did not change perceptibly through the course of adding water to the flask. The maximum capacity of the flask was approximately 100 grams (or mL of aqueous solution) which gave a total possible maximum load of 165 grams. Since the weight change on the balance through the course of a single experiment was typically in the range of 0.1 to 1.0 grams, it was concluded that the vertical position of the sample never changed during a single force pull measurement.

The micrometer head used in these studies had a 1/8-inch hardened steel spindle onto which a 1/4-inch diameter (3.175-mm radius) stainless steel rod was attached. To attach the 1/4-inch rod to the spindle of the micrometer a 1/8-inch hole was machined into one end and a set screw was used to hold the rod fixed. The end of the rod at which the liquid was contacted was machine polished with sharp edges and then roughened with emery paper to enhance wetting at the end of the rod. The side of the rod was polished smooth in order to reduce wetting on the outside of the rod. The radius of the rod was determined to be 3.175 mm by measuring the diameter with a micrometer. The micrometer head rested on a static stage built of acrylic plastic (1/2-inch thick). The sides of the stage were 15-cm high, the top was 16-cm across and it was 10 cm from

front to back. With these dimensions the apparatus fits easily inside the balance windscreen and straddles the 4-inch balance pan. The glass sample cell was specially constructed. Experiments showed that the evaporation rate (approximately 5 mg/min at 23 °C) of water from aqueous solutions was significant enough to affect the measured weight change during a surface tension measurement when making measurements in an open beaker. Because the rods used in this technique were typically 6-8 mm in diameter, a necked flask of the type depicted in Figure 3.4 with a neck diameter of approximately 1.0-cm was designed. The evaporative rate loss from the necked flask was less than 0.2 mg/min.

Although the radius of the rod was measured (by using calipers) to be 3.175 mm there was a significant variation among different rods in the effective radius which contacted the solution. Because of limitations in machine work on the particular rod used, the end of the rod was not perfectly flat and perpendicular to the edge of the rod, but rather somewhat rounded. The result of this was that the "effective" radius of the rod was determined to be 3.165 mm by assuming the surface tension of water to be 72.3 mN/m at 23 °C. Figure 3.7 is plot of calculated surface tension vs rod radius for a given observed maximum pull of 240.2 mg, showing the importance of very accurately knowing the rod radius.

The capacity of the flask was approximately 50 mL up to the bottom of the neck. Experiments were typically conducted as titration experiments in which 30 to 40-mL of water were initially placed in the flask. The maximum force was measured repeatedly to verify purity of the starting water. After the initial measurement an aliquot of

concentrated surfactant solution (e.g., approximately 10 times higher than the critical micelle concentrations) was added to the water. The total volume was known since the volume of each aliquot added was recorded. Therefore, the concentration was followed as it increased through sequential aliquots.

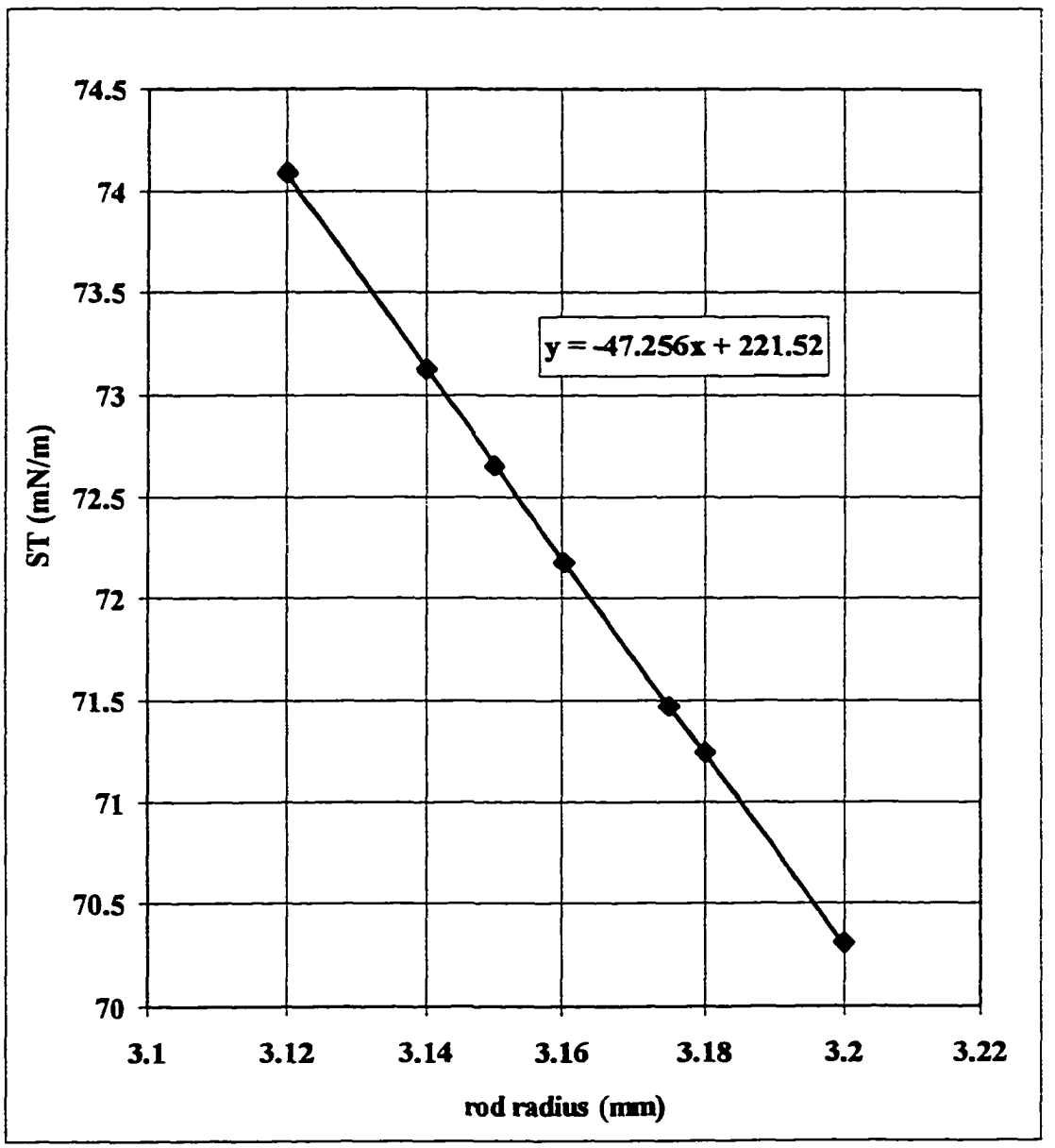

Figure 3.7. The derived value of the surface tension depended dramatically on the rod radius. Calculations were made with a measured force of 240.2 mg.

Force curve measurements using the IRP were generally made by taring the flask with sample in it to give an initial balance reading of zero. Of course the weight of sample (or water) initially in the flask was measured first. The rod/stage apparatus was set over the flask and the rod could be lowered quickly to within approximately 1 mm of the surface since visibility above the surface was clear. In experiments for which the entire force curve was to be measured, it was important to know the height of the end of the rod with respect to the level of the liquid. Therefore, the rod was very slowly lowered to make initial contact with the surface. There were two distinct ways to know when the rod contacted the surface. Visually, looking upward to the bottom of the surface, the instant of contact was immediately obvious. Also, there was a change in the force displayed on the balance (from zero). At the point of contact the dial reading on the micrometer head was recorded and used as the zero point. From this point, the rod was raised in fixed increments (of approximately 0.1 mm). At each height increment, a force measurement was also recorded. A force curve of the shape shown in Figure 3.8 was the result.

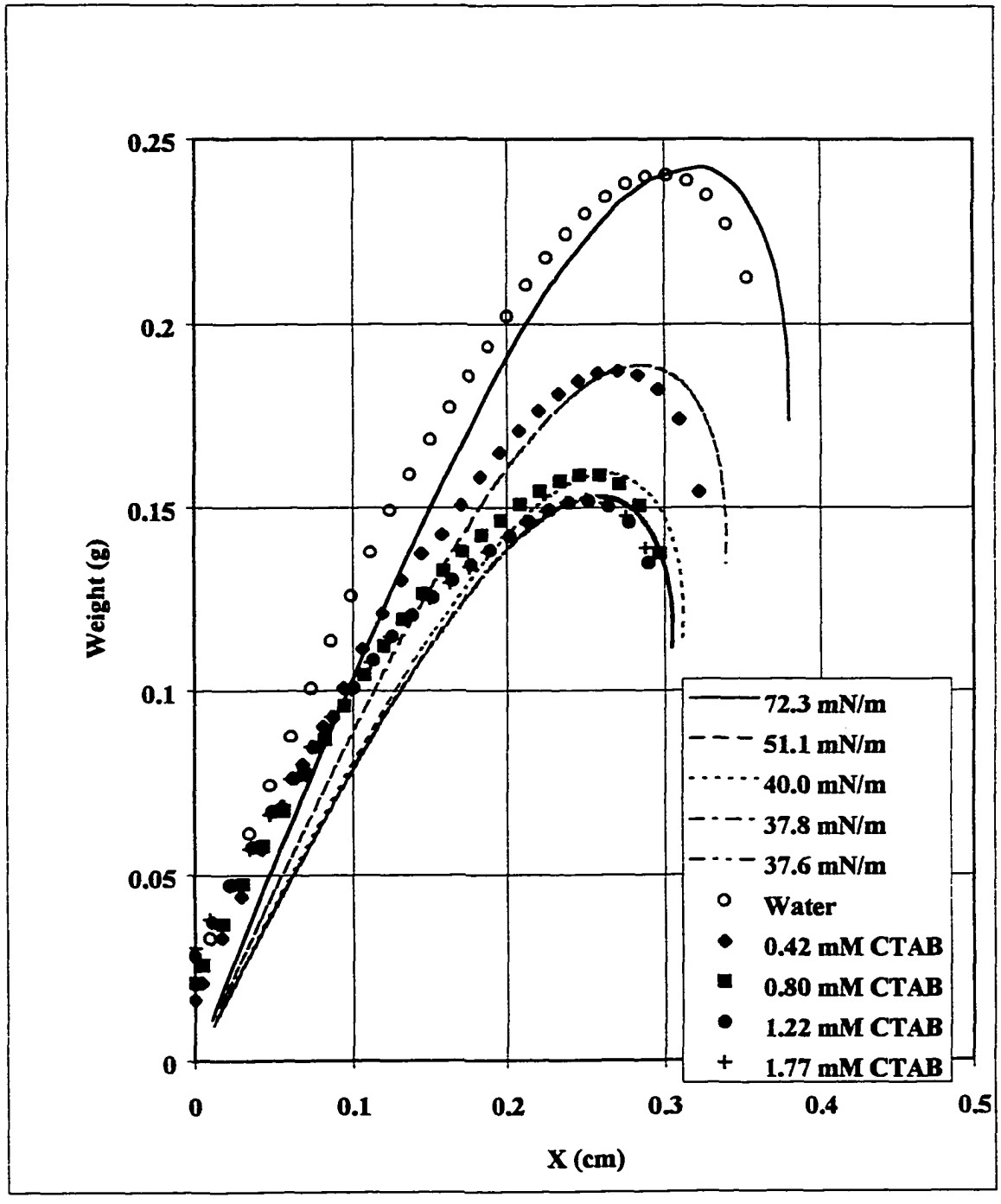

Figure 3.8. Force vs height curves for a series of CTAB solutions. Lines are calculated from theory (knowing the surface tension).

The second device, the DCIRP Tensiometer, was constructed as depicted in Figure 3.5. Surface tension measurements with the DCIRP (Figure 3.8) were made with the sample vessel sitting not on the balance pan, but on a stage next to the balance pan. The rod (or other probe) is held rigidly on the end of a 1/8 inch steel tube bent in an inverted "L" shape to hold the rod vertically while it is contacted with a sample solution. A block of acrylic polymer (4" x 2" x 1/2") which fits on top of the balance pan is machined to firmly hold the 1/8 inch tube. The sample stage of the DCIRP was the only moving component. A DC motor driven micrometer head (ORIEL Encoder Mike, with Dual Controller Model 18009) was used to drive the sample up to contact the rod. An encoder in the micrometer allowed values of the height to be determined from a digital readout on the controller. The speed could be controlled to be as slow as 0.01 mm/sec; therefore, a zero height could be established by stopping the movement at the instant contact was made. After contact, the sample was slowly lowered and a maximum force was determined by the same procedure described for the IRP, or the stage was stopped periodically to determine a force curve.

The DCIRP was devised because it permitted the movement of a small sample container (1 cm inner diameter test tube) in the horizontal plane. This was crucial since it was determined that accurate force measurements in the small samples required precise centering of the rod in the tube. Measurements made with the DCIRP required determining the force acting on the rod (through the directional converter arm) and not the sample. This is similar to the conventional techniques

used to measure surface tension with du Noüy ring or Wilhelmy plate. Indeed, both of these older methods have been tested on the DCIRP. Since the sample was not being weighed when using the DCIRP evaporation rate was not a problem and the specially constructed sample flask was not required.

The force curves of Figure 3.8 provide a comparison between experimental force measurements and force calculated by the integration of the Laplace equation. Since the calculated curve only relates force to the radial surface of the underside of the rod the initial value (at the point of contact) of force is zero. However, the experimentally determined initial force is on the order of 25 mg. Figure 3.6 illustrates the explanation for this phenomenon. It was obvious in the figure (and observed experimentally) that the outside of the rod was wetted by the liquid sample at the point of contact. As the rod was pulled up the liquid drained from the wall of the rod and the calculated and experimental forces matched at and near the point of maximum force.

In simply measuring surface tension, it is not necessary to know the point of contact of the rod with the liquid. Only the experimentally measured maximum force is required. Then Equations 3.9 and 3.10 can be employed to calculate surface tension.

To determine the feasibility of measuring surface tensions of aqueous solutions of cationic surfactants, we have obtained values of surface tension as a function of concentration for aqueous solutions of hexadecyltrimethylammonium bromide (cetyltrimethylammonium bromide or CTAB) at 23 °C. Results are plotted in Figure 3.9

as surface tension (γ) vs the logarithm of concentration (in mM). The measured weights at maximum pull varied from 242 mg for pure water to about 150 mg for the highest surfactant concentrations, which were well above the critical micelle concentration.

Values of the surface tensions plotted in the figure are intermediate between published du Noüy (21) and maximum bubble pressure (23) results for CTAB solutions, and the agreement among the various methods is quite good near the CMC. The rod-pull method avoids contact angle problems, which can cause results to be low in du Noüy experiments. The new method is considerably faster than the maximum bubble pressure technique, which yields surface tension values that are too large at low concentrations of surfactant unless extremely long bubble-formation times are employed. Sets of six replicate measurements, with the rod-pull method for each of several different liquid samples, indicate that the standard error in the maximum weight is typically 0.3 to 0.7 mg with our apparatus. This corresponded to standard deviations in surface tension of less than 0.25 mN m^{-1}. Results obtained for other pure liquids, and known solutions, are in good agreement with published surface tension data.

The results plotted in Figure 3.9 were the combination of 3 repeat titrations of CTAB using a 20.0 mM stock solution. The temperature varied from 22 to 23 °C since the experiments were conducted on different days and the solutions were not temperature controlled with a circulating water bath. The CMC (critical micelle concentration) determined from this experiment (0.92 mM) is in very good agreement with the commonly reported literature (22-24) values of 0.9-0.95 mM.

A CMC determination of the anionic surfactant sodium dodecyl sulfate (SDS) was also determined and results plotted in Figures 3.11. A CMC value of 8.0 mM for SDS is in very good agreement with accepted literature values (24).

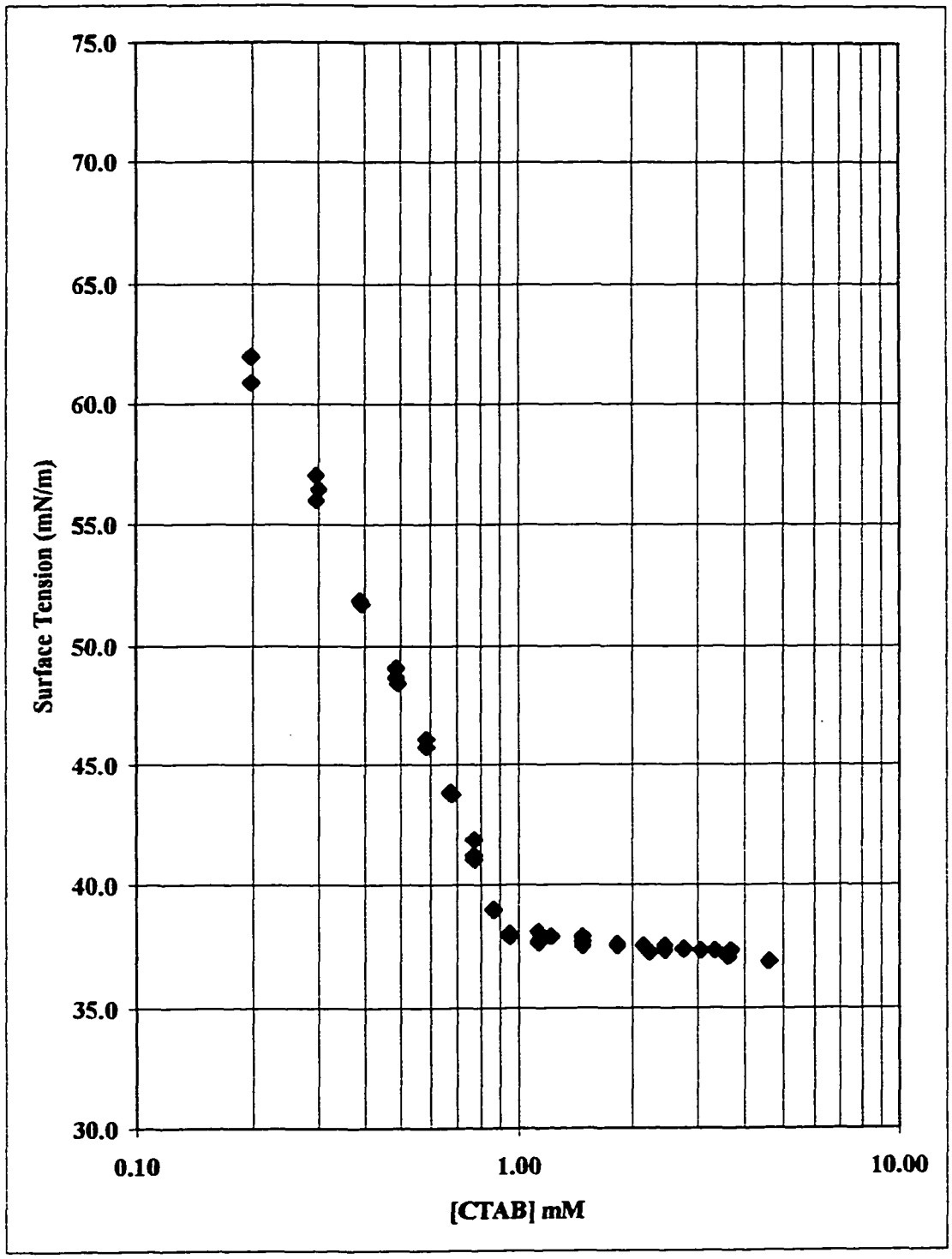

Figure 3.9. CMC determination of CTAB.

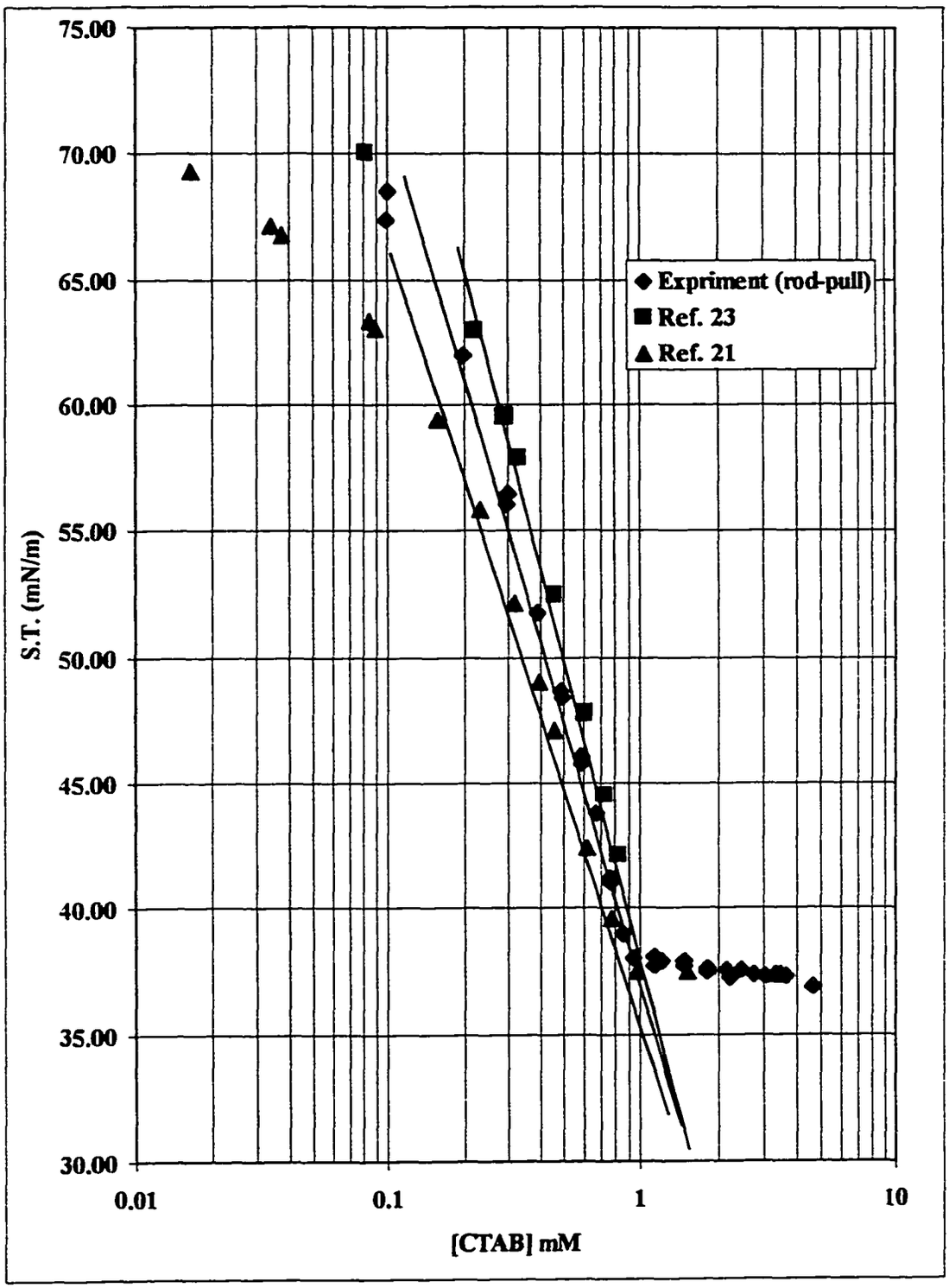

Figure 3.10. Comparison of present measurements with maximum bubble pressure measurements of Dharmawardana, et. al. (23) and Wilhelmy plate measurements of Aveyard, et. al. (21). The linear part of the curves before the CMC is used to calculate the surface excess, Γ.

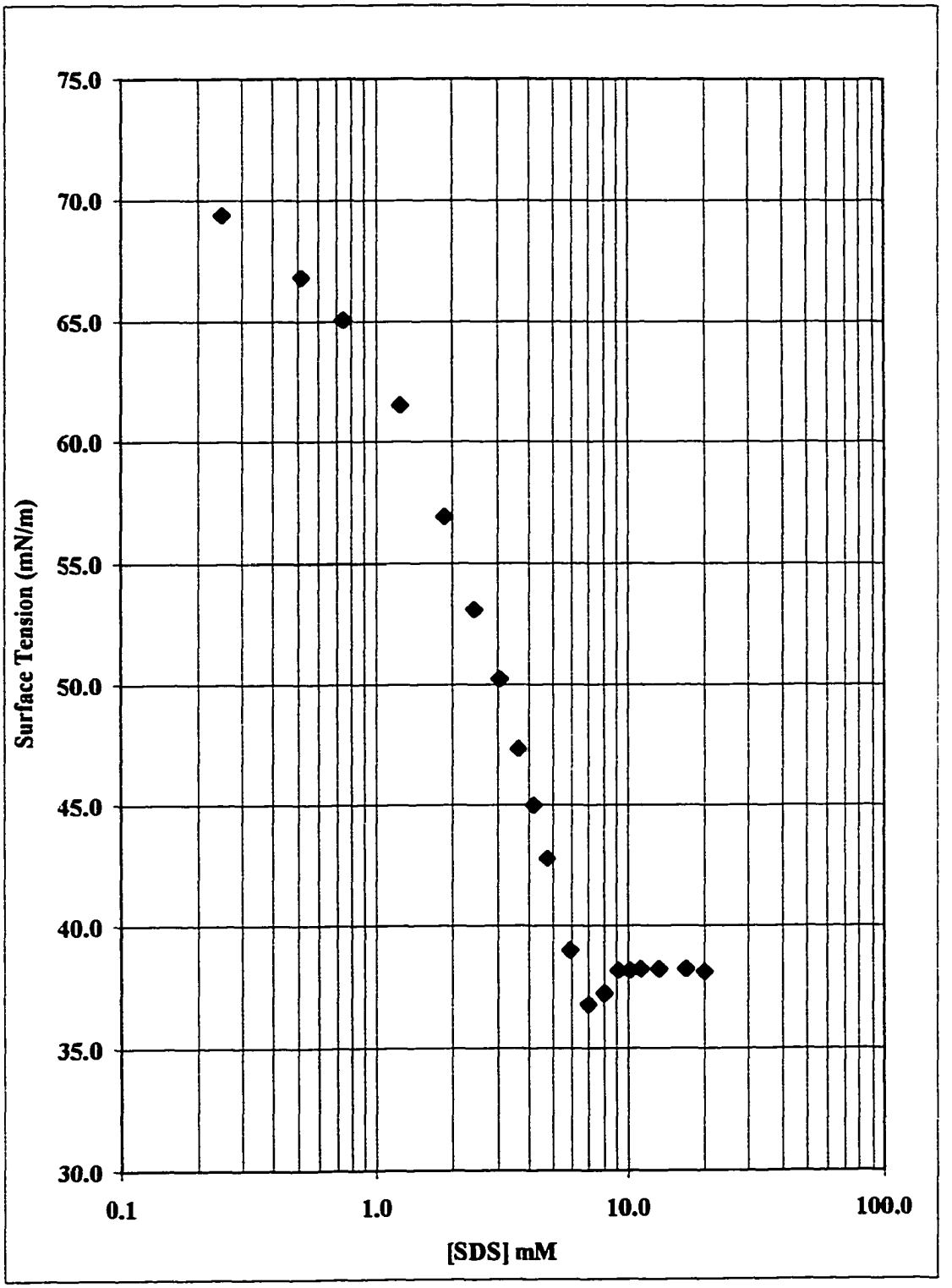

Figure 3.11. CMC Determination for SDS.

Results and Discussion

The experimental results plotted in Figure 3.8 are compared with curves calculated by integrating Equation 3.7. The initial force measured when the rod contacts the liquid is the result of liquid wetting the side of the rod. As the rod is pulled away from the free surface level the curve gradually approaches the calculated curve indicating that the side wetting is diminishing.

Near the maximum of the force curve, the calculated and experimental results match and it is at this maximum that the experimentally determined surface tensions are calculated. It is apparent from Figure 3.2 (or Figure 3.6) that after the angle ϕ becomes less than $\pi/2$ the liquid should have minimal contact with the side of the rod. However, since the critical maximum force occurs for $0 < \phi < \pi/2$, the tables generated originally by Padday (15) and by Equation 3.9 were only derived for this range.

The CMC measurements presented demonstrated the reliability of the new technique. The CMC curves are shown in Figures 3.9-3.11. A more subtle, yet important, physical property could also be extracted from these curves. The boundary between two phases is of course referred to as a surface or interface. In the case of measurement at a liquid-air interface the boundary is usually referred to as simply a surface, hence the term surface tension. Since adsorption of surfactant occurs at the surface, a layer develops in which the quantity of surfactant is different from that which would be present in a representative volume of the bulk solution not near the interface. The quantity of surfactant in that layer is referred to as the surface excess

quantity or the Gibbs adsorption amount. The Gibbs adsorption is derived from the Gibbs dividing surface, which is chosen parallel to the interface to define the layer thickness.

The surface excess concentration is given by

$$\Gamma^{\sigma}_{i} = n^{\sigma}_{i}/\sigma \qquad \text{Equation 3.11}$$

where n^{σ}_{i} is the amount (moles) of component i present at the surface. In Equation 3.11 σ in the denominator represents the surface area. In general, the symbol σ represents a surface quantity and n^{σ}_{i} is defined quantitatively as

$$n^{\sigma}_{i} = n_{i} - V^{\alpha}C^{\alpha}_{i} - V^{\beta}c^{\beta}_{i} \qquad \text{Equation 3.12}$$

where n_i is the total amount of component i, V^{β} the bulk volume and c^{β}_{i} the concentration of component i in the bulk phase. V^{α} and C^{α}_{i} represent similar definitions for a second phase. However, for surface tension measurements on surfactants the second phase is air so $V^{\alpha}C^{\alpha}_{i}$ is equal to zero.

The value of the surface excess could be determined from the linear portion of the surface tension vs log concentration curve before reaching the CMC. For very dilute surfactant solutions, the value of the surface excess (for 1:1 ionic surfactant) is given by the Gibbs equation,

$$\Gamma = -\frac{1}{2RT}\frac{d\gamma}{d\ln C} \qquad \text{Equation 3.13}$$

where R is the ideal gas constant, 8.314 J/K/mole, T the temperature (298 K) and $d\gamma/d\ln C$ is the slope of the CMC plot before the surfactant begins to form micelles.

The factor of 2 in the denominator arises because the activity of the electrolyte solution is given by $a_{cation}a_{anion}$ or C^2, if activity coefficients are neglected.

By taking the slopes of the linear portions of the CMC curves (Figure 3.10) for CTAB it is possible to compare the surface excess concentrations obtained by different methods. Using a du Nouy ring tensiometer, data from Aveyard, et.al. (22) gives a surface excess of $\Gamma = 2.72 \times 10^{-10}$ molecule/nm^2. Using maximum bubble pressure data from Dharmawardana, et. al. (23) give $\Gamma = 3.39 \times 10^{-10}$ molecule/nm^2. Experimental data from the rod pull method in the present work gives $\Gamma = 3.17 \times 10^{-10}$ molecule/nm^2.

In Figure 3.10 the surface tension vs concentration measurements for CTAB are compared with results of different experimental techniques from the literature. Note that the CMC values compare very well with these other techniques also. The slope of the linear portion of the curve, before the CMC is reached, is obviously different depending on the technique used. Dharmawardana et. al. (23) used a maximum bubble pressure technique and the slope of the curve is more negative leading to a higher calculated surface excess quantity ($\Gamma = 3.39 \times 10^{-10}$ molecule/nm^2) than the rod pull technique. The maximum bubble pressure method requires measurement of the pressure opposing the production of a bubble in a liquid. It is known that the maximum bubble pressure may yield large values of the surface tension. This results because diffusion of a highly surface active agent to the interface may not be fast enough to provide an equilibrium concentration as new surface forms during bubble growth. This diffusion control is particularly limiting at

low surfactant concentrations, well below the CMC of CTAB or when using surfactants with inherently lower CMC values. Although the force pull methods (rod pull, DuNoüy, Wilhelmy) also some generate new surface, it is important to note that a significant surface area already exists before the maximum pull is reached. As the probe is pulled upward and new surface is created the new area is fed not only by diffusion of surfactant from the bulk solution but also by rapid surface diffusion of surfactant molecules already present. As surfactant from the surface spreads to fill vacancies of newly created area then that spreading surface may also be fed by the bulk solution. This means that for experiments where a large surface already exists the diffusion flux from the bulk solution can much more readily equilibrate and replenish the surface excess.

Conclusions

In using the rod-pull method to investigate pure liquids and aqueous solutions of anionic, neutral, and cationic surfactants, no particular difficulties have been encountered in measuring the maximum weight with the rod-pull method. The presence of surfactants does increase the amount of liquid that rises, up the metal rod as the end of the rod first contacts the solution. Therefore, in the most careful research work, it is necessary to allow adequate time for drainage of the surfactant solution as the maximum pull is approached. Alternatively, the lower end of the metal rod could be enclosed in a Teflon sheath extending nearly to the tip.

The apparatus diagrammed in Figures 3.4 and 3.5 is readily modified to perform du Noüy ring and Wilhelmy plate experiments. Interfacial tensions as well as surface tensions have been obtained with the new apparatus. Buoyancy effects on the Wilhelmy plate can be inferred by using the micrometer to measure the distance from the bottom of the plate to the plane surface of the liquid or the liquid/liquid interface. Weights of several hundred mg to 1 g are commonly obtained in determining surface tension with either DuNoüy or Wilhelmy methods, so that balances accurate to 1 mg are usually quite suitable.

In making Wilhelmy surface tension measurements, it is convenient to determine the maximum pull by slowly raising the level of the plate to the point where rupture of the meniscus occurs. Then buoyancy corrections are applied to convert the maximum force to the force exerted at a height of zero (relative to the plane surface of the liquid). This equivalent force is the actual surface force corresponding to zero contact angle. Used in this way as a maximum pull method, the Wilhelmy technique avoids contact angle problems and obviates the need for the correction factors required with other common surface tension methods. The measured pull at any depth of immersion (corrected for buoyant effects) is equal to the product of the perimeter of the plate, the surface tension, and the cosine of the contact angle. Therefore once the surface tension has been determined, it is a simple matter to determine contact angles on a plate of any composition.

Evaporation of liquid from the flask may cause problems with highly volatile liquids. The glass vessel shown in Figure 3.4 helps eliminate these problems with

liquids like water, for which the weight loss during a measurement with the rod-pull method can be kept to less than a few tenths of a milligram. Enclosing the entire apparatus in an air-thermostated box can control temperature. In our opinion, the rod-pull surface tension method developed by Padday et al. should be much more widely used than it is, and the modification we propose should make it attractive for many applications. In obtaining surfactant titration data (such as those shown for CTAB in Figure 3.9) we have removed the sample flask before adding each increment of concentrated surfactant solution; stirring has been done manually outside the balance chamber. However, in an automated apparatus, increments of the titrant could be added without removing the sample. Mixing could then be accomplished with a retractable mechanical stirrer having blades that are poorly wetted by the solution.

A paper published describing the inverted vertical pull technique (25) was the basis for much of the work presented in this chapter. For completeness, the manuscript of a paper submitted in final form to the Journal of Colloids and Interface Science is included in the appendix. The paper describes other applications of the force-pull technique with the converter arm tensiometer including cylinder pull for maximum force and du Noüy ring for interfacial tension. Also described is the miniaturization of the rod-pull method for samples as small as 0.3 mL. Measurement of surface tension in small samples is very difficult for du Noüy ring and Wilhelmy plate because of the size of the probes. Sessile drop and spinning drop methods are possible with small samples of course but the measurement of contact angle and drop shape is difficult manually or involves the application of costly camera and digitization equipment.

In summary, the new surface tension techniques presented here are exciting alternatives to conventional methods. The key advantages of the inverted vertical pull method and the converter arm method are their inherent simplicity, low cost, convenience of automation, and robustness. The availability of top loading analytical balances in chemistry and engineering laboratories makes it possible to apply the techniques readily in most labs. Even including the cost of a top loading balance, these methods are more cost effective than conventional du Noüy ring instruments. At the time of this writing, a survey of instrument costs shows that the cost of a conventional manual du Noüy ring tensiometer is over three thousand dollars. A 1 mg top loading balance can be purchased for less than five hundred dollars (98/99 Fisher Scientific Catalog). Work is continuing towards developing automated versions of the instruments and towards optimizing techniques to determine surface tensions of very small samples (< 0.5 mL). The manuscript included in the appendix demonstrates that small sample measurements are indeed possible. Also, the techniques have been shown to provide surface or interfacial tension measurements with equal ease. It is predictable that these techniques, using top loading analytical balances, will become standard methods for surface and interfacial tension.

REFERENCES

1. Lecomte du Noüy, P., "A New Apparatus for Measuring Surface Tension", J. Gen Physiol., **1919**, 1, 521-524.
2. Wilhelmy, L. "Ueber die Abhängigkeit der Capillaritäts-Constanten des Alkohols con Substanz und Gestalt des benetzten festen Korpers", Ann. Physik. **1863**, 119, 177-217.
3. Bashforth, F.; Adams, J.C. "An Attempt to Test the Theory of Capillary Attraction", Cambridge Univ. Press, London/New York, **1883**.
4. Harkins, W. D.; Jordan, H. F. "A Method for the Determination of Surface and Interfacial Tension from the Maximum Pull on a Ring", J. Amer. Chem. Soc., **1930**, 52, 1751-1771.
5. Freud, B. B.; Freud, H. Z. "A Theory of the Ring Method for the Determination of Surface Tension", J. Amer. Chem. Soc., **1930**, 52, 1772-1782.
6. Zuidema, H. H.; Waters, G. W. "Ring Method for the Determination of Interfacial Tension", Indus. Eng. Chem., **1941**, 13(5), 312-313.
7. Couper, A.; *Physical Methods of Chemistry*, 2nd Ed., Volume IXA. Investigations of Surfaces and Interfaces -- Part A; B. W. Rossiter and R. C. Baetzold, Eds., Wiley-Interscience: New York, **1993**; p 1.
8. Padday, J. F. *Surface and Colloid Science*, Volume 1; E. Matijevic, Ed.; Wiley-Interscience: New York, **1969**; p 128.
9. Adamson, A. W. *Physical Chemistry of Surfaces*, Fifth Ed.; Wiley-Interscience: New York, **1990**.
10. Ambwani, D. S.; Fort, T. *Surface and Colloid Science*, Volume 11, Experimental Methods; R. D. Good and R. R. Stromberg, Eds.; Plenum Press: New York, **1979**; p 93.
11. Princen, H. M.; *Surface and Colloid Science*, Volume 2.; Egon Matijevic, Ed., Wiley-Interscience: New York,, **1969**, p 1.
12. Padday, J. F.; Russell, D. R. "The Measurement of the Surface Tension of Pure Liquids and Solutions", J. Coll. Sci. **1960**, 15, 503-511.
13. Huh, C.; Scriven, L. E. "Shapes of Axisymmetric Fluid Interfaces of Unbounded Extent", J. Coll. Int. Sci., **1969**, 30(3), 323-337.
14. Padday, J. F. "Tables of the Profiles of Axisymmetric Menisci", J. Electroanal. Interfacial Electrochem. **1972**, 37, 313.
15. Padday, J. F.; Pitt, A. R. "Axisymmetric Meniscus Profiles", J. Coll. Int. Sci., **1969**, 38(2), 323-334.
16. Padday, J. F.; Pitt, A. R.; and Pashley, R. M. "Axisymmetric Meniscus Profiles", J. Chem. Soc. Faraday Trans. 1, **1975**, *71*, 1919-1931.
17. Furlong, D. N.; Hartland, S. "Wall Effects in Measurement of Surface Tension Using a Vertical Cylinder, Part 1. – Theory", J. C. S. Faraday, 1, **1980**, 76, 457-466.

18. Furlong, D. N.; Hartland, S. "Wall Effects in Measurement of Surface Tension Using a Vertical Cylinder, Part2. – Experimental", J. C. S. Faraday, 1, **1980**, 467-472.
19. Lunkenheimer, K.; Wantke, K, -D. "Determination of the surface tension of surfactant solutions applying the method of Lecomte du Nouy (ring tensiometer)", Coll. Pol. Sci., **1981**, 259, 354-366.
20. Maigren, B.; Odberg, L. "Surface Tension Data from Slight Deformations of the Surface. The Ring Method", J. Coll. Int. Sci., **1982**, 88(1), 197-203.
21. Lyons, C. J.; Elbing, E.; Wilson, I. R. "The Rod-in-Free Surface Technique for Surface-Tension Measurement Using Small Rods", J. Coll. Int. Sci., **1984**, 102(1), 292-294.
22. Aveyard, R.; Cooper, P.; and Fletcher, P. D. I. "Solubilisation of Hydrocarbons in Surfactant Monolayers", J. Chem. Soc. Faraday Trans. 1, **1990**, 86, 3623.
23. Dharmawardana, U. R.; Christian, S. D.; Tucker, E. E.; Taylor, R. W.; Scamehorn, J. F. "A Surface Tension Method for Determining Binding Constants for Cyclodextrin Inclusion Complexes of Ionic Surfactants", Langmuir **1993**, 9, 2258-2263
24. Mukerjee, P.; Mysels, K. J. *Critical Micelle Concentrations of Aqueous Surfactant Systems*, United States Department of Commerce, National Bureau of Standards, Washington, DC, **1971**.
25. Christian, S.D.; Slagle, A.R.; Tucker, E.E.; Scamehorn, J.F. "Inverted Vertical Pull Surface Tension Method", Langmuir, **1998**, 14(11), 3126-3128.

Appendix to Chapter 3

This appendix contains the final manuscript, with revisions, submitted to the Journal of Colloid and Interface Science in December of 1998.

Directional Converter Arm Method for Surface and Interfacial Tension Measurements with a Top-loading Balance

Sherril D. Christian*, Andrew R. Slagle, Katsuhiko Fujio,
Edwin E. Tucker, and John F. Scamehorn
Institute for Applied Surfactant Research
The University of Oklahoma
Norman, OK 73019

ABSTRACT

A method is described for utilizing a top-loading balance, with a directional converter arm, in vertical pull surface force measurements. The Padday rod-pull technique, the du Noüy ring method, and the Wilhelmy plate method are utilized with rods, thin-walled tubes, wire rings, and plates either rigidly attached to the converter arm or hanging freely from a hook at the end of the arm. The robustness, large weighing capacity, and accuracy of top-loading balances makes them ideally suited for a variety of types of surface and interfacial tension measurements. The converter arm method can be used with a stainless steel rod (3 to 7 mm in diameter) in vertical pull surface tension measurements, with samples having volumes of only a few tenths

of a milliliter. Measurements on very small liquid volumes are feasible because the rod is firmly attached to the converter arm, rather than hanging freely as in measurements with balances mounted above the sample; therefore, the rod cannot swing toward and attach to the wall of small sample tubes. Automation of force and height measurements with the converter arm/top-loading balance method is straightforward.

INTRODUCTION

Previously (1), we showed the advantages of using a top-loading analytical balance in vertical pull surface tension and interfacial tension measurements. Our modified procedure utilizes measurement of changes in the apparent weight or mass of a liquid that occur as a rod, plate, ring, or tube contacts the liquid surface from above and is slowly raised to known vertical positions with a precision micrometer. This method inverts the usual vertical pull measuring procedure, in which a solid object is suspended from a microbalance or other sensitive balance mounted above the liquid. The stability of top-loading balances, coupled with the fact that objects being weighed remain in a fixed position, makes the use of these balances quite convenient in determining a wide array of surface and interfacial properties.

We describe here a complementary technique for utilizing top-loading balances in vertical pull surface force measurements. This method also exploits the robustness of these balances, with a modification permitting their use in measurement of the vertical force acting on objects mounted rigidly or hanging above a liquid sample. The du Noüy ring measurement (2) is readily performed with a thin-walled metal or glass tube attached directly to a metal arm extending from the balance. A modification of the Padday rod-pull method (3,4) permits accurate surface tensions to be measured for liquid samples as small as 0.3 mL.

APPARATUS

Figure 1 shows the arrangement of the two main components of the new measuring system: 1) a directional converter arm for making vertical pull measurements with a top-loading (load cell) balance; and 2) a stage, allowing precise vertical positioning of a liquid sample. The converter arm has an acrylic base (approximately 1.5 cm thick, 9 cm long, and 4 cm wide) resting freely on the circular pan of the top-loading balance. Extending upward from the center of the base is an approximately 1/8" stainless steel rod or tube, shaped in the form of an inverted letter **"J"**. The working end of the arm (aligned vertically) ordinarily extends outside the balance enclosure. The arm has an o.d. at its end of 0.125", permitting the rigid attachment of a tube, plate, ring, or rod by means of holders using set-screws. Alternatively, a small hook can be attached to the end of the arm, from which rings and other objects will hang freely. The dimensions shown in Figure 1 are typical for a converter arm extending outside the balance enclosure; it is possible to make the arm smaller so that the tube, plate, or rod is supported inside the case.

The stage resembles that of manual du Noüy balances, which employ a screw beneath the sample support to move the liquid gradually up and down. If the vertical movement is to be measured, the stage can be held (by spring-loading) against the spindle end of a micrometer, so that the vertical movement of the stage can be monitored with an encoder. Top-loading balances often come equipped with

microcomputer interfaces, so that simultaneous mass change and height data can be generated in semi-automatic or automatic measurement modes. The liquid in the glass vessel can be stirred magnetically and thermostatted (by circulation of liquid through a jacket) if necessary.

Top-loading balances can have significant advantages over traditional balances (using a torsion wire or a fulcrum and nulling mechanism) in measuring surface and interfacial tensions. Experimentally, we have shown that if objects are attached to or hung from the end of the converter arm, or placed directly on the pan of the balance, virtually the same mass is measured by the top-loading balance in each case. For objects weighing 1 to 2 grams (more than the usual mass change involved in surface force measurements) the mass determined with the balance is the same no matter where the weights are placed along the converter arm. This is because the torque caused by mass changes of the magnitude occurring in surface force experiments does not change the position of the total mass being weighed. The excellent stability of load cell weighing devices and the lack of vertical motion of the object being weighed enhance their utility. It should also be emphasized that both the converter arm and the inverted vertical pull methods have significant cost advantages compared to the very expensive microbalance systems that are frequently used for surface and interfacial tension measurements. Even a manual du Noüy apparatus now costs more than $3,000, while the cost of a top-loading balance (accurate to 1 mg), including computer interface, is less than $500.

MEASUREMENTS WITH THE PADDAY ROD-PULL METHOD

A method that is quite convenient for use with the top-loading balance is the rod-pull technique developed by Padday, et al. (3,4). We have recently shown the utility of the inverted vertical pull concept, implemented with solid rods of circular cross section, attached rigidly to a micrometer spindle (1). Use of the directional converter arm, with an attached rod, produces results in nearly exact agreement with those obtained with the inverted vertical pull measurements or conventional rod-pull measurements.

Figure 2 shows the orientation of the rod relative to the liquid as the liquid is lowered after contacting the rod. Initially, for a rod that is wetted by the liquid, some liquid rises up the side of the rod, contributing a component of force in the downward direction. As the liquid is lowered further, it will pass through a position in which the surface force is a maximum because the pull is straight up, as shown in the middle drawing in Figure 2. This is not the position of maximum pull, however, because buoyancy also contributes a `pull' in the same direction as the surface force. At some height greater than that in the middle drawing the combined surface and buoyant force will reach a maximum, provided that the column of liquid does not break before that point. In practice, with water and a variety of aqueous solutions of surface active

agents, the liquid wets the rod well enough so that the height corresponding to the maximum pull can be reached and exceeded without difficulty.

With water, organic liquids, and aqueous solutions, determination of mass vs. height data makes it possible to obtain the value of the mass at maximum pull, which is the single observation needed in calculating the surface tension. Figure 3 shows a typical mass vs. height diagram for a stainless steel rod having a radius of 3.16 mm, for liquid water at 23 °C (surface tension = 72.3 mN m^{-1}). Theoretical values of the mass change vs. height (the solid curve in Figure 3) are predicted by numerical integration of a nonlinear second order differential equation (3,4). Previous publications (1,3,4) have shown how the maximum mass (in common parlance, called the maximum weight) can be used to calculate the surface tension, for liquids of known density and for known values of the gravitational constant.

Experimental results are shown as points in the figure; they differ from theoretical predictions in several respects. There is an initial nonzero mass change contributed by liquid film rising up the rod, but as the maximum is approached, the liquid drains away and at the maximum pull virtually none of the liquid remains above the lower end of the rod. The experimental height at maximum pull is somewhat less than calculated, although the mass corresponding to maximum pull is virtually that calculated from theory. The horizontal discrepancy near the maximum is partly accounted for by the change in liquid level caused by lifting approximately

0.24 mL of liquid under the rod. The open diamonds in Figure 3 represent the experimental values corrected for the change in liquid level at each point. Wetting problems in the region near the point where the liquid detaches from the rod probably cause the force to be somewhat less than theoretical.

MEASUREMENTS WITH THE DU NOÜY METHOD

The du Noüy method (2,5), utilizing a Pt-Ir ring, has long been used to measure surface tensions of liquids and interfacial tensions of liquid/liquid interfaces. In measuring surface tension with the converter arm technique, the ring is either hung from a hook at the end of the converter arm, or attached rigidly to the arm to prevent the ring from swinging toward the wall of the container. First, the balance is zeroed (tared) with the ring out of the liquid. Then, the liquid sample is raised, either manually with a screw beneath the sample stage, or with a DC-motor driver and encoder (capable of setting and reading relative heights to about 1 micron). The liquid sample is raised until the ring passes through the air/liquid interface, ultimately breaking through this surface and becoming wetted by the liquid phase. Following this, the liquid sample is slowly lowered, and the mass change is monitored while the plane of the ring approaches the position of maximum pull; only the maximum mass change is recorded. Very small buoyant effects are detected for relative motion of the ring with no film attached, although these forces are usually negligible. Interfacial tension measurements are performed similarly, except that after zeroing the balance,

the ring is allowed to pass through both the liquid surface and the liquid/liquid interface; then the sample is lowered until the maximum pull is recorded.

In order to compare the new (converter arm) method with the conventional manual du Noüy method, several measurements were made with each technique, using pure heptane and a heptane/water interface at 23 °C. Measurements with the same ring yielded virtually identical results for the two methods: for the heptane/water interface, 50.0 ± 0.1 mN m^{-1} with the new method and 49.8 ± 0.1 mN m^{-1} with the new method; and for the heptane/air interface, 20.1 ± 0.2 mN m^{-1} with the new method and 20.0 ± 0.2 mN m^{-1} with the conventional method. These values are all in excellent agreement with literature values (6).

Although the du Noüy method (2, 5) commonly employs freely hanging rings made from thin Pt wire, there is no reason thin-walled metal or glass tubes cannot be used in place of the usually fragile rings. We have found that the rigidity of thin-walled metal tubes makes them useful in measurements of surface tension by the du Noüy method, employing the directional converter arm. One such tube (made from nickel-plated stainless steel) has been attached to the 0.125" o.d. end of the directional converter arm (see Figure 1). The cylinder has a length of 2 cm, a diameter of 15.50 mm, and a wall thickness of 0.43 mm. The upper end of the tube is held by a snugly-fitting plastic cap, threaded at the center to accept a 1/8" metal

screw. The screw connects to a holder, which is fixed to the end of the converter arm with set-screws.

An important variable in converting du Noüy force measurements into surface tension values is the ratio R/r, where R is the mean radius of the ring or tube and r is the radius of the wire or half the thickness of the tube wall. Ratios of R/r in the range 30 to 100 are common for the Pt-Ir rings used in conventional du Noüy experiments. For the tube used here, R = 7.96 mm and r = 0.215 mm, so that the value of R/r is 35.

In performing experiments with the stainless steel tube, the tube is separated from the cap, cleaned, and flamed briefly in a laboratory burner. After the tube has cooled, the cap and holder assembly are reattached, so that the tube is connected rigidly to the arm, in a vertical position. The tube position will not change as du Noüy force measurements are made.

With the tube in the desired position and the balance tared, the liquid sample is elevated until the end of the tube contacts the surface and penetrates a millimeter or so into the liquid. From this position, the liquid is slowly lowered until a maximum mass change is observed. With most liquids, it is possible to lower the liquid beyond the point at which the mass is a maximum, without detaching the film. Ordinarily, the maximum mass can be approached both from below and above - - that is, by alternately increasing and decreasing the height.

Measurements of mass vs. height have been obtained with the tube for liquid water at 23 °C. A plot similar to Figure 3 (not shown) is obtained, and the maximum mass attained is 0.765 g. As in the rod pull method, height measurements are not required in determining surface tension so long as the point of maximum pull can be reached. In the event that the film breaks before the point of maximum pull, data comprising a major portion of the mass vs. height curve (approaching but not reaching the maximum) can be analyzed to infer the value of the surface tension (6).

If the du Noüy method could be employed using a tube (or ring) of negligible wall (or wire) thickness, the maximum force exerted by two concentric films rising vertically would be equal to

$$W_{max}g = 4\pi R\gamma \qquad (1)$$

where W_{max} is the maximum measured mass change, g is the gravitational constant, R is the average of the inside and outside radii of the tube, and γ is the surface tension. However, a correction is required to account for buoyant effects (from liquid suspended directly under the tube wall) and for the fact that the films are not exactly vertical along their line of contact with the tube. Thus one writes

$$W_{max}gf = 4\pi R\gamma \qquad (2)$$

where f is a correction factor. Fortunately, f is known quite precisely as a function of the two dimensionless groups R/r and R^3/V, where V is the volume of liquid held up

by the tube, equal to the observed change in mass divided by the liquid density minus the air density.

The table below lists values of the correction factor f in equation 2, for a limited range of values of R/r and R^3/V (taken from reference 5). For R/r and R^3/V values outside this range, a more extensive table of f values should be consulted (5), or an equation relating f to R/r and R^3/V can be used (7).

Values of factor f in equation 2

R/r =	30	32	34	36	38	40
R^3/V						
0.56	.9281	.934	.940	.946	.951	.9567
0.58	.9247	.930	.938	.942	.947	.9532
0.60	.9215	.927	.933	.939	.944	.9496
0.62	.9184	.924	.930	.936	.941	.9467
0.64	.9150	.921	.927	.932	.938	.9439
0.66	.9121	.918	.925	.930	.935	.9408

From the measured value of the maximum pull for water at 23 °C (W_{max} = 0.765 g) one can calculate that the volume of water suspended (equal to the mass divided by density) is V = 0.77 mL. Thus, R^3/V (for a mean tube radius of 0.767 cm) is $0.767^3/0.77 = 0.59$. Recall that R/r = 35 for the tube. Using the table above, the value f = 0.938 is obtained by interpolation. Using equation 2, one calculates

$\gamma = fW_{max}g/(4\pi R) = (0.938)(0.765\ g)(980\ cm\ s^{-2})/(4)(3.14)(0.767\ cm)$

$= 73.0$ dyne $cm^{-1} = 73.0$ mN m^{-1}.

A MINIATURIZED ROD-PULL METHOD

Previously it was shown that enhanced values of the maximum force or mass could be obtained for metal cylinders (rods) contacting liquids contained in tubes having diameters only a factor of 1.5 to 4 greater than the rod diameters (8, 9). Theoretical calculations were shown to be in good agreement with experiment for rods and sample tubes having various diameters (8,9). Thus, for example, it was reported for liquid water that with a rod of radius 0.400 cm and a tube of radius 0.916 cm, the maximum mass change was 394 mg, compared to 350 mg for the same rod in a cylinder having an infinite tube radius (for which curvature is zero at large distances from the rod). Unfortunately, with the balance used in the previous experiments (8,9), it was difficult to reduce further the gap between the rod and the tube wall, because a freely swinging rod tends to move toward the wall and stick there.

The converter arm method is readily adapted to obtain surface tension data for quite small liquid samples (0.4 mL or less). Figure 4 shows an arrangement in which the 6.35 mm diameter rod contacts the liquid contained in a flat-bottomed glass tube having an inside diameter of 10.0 mm. The tube fits snugly into a vertical hole bored in a plastic or rubber-stopper base. With the stage elevated initially, the rod is aligned vertically, and as nearly as possible concentrically with the tube before liquid is

added. It is important to emphasize the convenience of being able to maintain the rod in a fixed position, preventing its movement toward the tube wall, even when the gap between the rod and the tube is only a millimeter or less.

After alignment, the stage is lowered and a 0.5 mL liquid sample is added to the tube. Then, as in the experiments with larger liquid samples, the stage is elevated until the rod penetrates a short distance into the liquid. The maximum mass is determined by slowly lowering the stage while monitoring the mass change. Again, the maximum mass can be approached both from above and below the optimum height without detaching the film from the rod. With water at 23 °C, using a 6.23 mm diameter stainless steel rod in a 10.55 mm (i. d.) tube, the maximum mass is determined to be 366 mg, compared to 234 mg obtained with a nearly plane surface (in an 8 cm i. d. glass sample vessel). The nearly 60% increase in the measured maximum pull in the small sample tube is an important benefit of the miniaturization.

In measurements with several stainless steel rods, the agreement between theoretical and observed values of the surface tension is quite good provided that a value of the rod radius that is 0.01 to 0.02 mm less than that measured with micrometer calipers is used in calculations. Imperfections in the face of the rod and the fact that the plane of the face may not be exactly perpendicular to the rod axis could lead to a force at maximum pull that is less than the calculated value. Figure 5 indicates the dependence of the calculated value of the maximum mass on rod radius,

for an assumed surface tension of 72.3 mN m^{-1} for liquid water at 23 °C, for a vessel of large tube diameter. A change in rod radius of only 0.002 cm causes a change in maximum mass of approximately 1%. An error of this magnitude in the maximum mass translates into an error of 1.4% or 1.0 mN m^{-1} in the calculated surface tension. It is convenient to calibrate each rod by making maximum mass measurements on a pure liquid such as water with a known surface tension. The inferred rod radius (obtained from standard curves such as that shown in Figure 5) can then be used in subsequent determinations of surface tensions for other liquids.

Data and calculations are shown in Figure 6 for a rod having an measured radius of 3.115 mm. Values of the calculated maximum mass, plotted against the inside diameter of the liquid tube, are in quite good agreement with observed values for an assumed rod radius of 3.100 mm. Figure 6 highlights the important effect of decreasing the glass tube radius on the magnitude of W_{max}, showing that both the inverted pull method and the new method utilizing the directional converter arm will be quite suitable for measurement of surface tensions of samples having volumes of 0.4 mL or less.

The calculated mass changes in Figure 6 are based on the assumption that the contact angle at the tube wall is zero, a condition which seems to be met for most aqueous solutions in glass sample tubes. The numerical integration can of course be performed for any chosen value of the contact angle at the container wall, making

this method useful for the determination of surface tensions in small vessels which are not completely wetted by the liquid. Although the integration is somewhat complicated, for most systems of interest we have been able to obtain accurate mass change vs. rod height profiles in less than a minute with desk-top personal computers.

AUTOMATION OF THE DIRECTIONAL CONVERTER ARM AND INVERTED VERTICAL PULL METHODS

The rod-pull technique, utilizing either the inverted vertical pull method described previously or the new directional converter arm method, should be quite readily modified for automatic or semi-automatic operation. So far, we have employed a stage driven by a stepper motor, with relative height measurements accurate to 1 μm, to obtain simultaneous mass and height information with the converter arm method. Mass and height changes can be monitored continuously as the liquid sample is driven upward to contact the rod and then withdrawn until the maximum pull is exceeded. Multiple determinations of the maximum pull are made, for increasing and decreasing heights of the end of the rod relative to the plane surface of the liquid. All of the logical steps required in programming the entire measurement cycle can be made from knowledge of the observed mass at known times, for the known (pre-determined) speed and direction of the stage driver. The reproducibility of repetitive measurements of the maximum pull in a single run and between runs is excellent, permitting determination of surface tension to within 0.3

mN m^{-1}, even with a balance only accurate to the nearest milligram. The miniaturization method described in the preceding section does not introduce difficulties in achieving microcomputer control of the measuring cycle.

In measurements on liquid samples with large surface areas, it is possible to use available titration systems designed to add known volumes of solutions of a surfactant or other component to an aqueous solution. Thus, the method of adding samples in automated Wilhelmy, du Noüy, and other surface or interfacial tension methods can be used directly with the rod-pull technique described here.

DISCUSSION

Use of the directional converter arm should facilitate many types of measurements of surface and interfacial forces. The du Noüy and rod-pull methods, using rings, tubes, or rods attached rigidly to the end of the arm, are particularly convenient in practice. Losses of liquid by evaporation do not ordinarily influence the change in mass determined for objects attached to or suspended from the converter arm.

Miniaturization of the rod-pull method can be accomplished by using a tube having an inside radius only 1 to 3 mm larger than the rod radius. The fact that the rod is rigidly attached to the converter arm makes this measurement much easier than

it would be if the rod were allowed to hang from a thin hook above the liquid sample. The ability to make accurate surface tension measurements on samples of volume 0.4 mL or less may offer particular advantages in clinical work, where lung fluids, blood sera, and other liquids may not be available in quantities larger than a fraction of a milliliter. An advantage in measurement is also achieved because the maximum pull is considerably increased, as predicted, when the gap between the rod and the sample tube wall becomes small.

Finally, it should be straightforward to develop fully automatic rod-pull, du Noüy, and Wilhelmy plate methods, utilizing the converter arm with top-loading balances. Because the end of the arm can extend outside the balance enclosure, liquid samples supported below the arm are readily stirred and thermostatted. Simultaneous readings of mass and height can be transmitted to a microcomputer, which can control the vertical movement (and if necessary, the horizontal movement) of the sample stage. With the rod, tube, ring, or plate connected directly to the directional converter arm, the problem of damping the motion of a hanging object before starting the measurement does not arise.

ACKNOWLEDGMENT

The authors would like to thank Professor Ahmed A. Taha for many helpful discussions.

Legends for Figures

Figure 1. Components of the surface tension system using a directional converter arm for vertical pull measurements with a top-loading balance. A rod is shown as the probe; however measurements have also been made with du Noüy rings, Wilhelmy plates, thin-walled metal tubes, and plastic films supported from the arm.

Figure 2. Liquid pulled up by a cylindrical metal rod.

Figure 3. Dependence of mass change measured with a stainless steel rod (Figure 2) on height, for liquid water at 23 °C. Rod radius is 0.3165 cm.

Figure 4. Stainless steel rod contacting liquid in a flat-bottomed glass tube having an inside diameter of 10.0 mm.

Figure 5. Dependence of the maximum mass on rod radius for liquid water at 23 °C. Sample tube radius is assumed to be infinite.

Figure 6. Experimental and calculated values of the maximum mass vs. sample tube diameter, for water at 23 °C for a rod having a nominal radius of 0.3115 cm. The calculated curve represents theoretical results for a rod having a radius of 0.3100 cm.

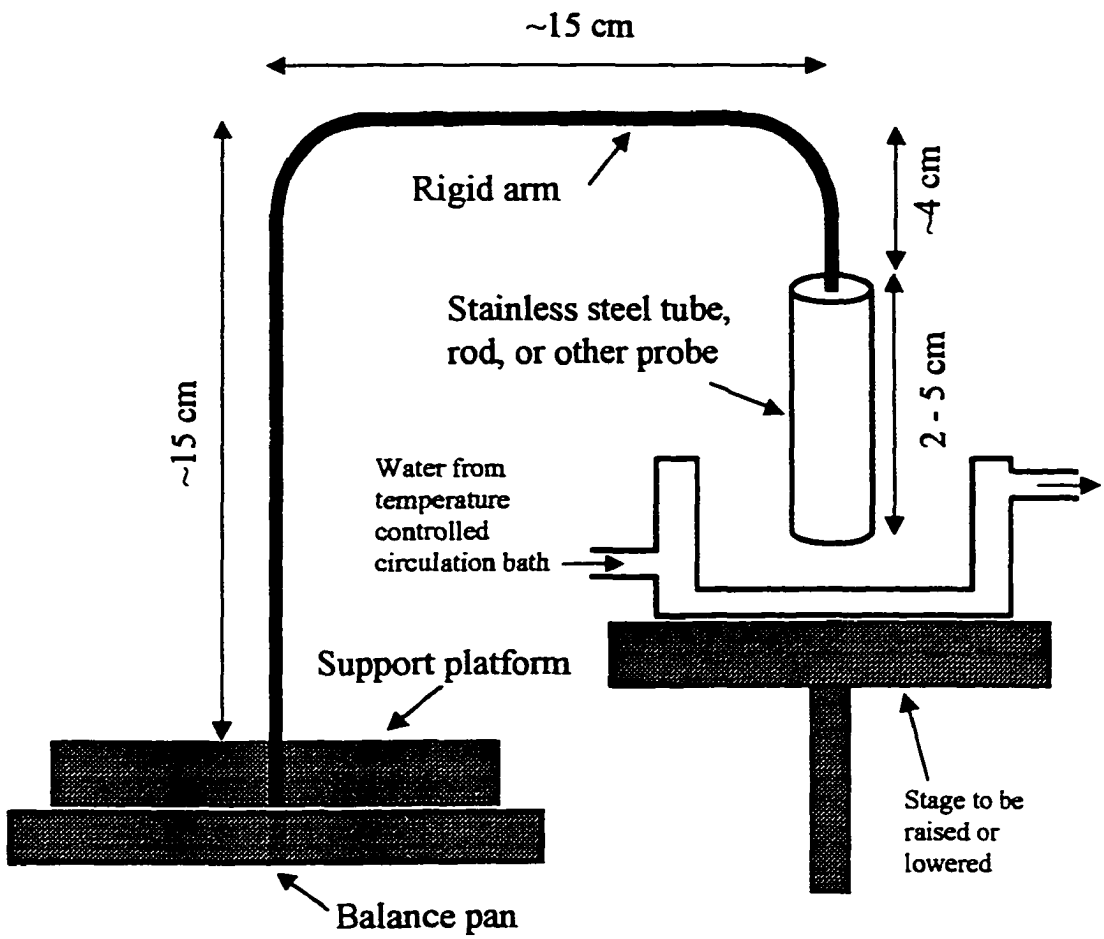
~15 cm
Rigid arm
~4 cm
Stainless steel tube,
rod, or other probe
2 - 5 cm
~15 cm
Water from
temperature
controlled
circulation bath
Support platform
Stage to be
raised or
lowered
Balance pan

Figure 1

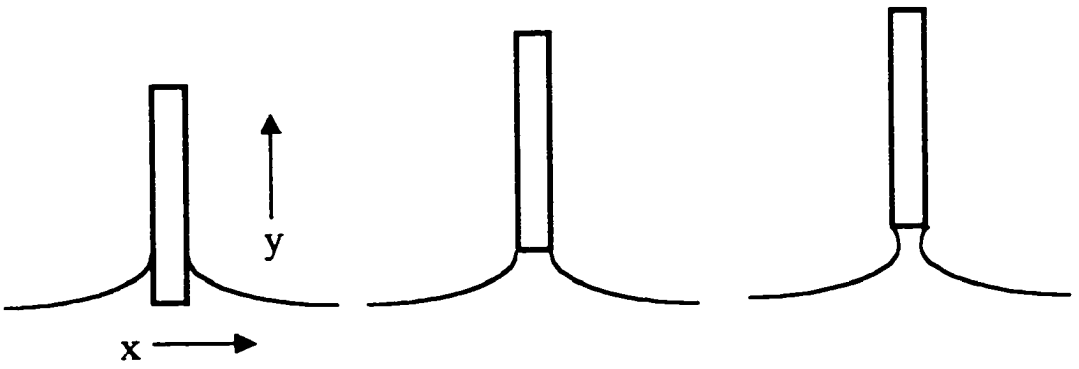

Figure 2

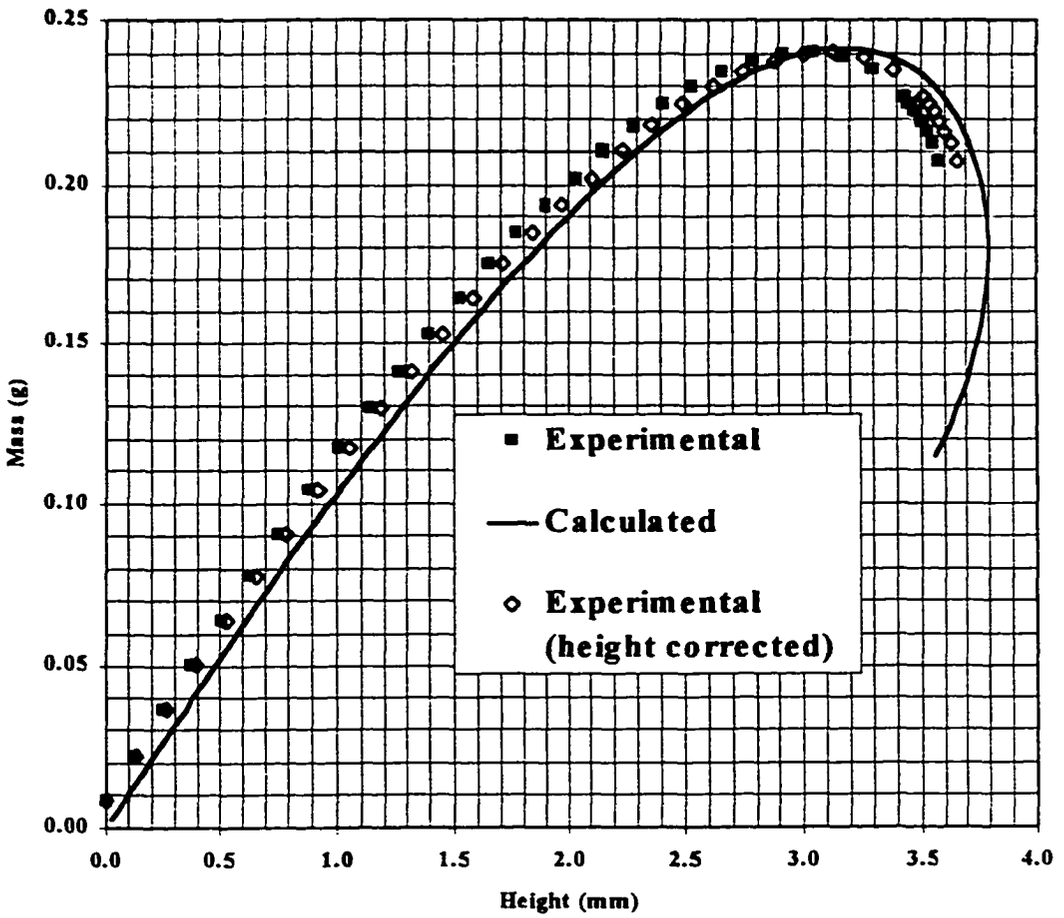
0.25
0.20
0.15
0.10
0.05
0.00
Mass (g)
0.0
0.5
1.0
1.5
2.0
2.5
3.0
3.5
4.0
Height (mm)
Experimental
Calculated
Experimental
(height corrected)

Figure 3

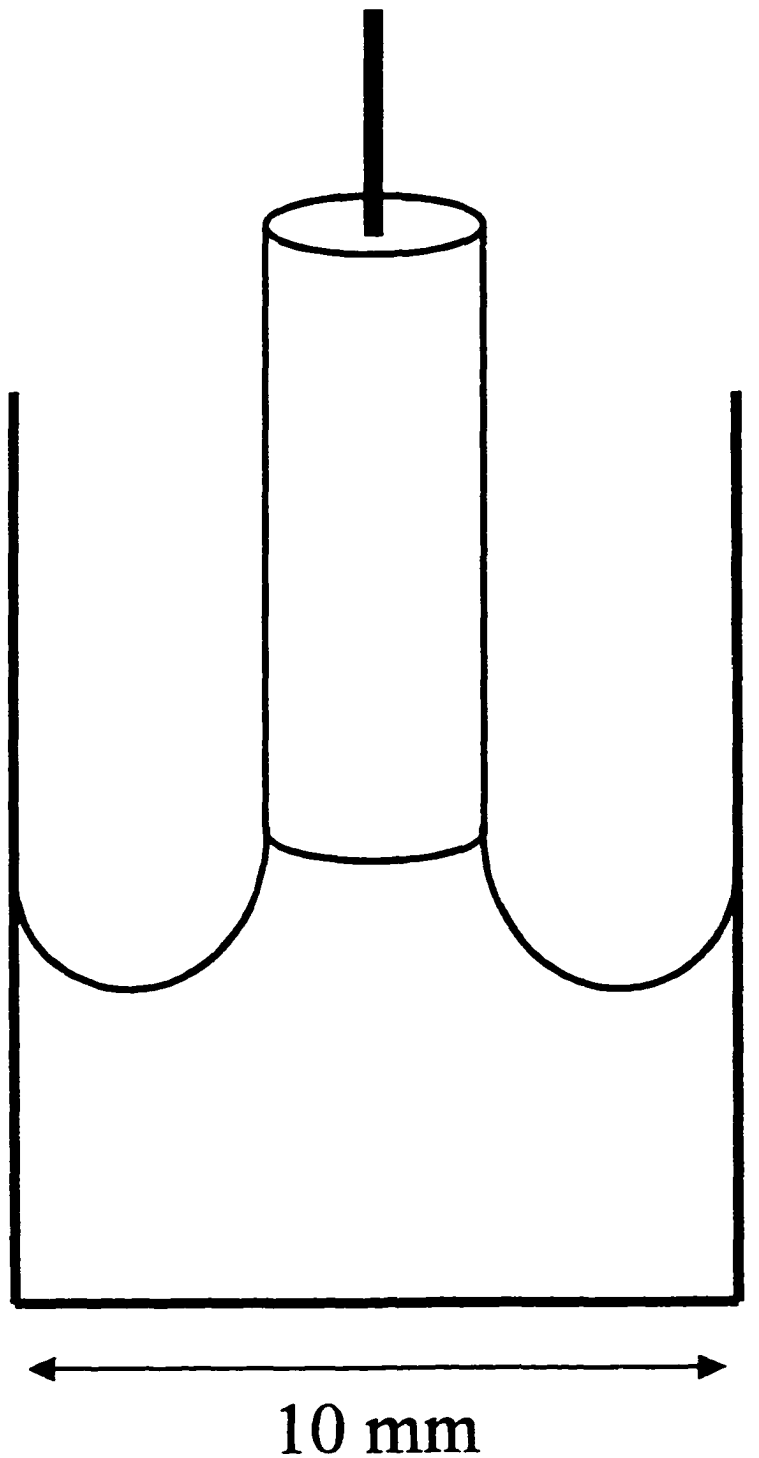

Figure 4

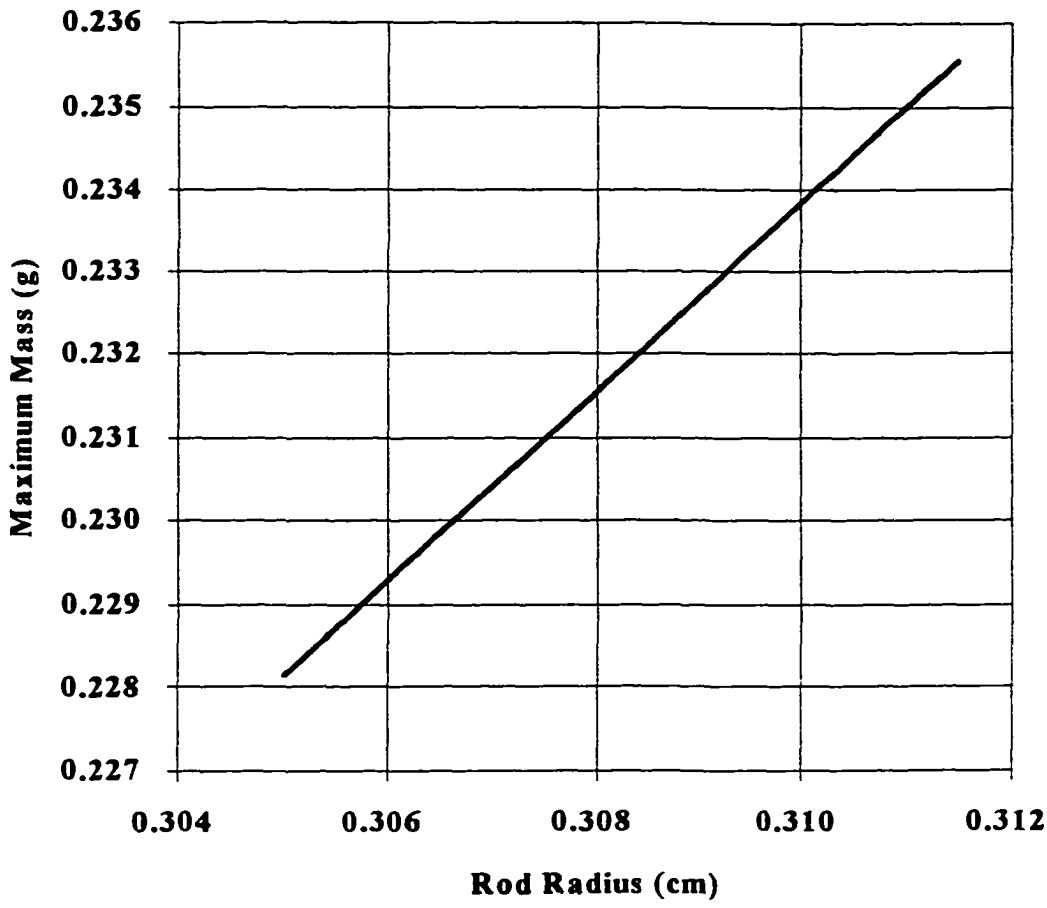
0.236
0.235
0.234
0.233
0.232
0.231
0.230
0.229
0.228
0.227
Maximum Mass (g)
0.304
0.306
0.308
0.310
0.312
Rod Radius (cm)

Figure 5

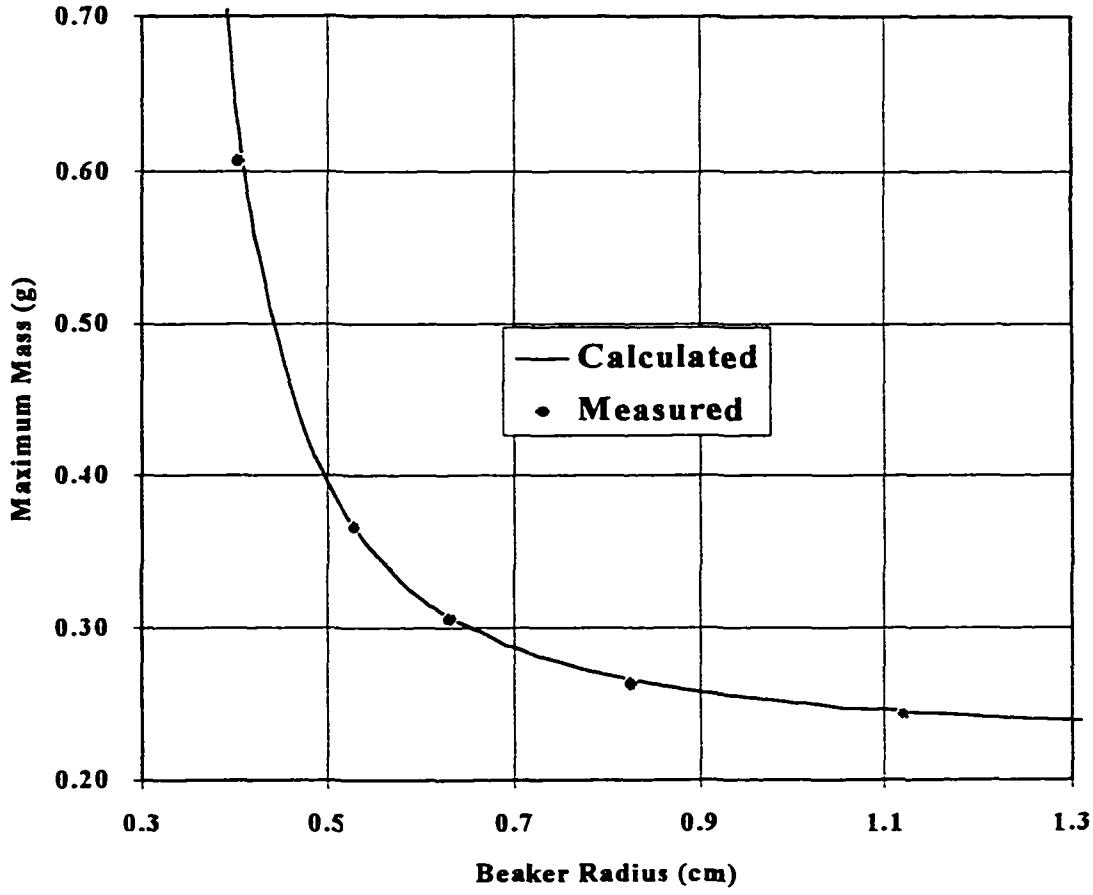
0.70
0.60
0.50
0.40
0.30
0.20
Maximum Mass (g)
Calculated
Measured
0.3
0.5
0.7
0.9
1.1
1.3
Beaker Radius (cm)

Figure 6

References

1. Christian, S. D., Slagle, A. R., Tucker, E. E., and Scamehorn, J. F., *Langmuir*, **14**, 3126 (1998).

2. a.) Lecomte du Noüy, P., *J. Gen Physiol.*, **1**, 521 (1919). b.) Harkins, W. D., and Jordan, H.F., *J. Amer. Chem. Soc.*, **52**, 1751 (1930). c.) Freud, D. B., Freud, H.Z., *J. Amer. Chem. Soc.*, **52**, 1772 (1930).

3. Padday, J. F. *J. Electroanal. Interfacial Electrochem.* **37**, 313 (1972).

4. Padday, J. F., Pitt, A. R., and Pashley, R. M. *J. Chem. Soc. Faraday Trans. 1*, **71**, 1919 (1974).

5. Couper, A. *in* "Physical Methods of Chemistry, 2nd Ed., Volume IXA. Investigations of Surfaces and Interfaces -- Part A", (B. W. Rossiter and R. C. Baetzold), p. 1, Wiley-Interscience, New York, 1993.

6. Adamson, A. W., "Physical Chemistry of Surfaces.", 5th Ed., Wiley-Interscience, New York, 1990.

7. Zuidema, H. H., and Waters, G. W., *Ind. Eng. Chem.*, **13**(5), 312 (1941).

8. Furlong, D. N., and Hartland, S., *J. C. S. Faraday I*, **76**, 457 (1980).

9. Furlong, D. N., and Hartland, S., *J. C. S. Faraday I*, **76**, 467 (1980).

IMAGE EVALUATION
TEST TARGET (QA-3)

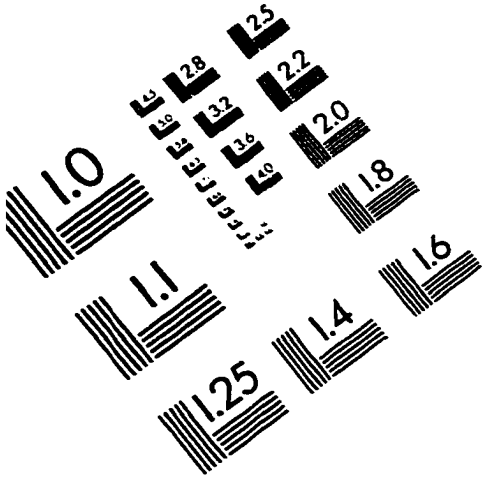

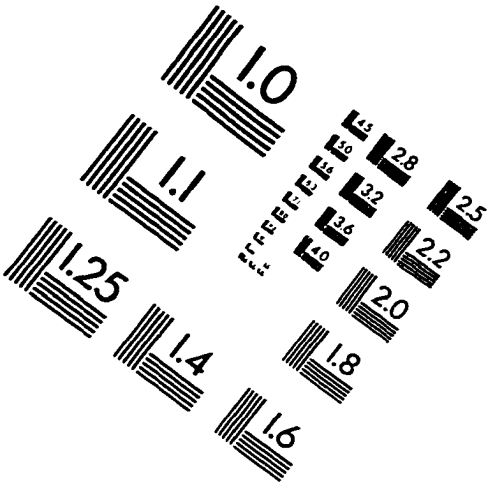

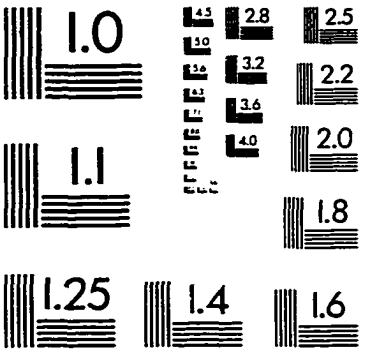

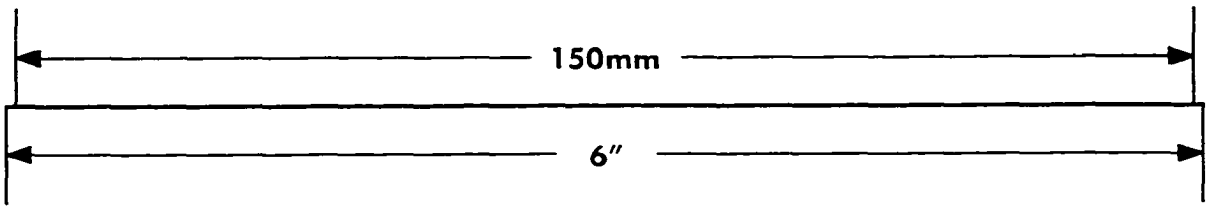

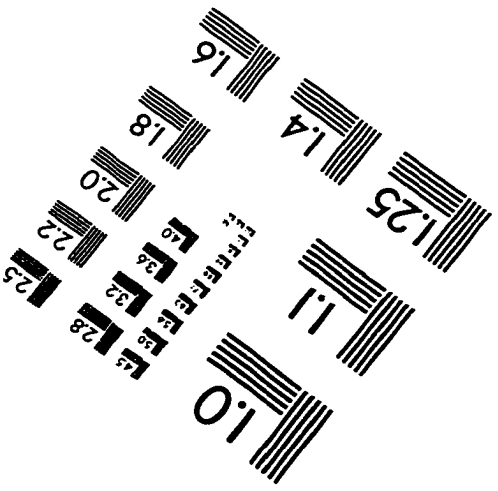

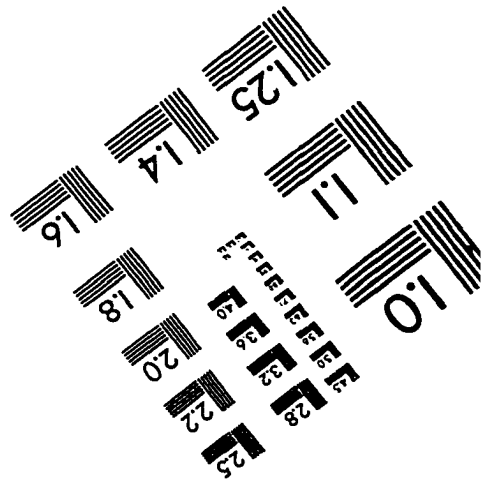

APPLIED IMAGE, Inc
1653 East Main Street
Rochester, NY 14609 USA
Phone: 716/482-0300
Fax: 716/288-5989

© 1993, Applied Image, Inc., All Rights Reserved